DISRUPTIONS IN HEPATIC ONE CARBON METABOLISM AND THE GUT MICROBIOME DURING THE PROGRESSION OF NON-ALCOHOLIC FATTY LIVER DISEASE

By

Russell Ryan Fling

A Dissertation

Submitted to
Michigan State University
in partial fulfillment off the requirements
for the degree of

Microbiology - Environmental Toxicology - Doctor of Philosophy

2022

ABSTRACT

DISRUPTIONS IN HEPATIC ONE CARBON METABOLISM AND THE GUT MICROBIOME DURING THE PROGRESSION OF NON-ALCOHOLIC FATTY LIVER DISEASE

By

Russell Ryan Fling

The etiology of non-alcoholic fatty liver disease is complex, with multiple contributing factors including dietary, environmental, gut microbiome and genetic mechanisms. Accumulating evidence suggests exposure to polychlorinated dibenzo-*p*-dioxins and similar compounds may increases risk for NAFLD development. These environmentally persistent dioxin-like compounds bind and activate the aryl hydrocarbon receptor (AhR), a transcription factor that regulates intestinal homeostasis, xenobiotic and central metabolism. In a AhR-dependent manner, mice orally gavaged with 2,3,7,8-tetrachlorodibenzo-*p*-dioxin (TCDD) exhibit steatosis progressing to steatohepatitis with fibrosis akin to NAFLD progression. NAFLD and hepatocellular carcinoma (HCC) is also closely correlated with dysregulation of central metabolism e.g., hepatic one carbon metabolism (OCM), and gut dysbiosis contributing to NAFLD progression and worsening prognosis. This report investigates mechanisms involved in the dysregulation of the gut microbiome and OCM associated pathways relevant to NAFLD progression through comparisons of molecular analyses of TCDD-treated mice to human NAFLD and HCC.

OCM describes the biosynthesis, homeostasis, and utilization of the cell's main methyl donor, *S*-adenosylmethionine (SAM) including high flux anabolic biosynthesis of polyamines, phosphatidylcholine and creatine. In later stages of NAFLD, OCM is dysregulated with altered OCM gene expression as well as SAM and *S*-adenosylhomocysteine (SAH) levels. To assess TCDD-elicited effects on OCM, mice were orally gavaged with TCDD every 4 days for 28 days. Serum and livers collected at early (8 days) and late (28 days) time points were subjected to metabolomic analyses with integration of chromatin immunoprecipitation sequencing (ChIP-seq), gene expression and protein levels. Results from these studies suggest that AhR-mediated

repression of OCM required prolonged repeated TCDD-treatment caused by indirect effects elicited by AhR activation e.g., oxidative stress.

Gut dysbiosis with disrupted enterohepatic bile acid metabolism is commonly associated with NAFLD and recapitulated in TCDD-treated mice. Similar to NAFLD, TCDD also increases systematic levels of secondary bile acids. These microbial transformed secondary bile acids are involved in modulation of host bile acid signaling pathways relevant to NAFLD. To investigate the effects of TCDD on the gut microbiota, the cecum contents of TCDD-treated mice were subjected to shotgun metagenomic sequencing. Taxonomic analysis identified dose-dependent increases in Lactobacillus species, notably *Lactobacillus reuteri*. Top enriched species were associated with increased abundances of bile salt hydrolase sequences, responsible for the initial deconjugation reaction in secondary bile acid metabolism. *L. reuteri* levels were also attributed to enrichment of microbial mevalonate-dependent isopentenyl diphosphate (IPP) biosynthesis genes, a pathway that was also elevated in cirrhosis patients. These results extend the role of Lactobacilli in the AhR/intestinal axis and NAFLD progression as well as highlight the similarities between TCDD-elicited phenotypes in mice to human NAFLD. Collectively, these studies evaluated TCDD-elicited mechanisms involved in disruptions in host and microbial metabolism, highlighting the AhR's role in NAFLD progression.

To my wife, I couldn’t have done it without you.

ACKNOWLEDGEMENTS

To my lovely wife, you are my better half. Your patience and understanding during my PhD work was vast (those cute gremlins will test you to your core!). You are the best mother as well as the smartest/kindest person I know. I have always been and will forever be in your debt.

To my family, thank you for your encouragement and support. Your love and help along this long journey also helped make this possible. Sarah thank you for visiting and helping, you are the most gracious and helpful guest. To my parents and sisters, your support and love helped me through difficult times and your help with the kids and house were immense. To Bob and Jean, your help and support, especially with the gremlins, made it possible for me to finish on time. It was 12 years of grad school and 2 kids. None of that would have been possible without your help.

To my advisor, Dr. Zacharewski, I would like to thank you for guidance through my development as a researcher. Your considerations and discussions regarding this research were not only immensely helpful, but generous and thoughtful.

To my committee Dr. Jones, Dr. Manning, Dr. Mansfield, and Dr. Vieille, thank you for your guidance in the development of my dissertation project. Your time and expertise pushed me to critically think about my project and was crucial for my develop during my academic scientific career.

To Rance, Kelly, Claire, Karina, Gio and Warren. I also could have not done this work without all of your help including your mentorship, knowledge and conducting the experiments. You are all talented and brilliant researchers and it was an honor to work with you.

TABLE OF CONTENTS

LIST OF FIGURES

KEY TO ABBREVIATIONS

3α/β-HDSH	3-α/β-hydroxysteroid dehydrogenase
5-MTHF	5-methyltetrhydrofolate
7α-HDSH	7α-hydroxysteroid dehydrogenase
AHCY	adenosylhomocysteinase
AhR	aryl hydrocarbon receptor
ALT	alanine transaminase
ArAT	aromatic amino acid aminotransferase
ARNT	aryl hydrocarbon nuclear translocator
AST	aspartate transaminase
BA	bile acid
BAAT	bile acid-CoA:amino acid N-acyltransferase
BHMT	betaine homocysteine N-methyltransferase
BMDL	benchmark dose lower confidence limit
BSH	bile salt hydrolase
CA	cholic acid
CBS	cystathionine β-synthase
CCl_4	carbon tetrachloride
CDCA	chenodeoxycholic acid
DCA	deoxycholic acid
DHA	docosahexaenoic acid
DRE	dioxin response element
FGF	fibroblast growth factor
FXR	farnesoid x receptor
GLP-1	glucagon-like peptide-1
GNMT	glycine N-methyltransferase
GPBAR1	G protein-coupled bile acid receptor 1

HCC	hepatocellular carcinoma
HFD	high fat diet
IAA	indole-3-acetate
IAId	indole-3-aldehyde
ILC3	group 3 innate lymphoid cells
IPP	isopentenyl diphosphate
IPyA	indol-3-pyruvic acid
LCA	lithocholic acid
MCD	methionine and choline deficient
NASH	non-alcoholic steatohepatitis
OCM	one carbon metabolism
PA	polyamine
PC	phosphatidylcholine
PCB	polychlorinated biphenyl
PCDD	polychlorinated dibenzo-p-dioxin
PCDF	polychlorinated dibenzofuran
pDRE	putative dioxin response element
PEMT	phosphatidylethanolamine N-methyltransferase
RORγt	retinoid-related orphan receptor γt
RXR	retinoid X receptor
SAH	*S*-adenosylhomocysteine
SAM	*S*-adenosylmethionine
SHP	small heterodimer partner
T2D	type 2 diabetes
TCDD	2,3,7,8-tetracholordibenzo-p-dioxin
TCDF	2,3,7,8-tetrachlorodibenzofuran
VLDL	very low density lipoprotein
β-MCA	beta-muricholic acid

CHAPTER 1: LITERATURE REVIEW

INTRODUCTION

Prevalence of non-alcoholic fatty liver disease (NAFLD) among adults is estimated at 25% of the global population and is second leading cause for liver transplants among adults in the United States [1]. NAFLD is defined as a range of pathologies from hepatic steatosis in early development progressing towards immune cell infiltration and inflammation, a.k.a. non-alcoholic steatohepatitis (NASH). NASH is found in ~6-8% of US adults or 25% of those with NAFLD[2]. A multiple-hit hypothesis proposes several factors contribute to the complex etiology of NALFD progression including associations with metabolic diseases and gut dysbiosis [3,4]. Emerging evidence suggests that environmental contaminants may play an underappreciated role in NAFLD progression [5–8] and gut microbiome homeostasis [9–14]. Particularly, 2,3,7,8-tetrachlorodibenzo-p-dioxin (TCDD), a persistent environmental organochlorine contaminant, induces a NAFLD-like phenotype in mice including gut dysbiosis with steatosis progressing to steatohepatitis with fibrosis paralleling NAFLD development in humans [11,13,15,16].

NON-ALCOHOLIC FATTY LIVER DISEASE EPIDEMIOLGY

NAFLD increases the risk to develop other metabolic disorders such as obesity, type 2 diabetes (T2D), and coronary heart disease. Globally, 55.5% (95% CI 47.3–63.7) of T2D patients are also afflicted with NAFLD [1]. In the US, NAFLD is present in ~25% of normal weight, ~67% of overweight, and ~94% of obese patients [17]. In a 16 year prospective study of >900,000 Americans, hepatocellular carcinoma in obese individuals was the greatest relative risk of 4.52 among diagnosed cancers [18]. Patients with NASH also have increased risk for cardiovascular events and atherosclerosis independent of other risk factors including metabolic disorders [19]. These co-occurring disorders have an underlying metabolic syndrome displaying dyslipidemia, hyperglycemia, hypertension, and visceral obesity with increased risk for progression of NAFLD to NASH and more severe liver diseases including cirrhosis and hepatocellular carcinoma [20].

NAFLD development and progression to NASH is not fully understood. Steatosis itself is benign and reversible through diet and drug interventions [21]. Steatosis can occur by excess energy intake with western diets high in sugar and carbohydrates [22]. While obesity highly correlates with NAFLD, obesity is not necessarily the cause and NAFLD can occur in non-obese individuals. Dysregulation of both adipose and/or hepatic lipid metabolism are factors that may contribute to NAFLD development [15,23,24]. Increased insulin resistance coupled with dysregulation of lipid metabolism are also drivers of steatosis. Altered lipid metabolism can result in a combination of increased adipose free fatty acid fluxes, reduced hepatic secretion of very low density lipoprotein (VLDL), decreased fatty acid beta-oxidation and/or increased hepatic lipogenesis [25,26].

Metabolic disorders including T2D and obesity increase the risk for progression to NASH with inflammation and fibrosis, however, the underlying mechanism is less understood. Increased hepatic inflammation through an inflammation-induced profibrogenic environment is mediated though activation of hepatic stellate cells (HSCs), recruited macrophages, resident macrophages (Kupffer cells), neutrophils and toll-like receptors (TLRs) [22,27]. Microbial components and hepatocyte damage can also create a proinflammatory environment. TLR4 activation is increased by pathogen associated molecular patterns (PAMPs), notably lipopolysaccharide, in NAFLD mouse models whereas TLR4 knockout models exhibit reduced steatosis, inflammation, and fibrosis [22]. TLR9 activation by damage associated molecular patterns (DAMPs) and TLR2 activation by bacterial and fungal components have also been implicated in inflammation and fibrosis [22]. In the early stages of liver damage, bone marrow-derived monocytes migrate to the liver where they can differentiate into pro-inflammatory M1 macrophages producing inflammatory cytokines i.e, TNF-α, interleukin (IL)-6 and IL-1, whereas resident Kupfer cells are predominantly the anti-inflammatory M2 phenotype. Both recruited M1 macrophages and Kupfer cells produce transforming growth factor beta 1 (TGF-β1), a profibrotic cytokine that induces the differentiation of quiescent stellate cells towards myofibroblasts responsible for ~80% of fibrillar collagen I

production in fibrotic livers [26,27]. To summarize, the development of NAFLD and progression to NASH and fibrosis is complex, involves activation of a diverse set of hepatic and immune cells and signaling pathways associated with inflammation, liver damage and gut dysbiosis.

DIOXIN AND DIOXIN-LIKE EXPOSURE IN HUMANS

While the underlying causes of metabolic syndrome are not fully understood, diet, sedentary life style, genetics and environmental contaminants are thought to contribute to the development of metabolic syndrome [5,28]. Persistent environmental pollutants including TCDD, as well as related polychlorinated dibenzo-*p*-dioxins (PCDDs), dibenzofurans (PCDFs), and coplanar polychlorinated biphenyls (PCBs) are ligands for the AhR and have been implicated in contributing to liver disease and NAFLD development [5,15,29,30]. Sources of environmental PCDDs originate from industrial processes. In the past, chlorine bleaching of pulp and production of chlorinated phenoxy acid herbicides including Agent Orange produced unwanted side products including PCDDs, however technology advancements and regulatory oversight have vastly reduced these sources from the early 1980s onward. Other sources of coplanar PCBs, PCDD and PCDF contamination include incomplete industrial combustion processes i.e., inefficient incinerator plants, local burning of solid fuels, and wild fires [31–33]. PCBs and PCDFs have long environmental half-lives with estimates of ~100 years for PCDDs and PCDFs in sediment and soil, while coplanar PCBs are ~10 years [34]. Human exposure to PCDDs and PCDFs occurs primarily through food from bioaccumulation in fish and fatty food products such as milk [35]. Occupation exposure related to combustion also exhibit elevated serum PCDD levels, such as fire fighters [36]. Levels of PCDD/Fs are detectable in the general population but have been declining over the past 20 years due to declining environmental exposure. However, PCDDs and PCBs are regularly detected in almost all adults, increase with age, and are higher among individuals with diets consisting of seafood [5,35,37]. In humans, half-lives of PCDD and PCDF congeners are estimated to be 6-10 years and 2-10 years, respectively [38]. Due to the long half-

lives in both the environment and humans, these persistent organic pollutants are often referred to as “forever chemicals”. PCBs and PCDD/Fs have been associated with liver and metabolic diseases. Positive correlations between serum alanine transaminase (ALT), a biomarker of liver injury, and PCB levels are in agreement across multiple studies [5,6,8,39]. Morbidly obese individuals also exhibit positive correlations between serum PCB levels and diabetes [6]. Bariatric patients have increased PCB levels associated with fat loss. Further, Human serum concentrations of PCBs have also been shown to reach AhR bioactive levels in sera of elderly patients [40].

THE AHR’S MECHANSIMS OF ACTION

Almost all if not all of TCDD’s toxicity is mediated through activation of the aryl hydrocarbon receptor, a basic helix-loop-helix/Per-Arnt-Sim transcription factor [41]. Upon ligand binding in the cytosol, the AhR translocates to the nucleus where it disassociates with its chaperone protein and dimerizes with the aryl hydrocarbon nuclear translocator (ARNT) [42]. The ligand-bound AhR/ARNT complex then acts as a transcription factor, binding to dioxin response elements (DREs) located upstream of target genes (Figure 1) [31,42]. The AhR is ubiquitously expressed in most tissues and regulates a wide diversity of gene networks from central metabolism, early development, immune responses, and tumorigenesis [43]. The better studied and understood role of the AhR is through direct regulation of host xenobiotic metabolizing enzymes for detoxification of hydrocarbons in the liver and lungs e.g., several cytochrome P450 cytochrome enzymes, UDP glucuronosyltransferase family 1 enzymes and glutathione-*S*-transferases [44]. However, the physiological role of the AhR and its true biological ligand are less clear. In the liver, the AhR has been implicated in regulation of energy homeostasis regarding circadian regulation [45], glucose metabolism [46] and lipid metabolism [15,24].

A diverse set of natural ligands from host, bacterial and dietary sources have been shown to bind and activate the AhR. Several host pathways produce intermediate metabolites with AhR

activity including tryptophan metabolism e.g., kynurenine and tryptamine, and heme metabolism e.g., bilirubin[47]. In the diet, Indole-3-carbinol is found in cruciferous vegetables and is metabolized into active AhR ligands [47]. Intestinal bacteria have also been shown to produce indole derivatives through catabolism of tryptophan including indole-3-aldehyde (IAld), indole-3-acetate (IAA), indol-3-pyruvic acid (IPyA), and indole-3-propionate[47]. An aromatic amino acid aminotransferase (ArAT) catalyzes the conversion of tryptophan to IPyA and the main route of IAA production in Lactobacillus and Bifidobacterium species utilizes the IPyA route [48]. *Lactobacillus reuteri* also uses the IPyA route and requires an ArAT, for IAld production, an endogenous AhR ligand that promotes intestinal IL-22 production [49].

THE ROLE OF THE AHR IN GUT HOMEOSTASIS

The AhR is also crucial for gut microbiome homeostasis and development. Mouse AhR knockout models exhibit gut dysbiosis, bacterial overgrowth [9,50] and increased susceptibility to pathogen infection [50]. In TH17 and group 3 innate lymphoid cells (ILC3), the AhR directly upregulates IL-22, a cytokine that promotes endothelial production of the antimicrobial peptide REG3γ [49,51,52]. IILC3 are defined by the expression of the retinoid-related orphan receptor γt (RORγt). RORγt interactions with the AhR are necessary for recruitment to dioxin response elements in the promoter of *Il22* [53]. Barrier maintenance through intestinal AhR-mediated IL-22 production is evident in $AhR^{-/-}$ mice which exhibit endothelial overgrowth of segmented filamentous bacteria [9,54]. Treatment with 2,3,7,8-tetrachlorodibenzofuran (TCDF), a PCDF AhR ligand, in wild type mice demonstrates almost complete lack of segmented filamentous bacteria endothelial growth [9]. IAld produced by *Lactobacillus reuteri* also upregulates this AhR-dependent pathway *in vivo,* preventing pathogen infection [49]. While AhR activation can impact the gut microbiome, the effects are preferentially targeted towards select phyla i.e., *Tenericutes*, *Proteobacteria*, *Verrucomicrobia* and *Actinobacteria*, with a trending decrease in *Firmicutes/Bacteroidetes* ratio in $AhR^{-/-}$ mice [54].

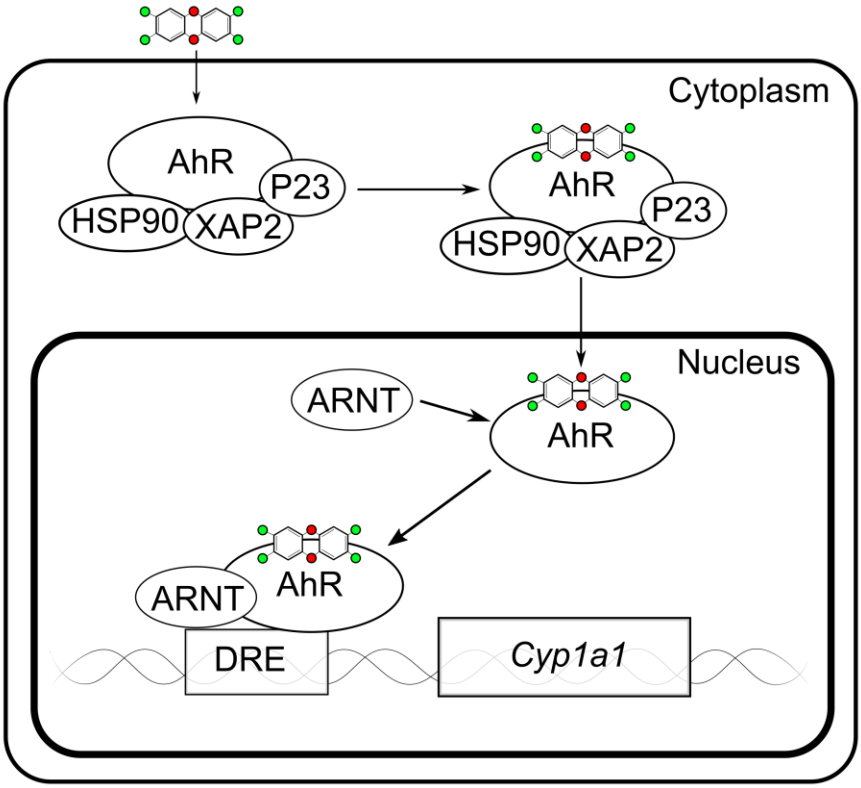

FIGURE 1. THE CANONICAL AHR MECHANISM OF ACTION

After entering the cytosol, TCDD binds to the AhR, translocates to the nucleus, and disassociates with chaperone proteins. In the nucleus, the ligand bound AhR forms a heterodimer with ARNT, promoting binding to dioxin response elements (DRE) located throughout the genome and regulating gene expression. *Abbreviations: Aryl hydrocarbon receptor nuclear translocator(ARNT), heat shock protein 90 (HSP90), Hepatitis B virus X protein associated protein 2 (XAP2), P23 (aka prostaglandin E synthase 3[PTGes3]).*

Bacterial community shifts are not consistent among treatment with different AhR ligands, including both endogenous/exogenous sources and study designs. TCDD exposure increases the Firmicutes/Bacteroidetes ratio with repeated exposure over longer periods of time (28 days to 26 weeks) whereas repeated exposure over shorter periods with TCDF (5 days) exhibited decreases in this ratio [9,12,16]. Interestingly, increases in total bile acid levels along with primary (host produced) and secondary (microbially modified) bile acid levels were consistent between TCDD and TCDF exposures [9,11].

HOST BILE ACID METABOLISM AND NAFLD

Bile acids (BAs) are amphipathic detergents that aid in the absorption of lipids and fat-soluble vitamins in the intestine. Primary BA biosynthesis occurs mainly in the liver through the classical *de novo* biosynthesis pathway (Figure 2), the liver being the only organ expressing all 14 enzymes necessary for *de novo* biosynthesis [55]. BAs also undergo enterohepatic circulation consisting of transport between the liver, gallbladder, and intestinal tract. BAs are secreted from hepatocytes into bile ducts, emptying in the gallbladder, and released into the duodenum during meal time. Almost all BAs entering intestinal lumen are actively transported in the distal small intestine back into portal circulation, whereas ~5% is lost to feces excretion [55]. Remaining bile acids reaching the colon can be modified by the gut microbiota into secondary bile acids e.g., deoxycholic acid (DCA) and lithocholic acid (LCA) (Figure 2). DCA can passively be reabsorbed in the colon, while LCA is mostly excreted in the feces [56].

BAs are synthesized from cholesterol in the liver. The two primary bile acids in humans are cholic acid (CA) and chenodeoxycholic acid (CDCA). In mice, CDCA is further metabolized to beta muricholic acid (β-MCA) making the majority of murine primary bile acids CA and β-MCA [56]. The first and rate limiting step in BA synthesis requires the cholesterol 7α -hydroxylase (CYP7A1). Sterol 12α-hydroxylase (CYP8B1) and sterol 27α -hydroxylase (CYP27A1) produce CA and CDCA, respectively (Figure 2). Bile acids are also conjugated to glycine or taurine

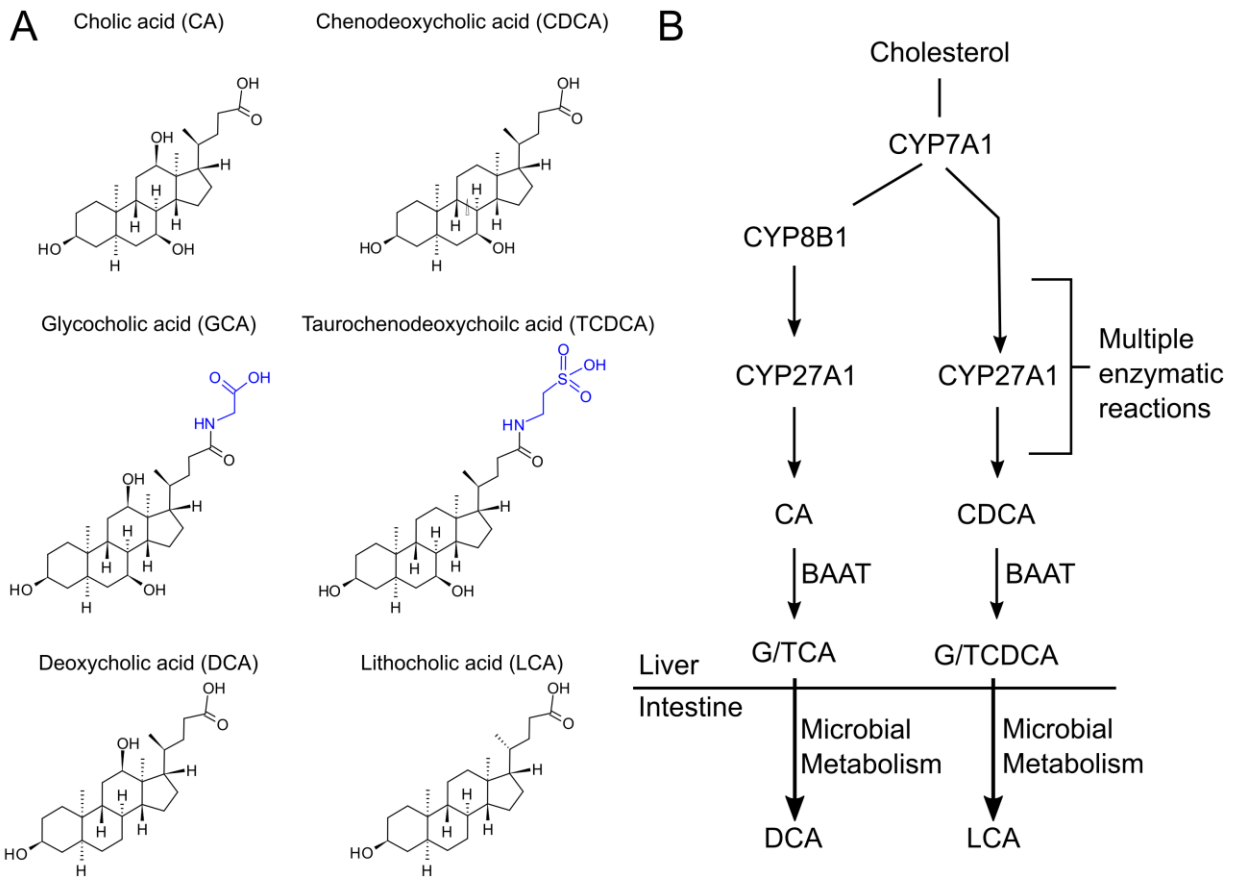

FIGURE 2. BILE ACID STRUCTURES AND BIOSYNTHESIS ROUTES

(A) Structures of predominant primary (cholic acid [CA] and chenodeoxycholic acid[CDCA]) and secondary bile acids (deoxycholic acid[DCA] and lithocholic acid[LCA]) in humans. **(B)** Summary of bile acid biosynthesis in humans including rate limiting enzyme, CYP7A1, and the bifurcation biosynthesis pathways of CA and CDCA, conjugation by BAAT to form glycine/taurine conjugated BAs (G/TCA, G/TCDCA) and microbial transformed secondary bile acids DCA and LCA. *Abbreviations: Cytochrome P450 Family 7 Subfamily A Member 1 (CYP7A1), Cytochrome P450 Family 8 Subfamily B Member 1 (CYP8B1), Cytochrome P450 Family 27 Subfamily A Member 1 (CYP27A1), Bile Acid-CoA:Amino Acid N-Acyltransferase (BAAT), glyco/taurocholic acid (G/TCA), glyco/taurochenodeoxycholic acid (G/TCDCA)*

mediated by bile acid-CoA:amino acid N-acyltransferase (BAAT). Human BA pools consist of glycine- and taurine-conjugated bile acids while murine BA pools are predominantly taurine-conjugated [56]. Regulation of BA enterohepatic circulation and *de novo* biosynthesis is partially mediated through the farnesoid x receptor (FXR), a nuclear hormone receptor highly expressed in the liver and small intestine [56]. BAs can bind the FXR, promoting heterodimer formation with the retinoid X receptor (RXR) resulting in transcriptional repression of BA metabolism through several alternate mechanisms in the small intestine and liver. The FXR/RXR heterodimer regulates *Cyp7a1* expression through FXR activation in the small intestine which leads to direct upregulation of fibroblast growth factor 19 (FGF19 in humans, FGF15 in mice) in ileal enterocytes. Intestinal FGF15/19 released into portal circulation binds to the FGF receptor 4 (FGFR4) located on sinusoidal membrane of hepatocytes resulting in reduced *Cyp7a1* expression (Figure 3) [55]. Another feedback repression mechanism involves another FXR target gene, the small heterodimer partner (*shp* aka *nrob2*). SHP is a nuclear receptor transcription factor that lacks a DNA-binding domain and forms non-functional heterodimers with a wide array of nuclear receptors e.g., the liver receptor homolog-1 (LRH-1), hepatocyte nuclear factor 4 alpha (HNF4-α), and the peroxisome proliferator-activated receptor gamma (PPARγ). The activated LRH-1 can bind to response elements upstream of *Cyp8B1* and promote its expression. In hepatocytes, activation of FXR leads to increased SHP levels and binding to LRH-1, inhibiting the expression of *Cyp8b1* [56]. Hepatic repression of *Cyp8b1* requires both FXR and SHP in the liver and is not dependent on intestinal signaling (Figure 3) [57].

Hepatic and serum total bile acid levels are increased in NAFLD patients [58–63]. Increased BA levels also positively correlate with disease progression from steatosis to steatohepatitis [61]. It is hypothesized that increased BA metabolism maintains lipid and cholesterol homeostasis by diverting cholesterol towards BA biosynthesis and promoting cholesterol excretion in bile. Cyp7a1$^{-/-}$ mice exhibit increased lipid accumulation, hepatic inflammation and cholesterol levels when challenged with a NAFLD-inducing methionine and

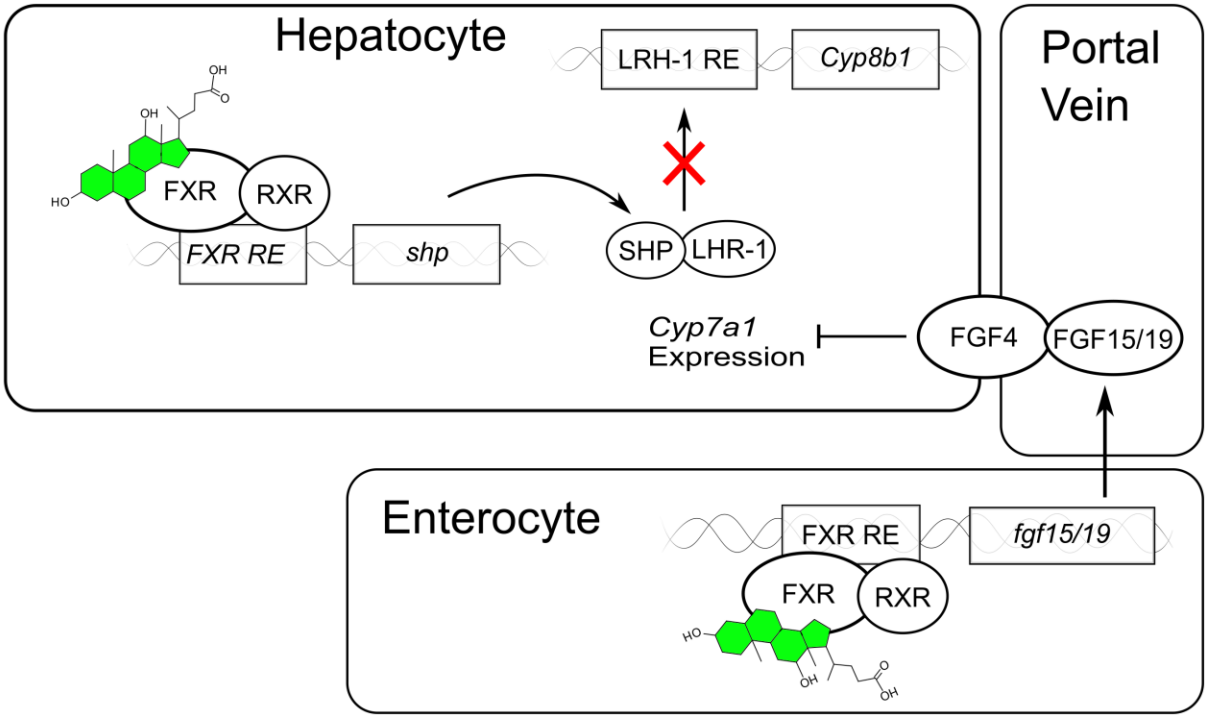

FIGURE 3. BA ACTIVATED FXR REGULATION OF BILE ACID BIOSYNTHESIS

Cyp7A1 and Cyp8B1 are the rate limiting steps in CA and CDCA biosynthesis, respectively. Intestinal knockouts in mice suggest FXR directly upregulates intestinal *Fgf15,* FGF15 secretion and FGF4 activation in hepatocytes, causing the inhibition of hepatic *Cyp7a1* expression. Alternatively, hepatic FXR activation directly upregulates *shp* expression. SHP forms non-functional heterodimers with the LRH-1, inhibiting LRH-1 mediated *Cyp8b1* expression. Ovals represent proteins. DNA response elements (RE) for respective transcription factors and upstream gene targets are also depicted. *Abbreviations: farnesoid x receptor (FXR), fibroblast growth factor 15/19 (Fgf15/19) retinoid x receptor (RXR), liver receptor homolog-1 (LRH-1)*

choline deficient (MCD) diet, while overexpression of *Cyp7a1* ameliorates the MCD effects [62]. Increased bile acid levels are also associated with activation of membrane g-protein coupled bile acid receptor 1 (GPBAR1, a.k.a. TGR5) signaling pathways, a membrane receptor involved in glucose homeostasis [65]. GPBAR1 activation promotes glucagon-like peptide-1 (GLP-1) production and secretion in L-cells, an enteroendocrine cell type located in the small intestine and large intestine [65]. Increase in systemic GLP-1 levels result in insulin release and decreases circulating glucose [66]. In addition to insulin regulation, GPBAR1 activation in macrophages promotes polarization from M1 pro-inflammatory phenotype towards an anti-inflammatory M2 phenotype [67]. The secondary BAs LCA followed by DCA are the most potent BA ligands for GPBAR1 [68]. Due to the beneficial metabolic impacts FXR and GPBAR1 mediated regulation of lipid/cholesterol levels, glucose homeostasis and inflammation, several pharmaceutical agonists targeting FXR and GPBAR1 signaling are in development for treatment of diabetes and NAFLD, some currently under human clinical trials [69].

MICROBIAL METABOLISM OF BILE ACIDS

Conjugated primary BAs can also be metabolized by the gut microbiome, producing a complex pool of secondary BAs that affect both host metabolism and the gut microbiome. The gateway reaction for microbial BA metabolism is deconjugation of the amino acid head groups (glycine or taurine) by bile salt hydrolases (BSHs) [70]. Deconjugated primary BAs can be further modified by oxidation, dehydroxylation, and epimerization reactions acting on hydroxyl groups of the core sterol in BAs [70]. DCA and LCA are produced from the 7α-dehydroxylation of CA or CDCA, respectively (Figure 4). Only a small subset of taxa from the Clostridium subcluster XIVa possess the *Bai* operon that codes for a multi-step enzymatic pathway responsible for the 7α/β-dehydroxylation [70]. Other BA metabolism enzymes include the 7α-hydroxysteroid dehydrogenase (7α-HDSH) that oxidizes the 7α hydroxyl group [71] and sequential oxidation/reduction reactions by separate 3-α/β-hydroxysteroid dehydrogenases (3α/β-HDSHs)

that epimerize the 3β hydroxy group of DCA, forming iso-DCA (Figure 4) [72]. The secondary bile acids produced by these microbial modification (7-keto-DCA, 3-keto-DCA and iso-DCA and iso-LCA) are also elevated in the plasma of NAFLD patients (Figure 4) [61]. BSHs are present in all major phyla in the gut microbiome with Actinobacteria, Firmicutes and Bacteroidetes phyla encompass the majority of BSH activity [73]. Isolates from human stool samples with BSH activity suggest Bacteroidetes have substrate specificity towards taurine-conjugated BAs, whereas Firmicutes and Actinobacteria taxa are able to deconjugate taurine- and glycine-conjugated BAs [73]. Deconjugation occurs throughout the entire intestinal tract, from small intestine to the colon, however, the greatest activity is reported in the large intestine of mice [74,75]. Alternatively 7α-dehydroxylation activity mainly occurs in the large intestine [75].

BSH activity may offer protective benefits against the detergent qualities of conjugated BAs. *In vitro* experiments suggest that BSH activity does impart bile tolerance. Knocking out *bsh* causes growth inhibition in the presence of bile acids in several bacterial species [73,76,77]. It is still not yet fully understood how BSH imparts its beneficial effects as deconjugated BAs exhibit higher antimicrobial activity versus conjugated BAs [77–79]. BSH activity may offer protection from bile acids in low pH environments like the proximal small intestine [76,80]. However, BSH's role *in vivo* is also not clear, possibly species and even strain specific. Work by Foley and colleagues have reported improved *in vivo* colonization of Δ*bsh L. gasseri* mutants compared to WT [81].

MICROBIAL BILE ACID METABOLISM AND NAFLD

Unconjugated primary BAs have higher hydrophobicity and lower solubility than conjugated BAs. BA and cholesterol precipitation following deconjugation is hypothesized to reduce re-absorption and increase BA and cholesterol excretion [82]. This relationship between BSH activity and lowering cholesterol effects has also been observed with probiotic supplementation of Lactobacillus species in humans and rodents [83–86]. More recently, it was

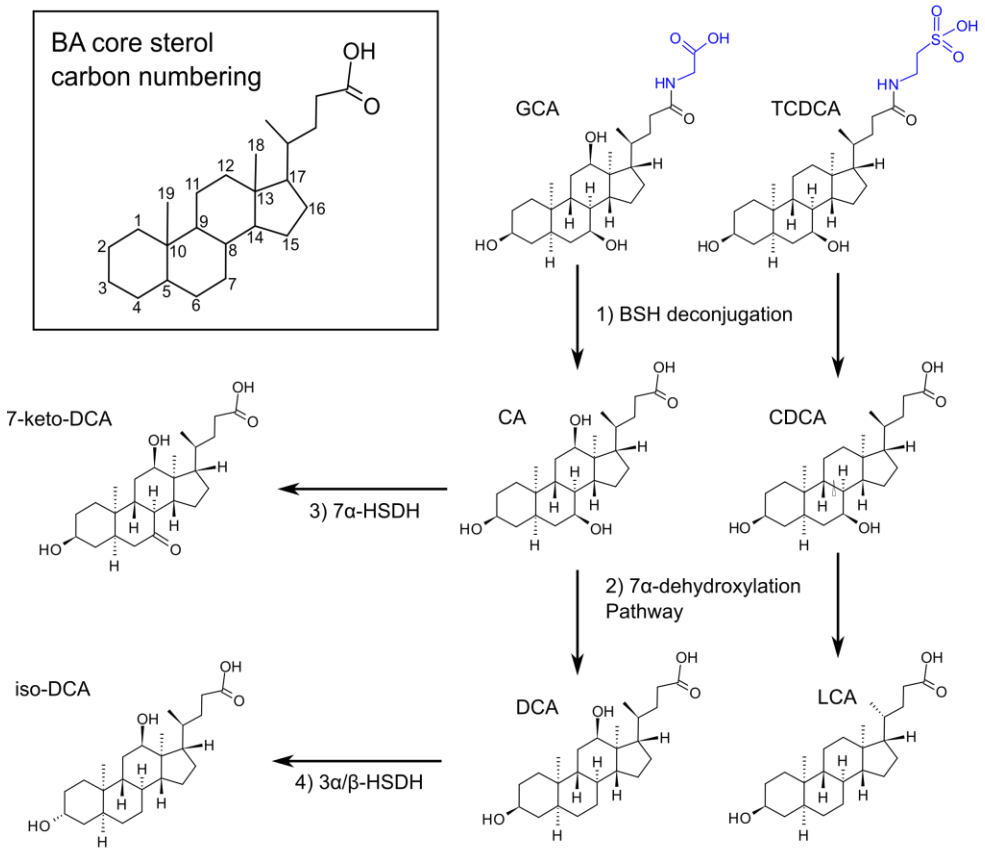

FIGURE 4. MICROBIAL METABOLISM OF SECONDARY BILE ACIDS.

1) Primary BAs are deconjugated by bacteria possessing BSH. Unconjugated primary BAs can be further modified by other BA metabolizing bacteria through a diverse set of BA modifications. Pictured is the 2) 7α-dehydroxylation pathway that modifies CA and CDCA to DCA and LCA, respectively. Other BA modifications pictured are 3) oxidation reactions by 7α-hydroxysteroid dehydrogenases (7α-HSDH) or 4) epimerization by consecutive 3α- and 3β- hydroxysteroid dehydrogenases (3α- & 3β-HSDH) reactions. *Abbreviations: 7-ketodeoxcycholic acid (7-keto-DCA), cholic acid (CA), chenodeoxycholic acid (CDCA), deoxycholic acid(DCA), glycocholic acid (GCA), isodeoxycholic acid (iso-DCA), , lithocholic acid (LCA), and taurochenodeoxycholic acid (TCDCA).*

shown that BSH's cholesterol lowering effects may also be mediated through FXR signaling both in the intestine and liver. Zhu and colleagues recently demonstrated BSH's role in hepatic and intestinal FXR activation. They provide evidence suggesting BSH activity with substrate preferences towards taurocholic acid over tauro-β-muricholic acid increased hepatic FXR signaling. BSH activity was associated with decreased intestinal FXR signaling concurrent with shifts in conjugated/unconjugated BAs [87]. When challenged with a high fat diet, Δbsh *Lactobacillus johnsonii* mutants lacked cholesterol lowering effects. complemented Δbsh *L. johnsonii* mutants containing a plasmid with high activity *bsh* where able to: 1) lower cholesterol levels, 2) decrease intestinal ileal *fxr* expression and 3) increase hepatic *fxr* expression. The FXR target gene *fgf15* was decreased in the intestine by the complemented *bsh* mutant versus the Δbsh mutant. Reduced intestinal FXR signaling resulted in increased hepatic *Cyp7a1* expression. Interestingly, the gut microbiomes of mice fed high fat diets supplemented with the complemented *bsh* mutant demonstrated increased biodiversity compared to Δbsh mutant supplemented mice. Further, the complemented *bsh* mutant increased other *bsh* containing species and supplemented mice microbiomes more resembled gut microbiomes of mice fed normal diets [87].

Rats fed a CA-enriched diet also have higher total BA levels and increased secondary BAs i.e., DCA, accompanied by increased relative abundance of Firmicutes bacteria. This suggests elevated BAs promote enrichment of BA tolerant/metabolizing species and/or increases microbial BA metabolism. DCA is the most abundant BA in feces [88] with high antimicrobial activity under biologically relevant concentrations and conditions [78]. DCA is also commonly increased aside primary BAs in NASH patients [59–61]. Further, the microbial secondary BA metabolism gene abundances of *bsh* and *baiCD* (the rate limiting enzyme in the 7α-dehydroxylation pathway), are also reported to be increased in NASH patients [89]. Alternatively, DCA levels are decreased concurrent with gene abundance of *bsh*, *baiCD* and DCA levels in non-obese patients with fibrosis [90]. These differences may be due to many factors including diet.

For example, levels of *baiCD* genes and fecal DCA concentrations are lower in human subjects fed a high fibre diet compared to a high fat diet [91].

NAFLD ANIMAL MODELS

Due to the complex pathophysiological mechanism involving multiple cell types and organs in the development and progression of NAFLD, *in vivo* models are still the gold standard for studying systemic changes in NAFLD progression. Several genetic, diet-based, and chemical-induced models mimic the disease progression in humans [92–94]. However, no model fully recapitulates the progression of steatosis to steatohepatitis with fibrosis and insulin resistance observed in humans. Many models require multiple “hits” to induce steatohepatitis and fibrosis. For example, the *ob/ob* genetic mouse model carries a mutation in the gene coding for leptin. Leptin deficiency in *ob/ob* mice results in spontaneous obesity with a diabetic phenotype. However, *ob/ob* mice also require a second hit to induce steatohepatitis e.g., administration of a high fat diet (HFD) or endotoxins [93]. Furthermore, *ob/ob* mice are resistant to fibrosis even when challenged with carbon tetrachloride (CCl_4), a carcinogen that induces oxidative stress, liver inflammation and fibrosis in wild type mice [92]. Leptin is necessary for production of TNF-α and TGFβ1 signaling, cytokines that evoke inflammation and collagen deposition. However, fibrosis can be induced in *ob/ob* mice following administration of leptin [92].

Several animal models for NAFLD use specialized diets. HFDs induce steatosis, hyperlipidemia, and insulin resistance after 10-12 weeks. At 34-36 weeks, elevated serum levels of ALT and aspartate transaminase (AST) levels are also observed, biomarkers of liver damage. The model fails to induce significant fibrosis even after 36-50 weeks of exposure [94]. The most common dietary model that does not require multiple hits to induce steatohepatitis is a methionine/choline deficient (MCD) diet. Mice fed a MCD diet develop steatosis rapidly with elevated ALT and AST levels within 2-8 weeks. Weight gain and insulin resistance are not observed like traditional NAFLD, rather mice have significant weight loss (~35%) after 4 weeks

[93]. MCD fed mice also demonstrate decreased VLDL secretion, and disrupted phosphatidylcholine (PC) biosynthesis [95]. Isolated hepatocytes from rats fed a choline deficient diet display severe inhibition of VLDL secretion that can be rescued by the addition of choline or methionine [96].

Many models have used other chemical exposures that target specific metabolic aspects of NAFLD. CCl_4 induces immune cell infiltration, microsteatosis, and dose-dependent increases in collagen deposition [94]. However, CCl_4 administration is not traditionally viewed as model that recapitulates NAFLD, rather often used as a second hit that induces steatohepatitis in dietary and genetic models. Streptozotocin is also used as model to study NAFLD and diabetes. Neonatal exposure induces a diabetic phenotype, accelerated steatosis with immune cell infiltration (6 weeks), fibrosis (8 weeks) and increased instances of hepatocellular carcinoma (after 20 weeks) when combined with a HFD [97].

One of the few models that recapitulates NAFLD development requiring no second hit is chemical exposure to TCDD in rodents. A single bolus dose (30 µg/kg TCDD) in mice induces hepatic lipid accumulation, increased free fatty acid levels, immune cell recruitment, and increased ALT levels [98,99]. Increased hepatic cholesterol levels and decreased serum levels also suggest increased hepatic cholesterol uptake and/or disrupted cholesterol metabolism [15,98,100]. Excess hepatic cholesterol is also evidenced by increased hepatic cholesterol esters partially mediated through reduced VLDL secretion [15]. Further, *in vitro* TCDD exposure in human hepatocytes and TCDD-exposed mice display increased hepatic free fatty acid import and accumulation with decreased gene expression and proteins levels associated with VLDL assembly [15,98,100]. Prolonged and repeated TCDD treatment in mice further progresses to steatohepatitis with fibrosis [30]. Like NAFLD, TCDD exposure in male mice also increased total serum BA levels concurrent with increased secondary BAs e.g., DCA and LCA, and conjugated secondary bile acids in the liver and feces, notably TLCA [11]. Mice treated for shorter periods (every day for 4 days) at similar levels demonstrate decreased serum secondary BA levels [101].

However, both short and prolonged exposure exhibited comparable hepatic repression of *Cyp7a1*, *Cyp8b1* and *Fgf4* [11,101]. Increased secondary bile acid levels after prolonged exposures suggest AhR mediated changes in gut environment may enrich for BA metabolizing species only after prolonged disruption of BA metabolism and may potentially correlate with progression to steatohepatitis and/or fibrosis.

ONE CARBON METABOLISM

One carbon metabolism (OCM) encompasses the biosynthesis, homeostasis, and utilization of the cell's main methyl donor, *S*-adenosylmethionine (SAM). Methyltransferases utilize SAM in a diverse set of reactions that participate in DNA/histone epigenetic regulation and metabolite biosynthesis [102]. Many NAFLD patients have disrupted OCM gene expression and metabolites correlated with NAFLD development and progression [103–107, 108-110]. In addition, several OCM gene knockout models in rodents cause a NAFLD phenotype with altered OCM metabolites with the spontaneous progression of NAFLD to NASH and increased incidence of HCC [117, 120-124]. SAM is also involved in several high flux hepatic anabolic metabolic pathways that utilize a high percentage of the total body's SAM pool including the biosynthesis of phosphatidylcholines (PC), polyamines (PAs), and creatine (CRE) [102,111].

The methylation reaction byproduct, *S*-adenosylhomocysteine (SAH), is converted back into methionine and ultimately the biosynthesis of SAM (Figure 5) [112]. SAH is metabolized to homocysteine (HCY) which can be re-methylated to methionine (MET) for SAM biosynthesis or diverted to the transsulfuration pathway for biosynthesis of cysteine and incorporation into glutathione in response to oxidative stress (Figure 5) [113]. Betaine homocysteine N-methyltransferase (BHMT) and methionine synthase (MTR) both contribute to the hepatic re-methylation of HCY back to MET using either betaine or 5-methyltetrhydrofolate (5-MTHF), respectively [112]. Betaine is derived from choline and 5-MTHF from folate. BMHT and MTR are linked by cytosolic and mitochondrial compartmentalized anaplerotic reactions. The generation of

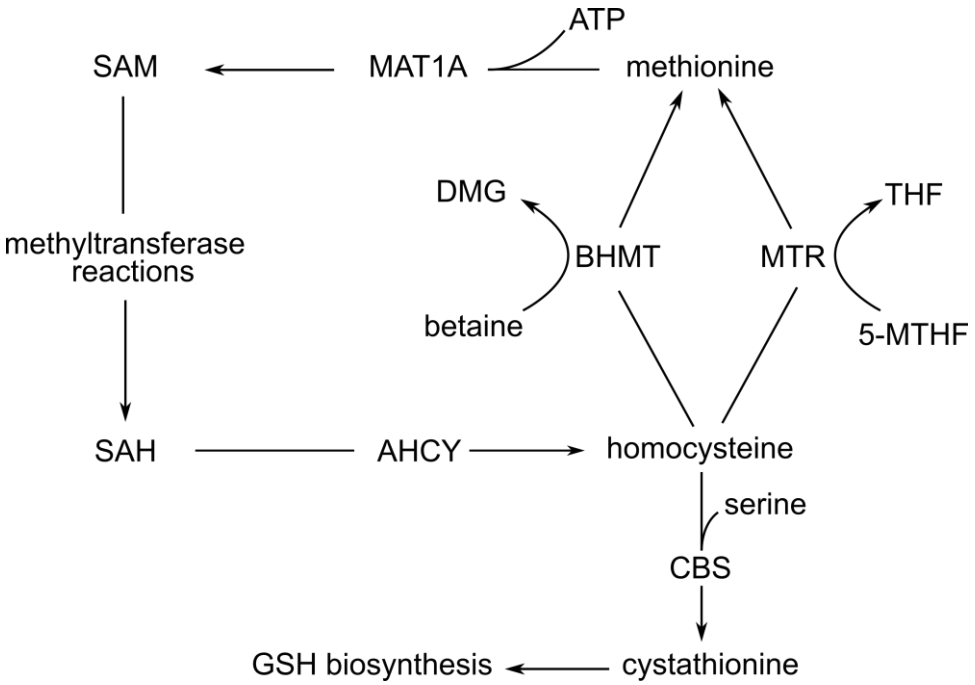

FIGURE 5. DIAGRAM OF GENES AND METABOLITES IN HEPATIC ONE CARBON METABOLISM

Included are SAM biosynthesis, transsulfuration pathway and alternative BHMT/MTR methionine biosynthesis pathways. *Abbreviations: 5-methyltetrahydrofolate (5-MTHF), Betaine homocysteine N-methyltransferase (BHMT), dimethylglycine (DMG), cystathionine beta-synthase (CBS), methionine adenosyltransferase 1 A (MAT1A), methionine synthase (MTR), S-adenosylhomocysteine hydrolase (ACHY), S-adenosylhomocysteine (SAH), S-adenosylmethionine (SAM)*

5-MTHF and betaine also generate intermediates in the metabolism of choline, glycine and serine that are separated in the cytosol and mitochondria (Figure 6) [114, 115]. The initial step in mitochondrial choline catabolism provides betaine that can be used for the methylation of HYC back to MET. De-methylation of betaine by cytosolic BHMT produces dimethylglycine (DMG) that can be converted to glycine by sequential catabolic reactions in the mitochondria by the glycine cleavage system. These 2 reactions also yield two molecules of 5,10-methylenetetrahydrofolate, an intermediate for 5-MTHF and 10-formyltetrahydrofolate used for purine biosynthesis (Figure 6) [114,115]. DMG, sarcosine and glycine from mitochondrial choline metabolism, produces $FADH_2$ and NADH that can be utilized by the mitochondrial electron transport chain for ATP production (Figure 6). GNMT, the most abundant hepatic methyltransferase, regulates SAM levels by methylating glycine to sarcosine, effectively redirecting excess methyl groups towards the folate one carbon pool (Figure 6) [115]. SAM allosterically activates cystathionine β-synthase (CBS) and inhibits methylenetetrahydrofolate reductase (MTHFR) that produces 5-MTHF. Conversely, 5-MTHF allosterically inhibits GNMT. Thus, high SAM levels divert HYC towards the transsulfuration pathway. Conversely, when SAM levels are low, 5-MTHF reserves are utilized for HYC methylation back to MET [116].

SAM biosynthesis catalyzed by methionine adenosyltransferase (MAT) consumes ATP and MET. In mammals, two MAT isoforms exist: methionine adenosyltransferase 1α (MAT1A) and methionine adenosyltransferase 2α (MAT2A). The predominant tertiary forms of MAT in the adult liver are MATI, MATII, and MATIII. MATI is a tetramer of α1 subunits whereas MATIII is a dimer of α1 subunits [117]. MATII consists of interactions between MAT2A and MAT2B subunits [117]. Under basal hepatic methionine levels, MATI has higher specific K_m than MATIII, whereas elevated methionine levels, such as meal times, favors MATIII for SAM biosynthesis when SAM concentrations are high [117]. Hepatic *Mat2a* expression is highest shortly after birth and steadily declines with age, but is expressed ubiquitously in most tissues while *Mat1a* is solely expressed in adult livers where *Mat2a* expression is low [117].

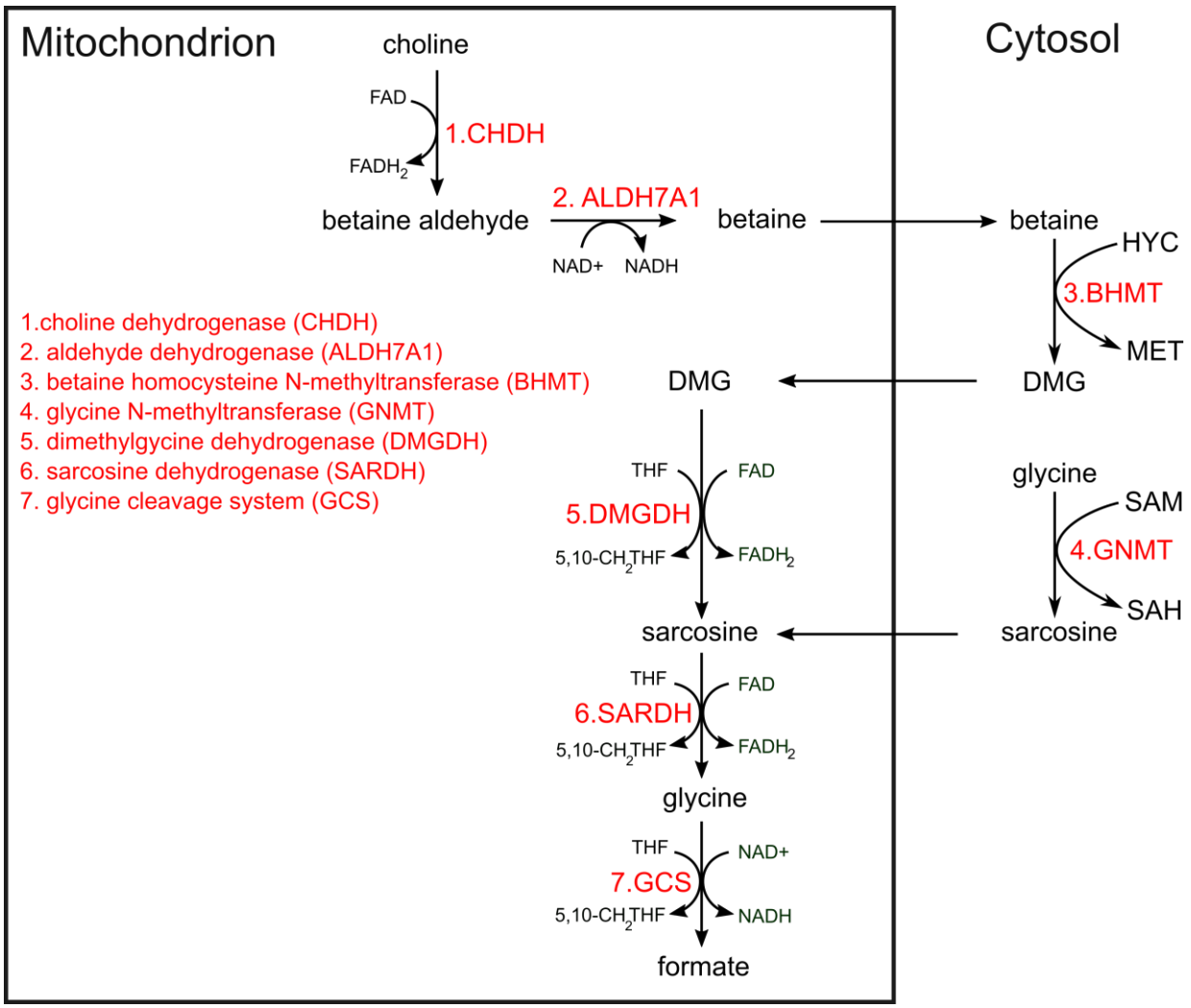

FIGURE 6. COMPARTMENTALIZATION OF ONE CARBON METABOLISM

Depicted is the compartmentalization of folate and betaine metabolism associated with OCM. Enzyme names are listed in red in figure. Abbreviations: 5,10-methylenetetrahydrofolate (5,10-CH_2THF), dimethylglycine (DMG), homocysteine (HYC), methionine (MET), *S*-adenosylhomocysteine (HYC), *S*-adenosylmethionine (SAM), tetrahydrofolate (THF)

ONE CARBON METABOLISM ASSOCIATIONS WITH NAFLD

Knockout of OCM associated genes in mice disrupts hepatic SAM levels and lipid metabolism. Of note, these genetic models exhibit deficiencies in packaging of triglycerides into VLDL particles resulting in reduced VLDL size/secretion and hepatic triglyceride accumulation [95,96,118,119]. GNMT knockout mice display a NAFLD phenotype with steatosis, steatohepatitis and fibrosis in 3 month old mice and spontaneously develop HCC after 8 months [120]. Concurrent with elevated hepatic SAM, *Gnmt*$^{-/-}$ mice also have increased polyamine biosynthesis and alterations in glucose metabolism with decreased serum glucose levels. There are also decreased fluxes in central metabolism including glycogen metabolism, gluconeogenesis and the citric acid cycle [121]. *Mat1a* knockout mice also have decreased hepatic SAM levels, decreased glutathione levels, increased lipid accumulation, hepatic inflammation, serum ALT levels, and spontaneously development HCC [118,122,123]. Disruptions in VLDL metabolism in 3-month old *Mat1a* knockout mice is ameliorated with SAM supplementation [118]. *Bhmt*$^{-/-}$ mice also demonstrate similar pathologies to *Mat1a* knockout mice including decreased SAM levels and SAM/SAH ratio with accumulation of hepatic betaine and HYC with spontaneous development of HCC [124]. Hepatic PC levels are also lower than wild type mice with reduced VLDL secretion [124].

Methionine and choline are essential dietary metabolites needed for hepatic lipid homeostasis and regulation of SAM levels. As previously mentioned, MCD diets elicit a NAFLD phenotype, however, they also alter OCM and associated metabolite levels i.e. lower hepatic SAM [125]. Mice fed choline deficient diets accumulate hepatic triglycerides while MET deficient diets reduce SAM levels suggesting hepatic lipid homeostasis relies more on choline availability and hepatic SAM homeostasis on MET availability [125]. Both choline and MET are involved in the generation of SAM and the biosynthesis of phosphatidylcholine through OCM. Choline catabolism provides betaine for SAM biosynthesis (Figure 5 & 6). In turn, phosphatidylethanolamine N-methyltransferase (PEMT) utilizes SAM in 3 sequential methylation reactions of

phosphatidylethanolamine (PE) to form PC (Figure 7). Alternatively, choline can be used for PC *de novo* biosynthesis of the PC headgroup through the cytidine diphosphate-choline (CDP)-choline pathway, aka the Kennedy pathway (Figure 7) [126]. The CDP-choline pathway accounts for ~70% of total hepatic PC biosynthesis while remaining PC biosynthesis is achieved through the predominantly hepatic expressed PEMT pathway [127]. PEMT localizes to the hepatocyte's canalicular membrane and mitochondria associated membrane of the endoplasmic reticulum [127,128].

$PEMT^{-/-}$ mice under normal diets do not display any NAFLD pathologies and only exhibit a NAFLD phenotype when challenged with a high fat diet that induces hepatic triglyceride accumulation and elevated ALT levels [129]. $PEMT^{-/-}$ mice also exhibit disrupted VLDL metabolism, with a ~50% reduction in secreted triglycerides, ~70% reduction in hepatic apoB100 secretion, and reduced PC levels in VLDL particles [119]. $PEMT^{-/-}$ mice fed a choline deficient diet develop liver failure within 3-5 days highlighting the essential role of choline in PC biosynthesis when both PEMT and CDP-choline pathways are blocked. Interestingly, a double knockout in mice of PEMT and ATP-binding cassette, sub-family , member 4 (*Abcb4*) survived >90 days when fed a choline deficient diet [130]. *Abcb4* is a PC flippase located on the canalicular membrane involved in hepatic biliary PC secretion. Results from double knockout mice studies suggests severe liver injury in PEMT-/- mice may be attributed to reduced PC biosynthesis capacity and rapid depletion of PC through hepatic biliary secretion [131]. PEMT production of PC may also serve as alternative pathway to the CDP-choline pathway when mice are fasting and choline availability is low i.e., during sleep [131].

The PEMT and CDP-choline pathways also produce PC species that differ by fatty acid composition. The PEMT pathway favors production of PC with longer chain polyunsaturated fatty acids, notably species containing docosahexaenoic acid (DHA, PC 16:0/22:6) in both human and mice [132,133]. Conversely, the CDP-choline pathway produces shorter saturated fatty acid PCs e.g., 16:0/18:0[133]. PC species produced by PEMT are highly enriched with DHA in human and

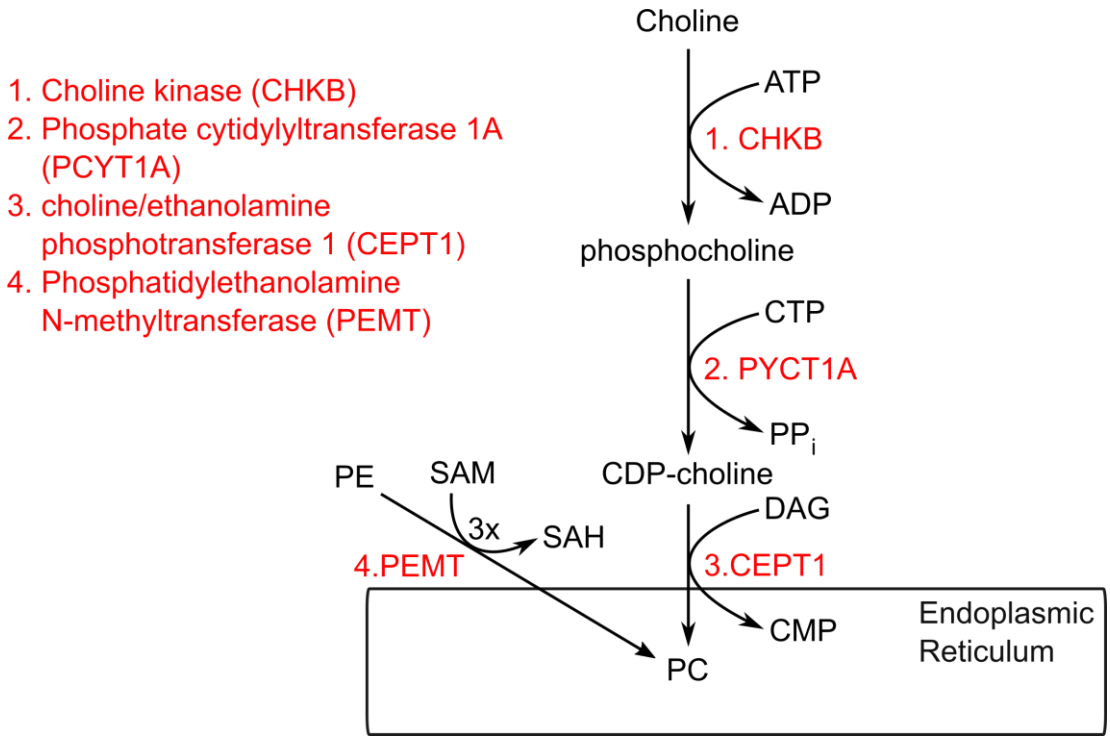

FIGURE 7. BIOSYNTHESIS OF PHOSPHATIDYLCHOLINE (PC)

PC is synthesized through alternate CDP-choline or phosphatidylethanolamine N-methyltransferase(PEMT) pathways. Associated enzymes are numbered and names denoted in the figure. *Abbreviations: cytidine diphosphate-choline (CDP), cytidine monophosphate-choline (CMP), cytidine triphosphate-choline (CTP), Diacyl glyceride (DAG), S-adenosylhomocysteine (SAH), S-adenosylmethionine (SAM)*

mice plasma, suggesting the PEMT pathway is the primary biosynthesis route of PC incorporated into VLDL particles secreted from the liver [132,133]. $PEMT^{-/-}$ mice exhibit decreased serum triglycerides and depleted serum levels of PC containing DHA concurrent with elevated hepatic PE containing DHA. Further, choline supplementation is not able to rescue reduced VLDL secretion in $PEMT^{-/-}$ mice [119,133].

Genetics may also play a role in NAFLD development and progression from steatosis to steatohepatitis with fibrosis and HCC. A well-studied factor implicated in human NAFLD development are polymorphisms in the Patatin-like phospholipase domain-containing protein 3 (*Pnpla3*) [134]. The human PNPLA3 I148M variant is associated with elevated lipid levels and reduced VLDL secretion [135]. Interestingly, the human HepG2 cell line is homozygous for the I148M variant [136]. Several OCM polymorphisms have also been associated with higher risk for NAFLD including *Pemt* [108,137] and methylenetetrahydrofolate reductase (*Mthfr)* [138]. MTHFR produces 5-MTHF from 5,10-CH_2THF, providing MTR methyl donors for the re-methylation of HYC back to MET (Figure 6). The heterozygous V175M PEMT polymorphism results in reduced function and was found in 70% of NAFLD subjects but only ~40% of the Caucasian population [108]. Non-obese Japanese with NASH and the PEMT V175M polymorphism demonstrated ~6 fold increased allele frequency, however the heterozygous allele frequency in the Japanese general population was much lower than Caucasian population [137].

DISRUPTIONS OF OCM IN HEPATOCELLULAR CARCINOMA

In liver diseases, notably HCC and cirrhosis, *Mat1a* expression is often decreased concomitant with increased *Mat2a* expression and reduced SAM/SAH ratio referred to as the MAT1A/MAT2A switch [139,140]. Reduced *Mat1a* expression and low SAM levels are most pronounced in HCC patients with poor prognosis [105,139]. The repression of *Gnmt* and *Bhmt* is also reported in several cancers including pancreatic carcinoma and HCC with poor prognoses, as well as cancer derived cell lines e.g., HepG2 [105,109,110,141]. Moreover, the promoter region

of these genes exhibit differential methylation in HCC. For example, *Mat1a* promoter regions are hypermethylated while *Mat2a* promoter regions are hypomethylated in HCC, resulting in decreased *Mat1a*/*Mat2a* ratio of gene expression. These MAT expression patterns in cells is reflected in a decreased SAM/SAH ratio [142,143]. The MAT1A/MAT2A switch in NAFLD patients is also associated with global DNA hypomethylation [103,143]. The SAM/SAH ratio is thought to play critical roles in DNA methylation status and SAM supplementation has been proposed to treat liver diseases e.g., cirrhosis, alcoholic liver disease, and HCC, with varying degrees of success [144,145].

In addition to regulating SAM/SAH levels, *Mat2a* and *Gnmt* may impact cancer progression through nuclear translocation and interactions. MATII (MAT2A and MAT2B heterodimer) is found in the nucleus and interacts with several chromatin associated complexes and transcription factors including MAF bZIP transcription factor K (MAFK), a DNA-binding oncogene [146]. GNMT is typically a cytosolic protein with SAM binding and 5-MTHF allosteric binding activity. Interestingly, GNMT can also bind polyaromatic hydrocarbons which results in translocation to the nucleus in the presence of aflatoxin or benzo[*a*]pyrene (BaP), a low affinity AhR agonist [147]. CYP1A1 (also a canonical AhR gene target) is involved in the xenobiotic metabolism and toxicity of these metabolites, suggesting GNMT may coregulate their detoxification [147]. Interestingly, TCDD has low GNMT binding affinity compared to BaP [148]. Mutation of phosphorylation sites identified on the serine 9 of GNMT results in impaired GNMT nuclear translocation and increased *Cyp1a1* expression when exposed to BaP [147]. GNMT is also viewed as a cancer suppressor with induction inhibiting G2/M cell cycle progression and cancer proliferation [147]. GNMT nuclear translocation appears necessary for its anticancer effects. However, its main catalytic activity i.e., methylation of glycine, may not be required, suggesting alternative GNMT functions in cancer suppression beyond SAM/SAH level regulation [110,149].

Polyamine (PA) levels and biosynthesis are also elevated in cancer and linked to SAM catabolism [150]. While canonical OCM pathway uses SAM as a methyl donor, SAM can also be decarboxylated and donate its aminopropyl group for the biosynthesis of PAs spermine and spermidine from putrescine [150]. PAs are aliphatic cations that are fully protonated at physiological pH, associating with negatively charged molecules e.g., DNA, RNA and phospholipids. PAs serve diverse biological roles in regulation of cellular metabolism including protein translation, cell proliferation, circadian rhythm and mitochondrial membrane integrity [150–152]. Ornithine decarboxylase (*Odc*) catalyzes the rate limiting step of PA biosynthesis. *Odc* along with several other PA biosynthesis associated genes are upregulated in cancers by the proto-oncogene MYC transcription factors, c-MYC and n-MYC [152]. Regulation of ODC and subsequently PA metabolism is tightly regulated by feedback mechanisms. The ODC antizyme (OAZ) binds to ODC, promoting ODC proteasomal degradation. Conversely antizyme inhibitor 1 (AZIN1) binds OAZ and prevents interactions with ODC, preventing ODC degradation [150]. TCDD and other AhR ligands consistently induce hepatic ODC activity in rodent models [153–155]. However, TCDD effects on PA metabolism are not consistent with the reported inhibition of ODC activity [156,157]. The AhR can also promote *Odc* and *Azin1* expression through DRE-dependent mechanisms in multiple myeloma plasma cells [158]. Expression levels of *Odc* and *Azin1* are also prognostic of cancer patient survival [152]. Due to the prominent role of PA metabolism in cancer proliferation, several pharmaceuticals targeting ODC and AZIN1 enzymatic activity have been evaluated in clinical trials with mixed results [150,152].

CONCLUSION

The etiology of NAFLD is multi-faceted and complex involving environmental, genetic, diet and microbial factors that contribute to the development of steatosis to steatohepatitis with fibrosis and increased the risk of HCC [9,22,30,92,108]. Metabolic syndrome is also associated with the progression to more severe health outcomes i.e., NASH, fibrosis, cirrhosis, and HCC [17–20].

The liver serves as a central metabolic hub for lipid and xenobiotic metabolism where enterohepatic circulation bridges metabolic and immune system interactions between the liver and the gut microbiome. Of note, dysregulation of hepatic biosynthesis and microbial BA metabolism plays important roles in intestinal/hepatic immune system signaling, cholesterol metabolism, and lipid transport, pathways that are also dysregulated in NAFLD [55,84,87]. Hepatic OCM is another critical metabolic pathway involved in hepatic lipid homeostasis that is disrupted in NAFLD. Genetic and dietary models have provided mechanistic insights into the dysregulation of OCM in NAFLD progression, development of HCC, and correlation with poorer prognosis [93,105,108,109,112,118,129]. Moreover, several biomarkers, drugs, and probiotics have been utilized for the characterization and treatment of NAFLD with many of these diagnostic and pharmaceutical tools targeting OCM modulation and host/microbiome BA signaling pathways [69,84,144,145,150,152]. Animal models exposed to TCDD have demonstrated the diverse roles AhR plays in the regulation of hepatic lipid & xenobiotic metabolism, immune/microbiota signaling, and gut microbiome homeostasis [9,45,46,49,54]. Further elucidating the mechanistic roles of AhR in the etiology of NAFLD could provide better context for the contribution environmental contaminants play in NAFLD development and identify novel biomarkers and pharmaceutical targets for the diagnosis and treatment of NAFLD.

RATIONALE

Emerging evidence suggests the multifactorial etiology of NAFLD involves exposure to persistent environmental containments [5,7,8,28]. Repeated TCDD treatment in mice elicits a NAFLD-like phenotype with the progression of steatosis to steatohepatitis with fibrosis that is associated with the dysregulation of hepatic metabolism of glutathione, polyamines, and VLDLs [29,98,154,224]. These metabolic pathways are connected to one carbon metabolism (OCM). OCM encompasses the biosynthesis and utilization of *S*-adenosylmethionine (SAM), the cells main methyl donor. SAM availability is tightly regulated by allosteric and epigenetic regulatory

mechanisms that affects methyltransferase activity involved in high flux anabolic pathways crucial for lipid homeostasis and cell regulation [102, 116, 118]. OCM is often dysregulated in human NAFLD and HCC and associated with poorer prognosis [50,105,150,225]. However, AhR-mediated mechanisms involved in OCM regulation in the context of a TCDD-elicited NAFLD progression has not been fully investigated. The AhR is also crucial for homeostasis of gut microbiome and intestinal immune system, acting through AhR mediated host/microbiome signaling pathways critical for intestine barrier function and defenses against pathogens [49,52,163]. TCDD-treated mice exhibit gut dysbiosis and dysregulated bile acid (BA) metabolism concurrent with elevated primary and secondary bile acids similar to late stage NAFLD in humans [14,16,63,163]. These secondary bile acids activate hepatic and intestinal BA receptors involved in regulation of bile acid and glucose metabolism [68]. However, there is a dearth of studies investigating the effects on secondary bile acid metabolic pathways in the gut microbiome affected by TCDD treatment in mice.

HYPOTHESIS

TCDD-elicited activation of the AhR affects hepatic one carbon metabolism and the gut microbiome, contributing to the progression of steatosis to steatohepatitis with fibrosis.

SPECIFIC AIMS

Specific Aim 1: Evaluate disruptions in hepatic OCM in the context of TCDD-elicited NAFLD progression through the integration of multi-omics analyses of OCM gene expression, proteins, and metabolites.

Specific Aim 2: Investigate disruptions in the gut microbiome through metagenomic taxonomic and functional analyses associated with TCDD-elicited shifts in community and microbial metabolic pathways associated with NAFLD.

REFERENCES

REFERENCES

1. Younossi, Z.M.; Golabi, P.; de Avila, L.; Paik, J.M.; Srishord, M.; Fukui, N.; Qiu, Y.; Burns, L.; Afendy, A.; Nader, F. The Global Epidemiology of NAFLD and NASH in Patients with Type 2 Diabetes: A Systematic Review and Meta-Analysis. *Journal of Hepatology* **2019**, *71*, 793–801, doi:10.1016/j.jhep.2019.06.021.

2. Michelotti, G.A.; Machado, M.; Michelotti, G.A.; Machado, M.V.; Diehl, A.M.; Machado, M.V.; Diehl, A.M. NAFLD-Mltidisciplinary Nutritional Management View Project Genetic Ancestry and Chronic Liver Diseases View Project NAFLD, NASH and Liver Cancer. *Nat. Rev. Gastroenterol. Hepatol* **2013**, *10*, 656–665, doi:10.1038/nrgastro.2013.183.

3. Tilg, H.; Adolph, T.E.; Moschen, A.R. Multiple Parallel Hits Hypothesis in Nonalcoholic Fatty Liver Disease: Revisited After a Decade. *Hepatology* **2021**, *73*, 833–842, doi:10.1002/hep.31518.

4. Buzzetti, E.; Pinzani, M.; Tsochatzis, E.A. The Multiple-Hit Pathogenesis of Non-Alcoholic Fatty Liver Disease (NAFLD). *Metabolism* **2016**, *65*, 1038–1048, doi:10.1016/j.metabol.2015.12.012.

5. Cave, M.; Appana, S.; Patel, M.; Falkner, K.C.; McClain, C.J.; Brock, G. Polychlorinated Biphenyls, Lead, and Mercury Are Associated with Liver Disease in American Adults: NHANES 2003-2004. *Environmental Health Perspectives* **2010**, *118*, 1735–1742, doi:10.1289/ehp.1002720.

6. Rantakokko, P.; Männistö, V.; Airaksinen, R.; Koponen, J.; Viluksela, M.; Kiviranta, H.; Pihlajamäki, J. Persistent Organic Pollutants and Non-Alcoholic Fatty Liver Disease in Morbidly Obese Patients: A Cohort Study. *Environ Health* **2015**, *14*, 79, doi:10.1186/s12940-015-0066-z.

7. Zheng, S.; Yang, Y.; Wen, C.; Liu, W.; Cao, L.; Feng, X.; Chen, J.; Wang, H.; Tang, Y.; Tian, L.; et al. Effects of Environmental Contaminants in Water Resources on Nonalcoholic Fatty Liver Disease. *Environment International* **2021**, *154*, 106555, doi:10.1016/j.envint.2021.106555.

8. Serdar, B.; LeBlanc, W.G.; Norris, J.M.; Dickinson, L.M. Potential Effects of Polychlorinated Biphenyls (PCBs) and Selected Organochlorine Pesticides (OCPs) on Immune Cells and Blood Biochemistry Measures: A Cross-Sectional Assessment of the NHANES 2003-2004 Data. *Environmental Health* **2014**, *13*, 114, doi:10.1186/1476-069X-13-114.

9. Zhang, L.; Nichols, R.G.; Correll, J.; Murray, I.A.; Tanaka, N.; Smith, P.B.; Hubbard, T.D.; Sebastian, A.; Albert, I.; Hatzakis, E.; et al. Persistent Organic Pollutants Modify Gut Microbiota–Host Metabolic Homeostasis in Mice through Aryl Hydrocarbon Receptor Activation. *Environmental Health Perspectives* **2015**, *123*, 679–688, doi:10.1289/ehp.1409055.

10. Nichols, R.G.; Zhang, J.; Cai, J.; Murray, I.A.; Koo, I.; Smith, P.B.; Perdew, G.H.; Patterson, A.D. Metatranscriptomic Analysis of the Mouse Gut Microbiome Response to the Persistent

Organic Pollutant 2,3,7,8-Tetrachlorodibenzofuran. *Metabolites* **2019**, *10*, 1, doi:10.3390/metabo10010001.

11. Fader, K.A.; Nault, R.; Zhang, C.; Kumagai, K.; Harkema, J.R.; Zacharewski, T.R. 2,3,7,8-Tetrachlorodibenzo-p-Dioxin (TCDD)-Elicited Effects on Bile Acid Homeostasis: Alterations in Biosynthesis, Enterohepatic Circulation, and Microbial Metabolism. *Sci Rep* **2017**, *7*, 5921, doi:10.1038/s41598-017-05656-8.

12. Stedtfeld, R.D.; Brett Sallach, J.; Crawford, R.B.; Stedtfeld, T.M.; Williams, M.R.; Waseem, H.; Johnston, C.T.; Li, H.; Teppen, B.J.; Kaminski, N.E.; et al. TCDD Administered on Activated Carbon Eliminates Bioavailability and Subsequent Shifts to a Key Murine Gut Commensal. *Applied Microbiology and Biotechnology* **2017**, *101*, 7409–7415, doi:10.1007/s00253-017-8460-9.

13. Stedtfeld, R.D.; Chai, B.; Crawford, R.B.; Stedtfeld, T.M.; Williams, M.R.; Xiangwen, S.; Kuwahara, T.; Cole, J.R.; Kaminski, N.E.; Tiedje, J.M.; et al. Modulatory Influence of Segmented Filamentous Bacteria on Transcriptomic Response of Gnotobiotic Mice Exposed to TCDD. *Frontiers in microbiology* **2017**, *8*, 1708, doi:10.3389/fmicb.2017.01708.

14. Stedtfeld, R.D.; Stedtfeld, T.M.; Fader, K.A.; Williams, M.R.; Bhaduri, P.; Quensen, J.; Zacharewski, T.R.; Tiedje, J.M.; Hashsham, S.A. TCDD Influences Reservoir of Antibiotic Resistance Genes in Murine Gut Microbiome. *FEMS Microbiology Ecology* **2017**, *93*, doi:10.1093/femsec/fix058.

15. Nault, R.; Fader, K.A.; Lydic, T.A.; Zacharewski, T.R. Lipidomic Evaluation of Aryl Hydrocarbon Receptor-Mediated Hepatic Steatosis in Male and Female Mice Elicited by 2,3,7,8- Tetrachlorodibenzo-p-dioxin., doi:10.1021/acs.chemrestox.6b00430.

16. Lefever, D.E.; Xu, J.; Chen, Y.; Huang, G.; Tamas, N.; Guo, T.L. TCDD Modulation of Gut Microbiome Correlated with Liver and Immune Toxicity in Streptozotocin (STZ)-Induced Hyperglycemic Mice. *Toxicology and Applied Pharmacology* **2016**, *304*, 48–58, doi:10.1016/j.taap.2016.05.016.

17. Anstee, Q.M.; Targher, G.; Day, C.P. Progression of NAFLD to Diabetes Mellitus, Cardiovascular Disease or Cirrhosis. *Nat Rev Gastroenterol Hepatol* **2013**, *10*, 330–344, doi:10.1038/nrgastro.2013.41.

18. Calle, E.E. Overweight, Obesity, and Mortality from Cancer in a Prospectively Studied Cohort of U.S. Adults. *The New England Journal of Medicine* **2003**, 14.

19. Deprince, A.; Haas, J.T.; Staels, B. Dysregulated Lipid Metabolism Links NAFLD to Cardiovascular Disease. *Molecular Metabolism* **2020**, *42*, 101092, doi:10.1016/j.molmet.2020.101092.

20. Alberti, K.G.M.M.; Zimmet, P.; Shaw, J. Metabolic Syndrome-a New World-Wide Definition. A Consensus Statement from the International Diabetes Federation. *Diabet Med* **2006**, *23*, 469–480, doi:10.1111/j.1464-5491.2006.01858.x.

21. Musso, G.; Gambino, R.; Cassader, M.; Pagano, G. A Meta-Analysis of Randomized Trials for the Treatment of Nonalcoholic Fatty Liver Disease. *Hepatology* **2010**, *52*, 79–104, doi:10.1002/hep.23623.

22. Wree, A.; Broderick, L.; Canbay, A.; Hoffman, H.M.; Feldstein, A.E. From NAFLD to NASH to Cirrhosis—New Insights into Disease Mechanisms. *Nature Reviews Gastroenterology & Hepatology* **2013**, *10*, 627–636, doi:10.1038/nrgastro.2013.149.

23. Byrne, C.D.; Targher, G. NAFLD: A Multisystem Disease. *Journal of Hepatology* **2015**, *62*, S47–S64, doi:10.1016/j.jhep.2014.12.012.

24. Cholico, G.N.; Fling, R.R.; Zacharewski, N.A.; Fader, K.A.; Nault, R.; Zacharewski, T. *Thioesterase Induction by 2,3,7,8-Tetrachlorodibenzo-p-Dioxin Results in a Futile Cycle That Inhibits Hepatic β-Oxidation*; Pharmacology and Toxicology, 2021;

25. Lambert, J.E.; Ramos–Roman, M.A.; Browning, J.D.; Parks, E.J. Increased De Novo Lipogenesis Is a Distinct Characteristic of Individuals With Nonalcoholic Fatty Liver Disease. *Gastroenterology* **2014**, *146*, 726–735, doi:10.1053/j.gastro.2013.11.049.

26. Koyama, Y.; Brenner, D.A. Liver Inflammation and Fibrosis. *Journal of Clinical Investigation* **2017**, *127*, 55–64, doi:10.1172/JCI88881.

27. Zhang, C.-Y.; Yuan, W.-G.; He, P.; Lei, J.-H.; Wang, C.-X. Liver Fibrosis and Hepatic Stellate Cells: Etiology, Pathological Hallmarks and Therapeutic Targets. *WJG* **2016**, *22*, 10512, doi:10.3748/wjg.v22.i48.10512.

28. Warner, M.; Mocarelli, P.; Brambilla, P.; Wesselink, A.; Samuels, S.; Signorini, S.; Eskenazi, B. Diabetes, Metabolic Syndrome, and Obesity in Relation to Serum Dioxin Concentrations: The Seveso Women's Health Study. *Environmental Health Perspectives* **2013**, *121*, 906–911, doi:10.1289/ehp.1206113.

29. Fader, K.A.; Nault, R.; Ammendolia, D.A.; Harkema, J.R.; Williams, K.J.; Crawford, R.B.; Kaminski, N.E.; Potter, D.; Sharratt, B.; Zacharewski, T.R. 2,3,7,8-Tetrachlorodibenzo-p-Dioxin Alters Lipid Metabolism and Depletes Immune Cell Populations in the Jejunum of C57BL/6 Mice. *Toxicological Sciences* **2015**, *148*, 567–580, doi:10.1093/toxsci/kfv206.

30. Nault, R.; Fader, K.A.; Ammendolia, D.A.; Dornbos, P.; Potter, D.; Sharratt, B.; Kumagai, K.; Harkema, J.R.; Lunt, S.Y.; Matthews, J.; et al. Dose-Dependent Metabolic Reprogramming and Differential Gene Expression in TCDD-Elicited Hepatic Fibrosis. *Toxicological Sciences* **2016**, *154*, 253–266, doi:10.1093/toxsci/kfw163.

31. Lindén, J.; Lensu, S.; Tuomisto, J.; Pohjanvirta, R. Dioxins, the Aryl Hydrocarbon Receptor and the Central Regulation of Energy Balance. **2010**, doi:10.1016/j.yfrne.2010.07.002.

32. Mukerjee, D. Health Impact of Polychlorinated Dibenzo-p-Dioxins: A Critical Review. *Journal of the Air & Waste Management Association* **1998**, *48*, 157–165, doi:10.1080/10473289.1998.10463655.

33. Vorkamp, K. An Overlooked Environmental Issue? A Review of the Inadvertent Formation of PCB-11 and Other PCB Congeners and Their Occurrence in Consumer Products and in the Environment. *Science of The Total Environment* **2016**, *541*, 1463–1476, doi:10.1016/j.scitotenv.2015.10.019.

34. Sinkkonen, S.; Paasivirta, J. Degradation Half-Life Times of PCDDs, PCDFs and PCBs for Environmental Fate Modeling. *Chemosphere* **2000**, *40*, 943–949, doi:10.1016/S0045-6535(99)00337-9.

35. Fernández-González, R.; Yebra-Pimentel, I.; Martínez-Carballo, E.; Simal-Gándara, J. A Critical Review about Human Exposure to Polychlorinated Dibenzo-p-Dioxins (PCDDs), Polychlorinated Dibenzofurans (PCDFs) and Polychlorinated Biphenyls (PCBs) through Foods. *Critical Reviews in Food Science and Nutrition* **2015**, *55*, 1590–1617, doi:10.1080/10408398.2012.710279.

36. Chernyak, Y.I.; Shelepchikov, A.A.; Brodsky, E.S.; Grassman, J.A. PCDD, PCDF, and PCB Exposure in Current and Former Firefighters from Eastern Siberia. *Toxicology Letters* **2012**, *213*, 9–14, doi:10.1016/j.toxlet.2011.09.021.

37. Seo, S.-H.; Kwon, S.-Y.; Choi, S.-D.; Chang, Y.-S. Twenty-Year Trends and Exposure Assessment of Polychlorinated Dibenzodioxins and Dibenzofurans in Human Serum from the Seoul Citizens. *Chemosphere* **2021**, *273*, 128558, doi:10.1016/j.chemosphere.2020.128558.

38. Milbrath, M.O.; Wenger, Y.; Chang, C.-W.; Emond, C.; Garabrant, D.; Gillespie, B.W.; Jolliet, O. Apparent Half-Lives of Dioxins, Furans, and Polychlorinated Biphenyls as a Function of Age, Body Fat, Smoking Status, and Breast-Feeding. *Environmental Health Perspectives* **2009**, *117*, 417–425, doi:10.1289/ehp.11781.

39. Cave, M.C.; Pinkston, C.M.; Rai, S.N.; Wahlang, B.; Pavuk, M.; Head, K.Z.; Carswell, G.K.; Nelson, G.M.; Klinge, C.M.; Bell, D.A.; et al. Circulating MicroRNAs, Polychlorinated Biphenyls, and Environmental Liver Disease in the Anniston Community Health Survey. *Environ Health Perspect* **2022**, *130*, 017003, doi:10.1289/EHP9467.

40. Park, W.H.; Kang, S.; Lee, H.K.; Salihovic, S.; Bavel, B. van; Lind, P.M.; Pak, Y.K.; Lind, L. Relationships between Serum-Induced AhR Bioactivity or Mitochondrial Inhibition and Circulating Polychlorinated Biphenyls (PCBs). *Sci Rep* **2017**, *7*, 9383, doi:10.1038/s41598-017-09774-1.

41. Harrill, J.A.; Layko, D.; Nyska, A.; Hukkanen, R.R.; Manno, R.A.; Grassetti, A.; Lawson, M.; Martin, G.; Budinsky, R.A.; Rowlands, J.C.; et al. Aryl Hydrocarbon Receptor Knockout Rats Are Insensitive to the Pathological Effects of Repeated Oral Exposure to 2,3,7,8-Tetrachlorodibenzo-p-Dioxin. **2015**, doi:10.1002/jat.3211.

42. Mandal, P.K. Dioxin: A Review of Its Environmental Effects and Its Aryl Hydrocarbon Receptor Biology. *Journal of Comparative Physiology B: Biochemical, Systemic, and Environmental Physiology* **2005**, *175*, 221–230, doi:10.1007/s00360-005-0483-3.

43. Gonzalez, F.J.; Fernandez-Salguero, P.M. The Aryl Hydrocarbon Receptor: Studies Using the AHR-Null Mice. *DRUG METABOLISM AND DISPOSITION Drug Metab Dispos* **1998**, *26*, 1194–1198.

44. Yeager, R.L.; Reisman, S.A.; Aleksunes, L.M.; Klaassen, C.D. Introducing the “TCDD-Inducible AhR-Nrf2 Gene Battery.” *Toxicological Sciences* **2009**, *111*, 238–246, doi:10.1093/toxsci/kfp115.

45. Fader, K.A.; Nault, R.; Doskey, C.M.; Fling, R.R.; Zacharewski, T.R. 2,3,7,8-Tetrachlorodibenzo-p-Dioxin Abolishes Circadian Regulation of Hepatic Metabolic Activity in Mice. *Scientific Reports* **2019**, *9*, 1–18, doi:10.1038/s41598-019-42760-3.

46. Nault, R.; Fader, K.A.; Kirby, M.P.; Ahmed, S.; Matthews, J.; Jones, A.D.; Lunt, S.Y.; Zacharewski, T.R. Pyruvate Kinase Isoform Switching and Hepatic Metabolic Reprogramming by the Environmental Contaminant 2,3,7,8-Tetrachlorodibenzo-p-Dioxin. *Toxicological Sciences* **2016**, *149*, 358–371, doi:10.1093/toxsci/kfv245.

47. Dvořák, Z.; Poulíková, K.; Mani, S. Indole Scaffolds as a Promising Class of the Aryl Hydrocarbon Receptor Ligands. *European Journal of Medicinal Chemistry* **2021**, *215*, 113231, doi:10.1016/j.ejmech.2021.113231.

48. Zelante, T.; Puccetti, M.; Giovagnoli, S.; Romani, L. Regulation of Host Physiology and Immunity by Microbial Indole-3-Aldehyde. *Current Opinion in Immunology* **2021**, *70*, 27–32, doi:10.1016/j.coi.2020.12.004.

49. Zelante, T.; Iannitti, R.G.; Cunha, C.; DeLuca, A.; Giovannini, G.; Pieraccini, G.; Zecchi, R.; D'Angelo, C.; Massi-Benedetti, C.; Fallarino, F.; et al. Tryptophan Catabolites from Microbiota Engage Aryl Hydrocarbon Receptor and Balance Mucosal Reactivity via Interleukin-22. *Immunity* **2013**, *39*, 372–385, doi:10.1016/j.immuni.2013.08.003.

50. Lawrence, B.P.; Vorderstrasse, B.A. New Insights into the Aryl Hydrocarbon Receptor as a Modulator of Host Responses to Infection. *Semin Immunopathol* **2013**, *35*, 615–626, doi:10.1007/s00281-013-0395-3.

51. Schnupf, P.; Gaboriau-Routhiau, V.; Cerf-Bensussan, N. Host Interactions with Segmented Filamentous Bacteria: An Unusual Trade-off That Drives the Post-Natal Maturation of the Gut Immune System. *Seminars in Immunology* **2013**, *25*, 342–351, doi:10.1016/j.smim.2013.09.001.

52. Qui, J.; Zhou, L.; Qiu, J.; Zhou, L. Aryl Hydrocarbon Receptor Promotes RORγt+ ILCs and Controls Intestinal Immunity and Inflammation. *Semin Immunopathol* **2013**, *35*, 657–670, doi:10.1016/j.biotechadv.2011.08.021.Secreted.

53. Qiu, J.; Heller, J.J.; Guo, X.; Chen, Z.M.E.; Fish, K.; Fu, Y.X.; Zhou, L. The Aryl Hydrocarbon Receptor Regulates Gut Immunity through Modulation of Innate Lymphoid Cells. *Immunity* **2012**, *36*, 92–104, doi:10.1016/j.immuni.2011.11.011.

54. Murray, I.A.; Nichols, R.G.; Zhang, L.; Patterson, A.D.; Perdew, G.H. Expression of the Aryl Hydrocarbon Receptor Contributes to the Establishment of Intestinal Microbial Community Structure in Mice. *Scientific Reports* **2016**, *6*, 33969, doi:10.1038/srep33969.

55. Chiang, J.Y.L. Bile Acids: Regulation of Synthesis. *Journal of Lipid Research* **2009**, *50*, 1955–1966, doi:10.1194/jlr.R900010-JLR200.

56. Chow, M.D.; Lee, Y.H.; Guo, G.L. The Role of Bile Acids in Nonalcoholic Fatty Liver Disease and Nonalcoholic Steatohepatitis. *Molecular Aspects of Medicine* **2017**, *56*, 34–44, doi:10.1016/j.mam.2017.04.004.

57. Kim, I.; Ahn, S.H.; Inagaki, T.; Choi, M.; Ito, S.; Guo, G.L.; Kliewer, S.A.; Gonzalez, F.J. Differential Regulation of Bile Acid Homeostasis by the Farnesoid X Receptor in Liver and Intestine. *Journal of Lipid Research* **2007**, *48*, 2664–2672, doi:10.1194/jlr.M700330-JLR200.

58. Dasarathy, S.; Yang, Y.; McCullough, A.J.; Marczewski, S.; Bennett, C.; Kalhan, S.C. Elevated Hepatic Fatty Acid Oxidation, High Plasma Fibroblast Growth Factor 21, and Fasting Bile Acids in Nonalcoholic Steatohepatitis. *European Journal of Gastroenterology & Hepatology* **2011**, *23*, 382–388, doi:10.1097/MEG.0b013e328345c8c7.

59. Ferslew, B.C.; Xie, G.; Johnston, C.K.; Su, M.; Stewart, P.W.; Jia, W.; Brouwer, K.L.R.; Sidney Barritt, A. Altered Bile Acid Metabolome in Patients with Nonalcoholic Steatohepatitis. *Dig Dis Sci* **2015**, *60*, 3318–3328, doi:10.1007/s10620-015-3776-8.

60. Aranha, M.M.; Cortez-Pinto, H.; Costa, A.; da Silva, I.B.M.; Camilo, M.E.; de Moura, M.C.; Rodrigues, C.M.P. Bile Acid Levels Are Increased in the Liver of Patients with Steatohepatitis: *European Journal of Gastroenterology & Hepatology* **2008**, *20*, 519–525, doi:10.1097/MEG.0b013e3282f4710a.

61. Nimer, N.; Choucair, I.; Wang, Z.; Nemet, I.; Li, L.; Gukasyan, J.; Weeks, T.L.; Alkhouri, N.; Zein, N.; Tang, W.H.W.; et al. Bile Acids Profile, Histopathological Indices and Genetic Variants for Non-Alcoholic Fatty Liver Disease Progression. *Metabolism* **2021**, *116*, 154457, doi:10.1016/j.metabol.2020.154457.

62. Kalhan, S.C.; Guo, L.; Edmison, J.; Dasarathy, S.; McCullough, A.J.; Hanson, R.W.; Milburn, M. Plasma Metabolomic Profile in Nonalcoholic Fatty Liver Disease. *Metabolism: Clinical and Experimental* **2011**, *60*, 404–413, doi:10.1016/j.metabol.2010.03.006.

63. Puri, P.; Daita, K.; Joyce, A.; Mirshahi, F.; Santhekadur, P.K.; Cazanave, S.; Luketic, V.A.; Siddiqui, M.S.; Boyett, S.; Min, H.; et al. The Presence and Severity of Nonalcoholic Steatohepatitis Is Associated with Specific Changes in Circulating Bile Acids. *Hepatology* **2018**, *67*, 534–548, doi:10.1002/hep.29359.

64. Liu, H.; Pathak, P.; Boehme, S.; Chiang, JohnY.L. Cholesterol 7α-Hydroxylase Protects the Liver from Inflammation and Fibrosis by Maintaining Cholesterol Homeostasis. *Journal of Lipid Research* **2016**, *57*, 1831–1844, doi:10.1194/jlr.M069807.

65. Petersen, N.; Greiner, T.U.; Torz, L.; Bookout, A.; Gerstenberg, M.K.; Castorena, C.M.; Kuhre, R.E. Targeting the Gut in Obesity: Signals from the Inner Surface. *Metabolites* **2022**, *12*, 39, doi:10.3390/metabo12010039.

66. Pols, T.W.H.; Noriega, L.G.; Nomura, M.; Auwerx, J.; Schoonjans, K. The Bile Acid Membrane Receptor TGR5: A Valuable Metabolic Target. *Dig Dis* **2011**, *29*, 37–44, doi:10.1159/000324126.

67. Shi, Y.; Su, W.; Zhang, L.; Shi, C.; Zhou, J.; Wang, P.; Wang, H.; Shi, X.; Wei, S.; Wang, Q.; et al. TGR5 Regulates Macrophage Inflammation in Nonalcoholic Steatohepatitis by Modulating NLRP3 Inflammasome Activation. *Front. Immunol.* **2021**, *11*, 609060, doi:10.3389/fimmu.2020.609060.

68. Li, Y.; Jadhav, K.; Zhang, Y. Bile Acid Receptors in Non-Alcoholic Fatty Liver Disease. *Biochemical Pharmacology* **2013**, *86*, 1517–1524, doi:10.1016/j.bcp.2013.08.015.

69. Evangelakos, I.; Heeren, J.; Verkade, E.; Kuipers, F. Role of Bile Acids in Inflammatory Liver Diseases. *Semin Immunopathol* **2021**, *43*, 577–590, doi:10.1007/s00281-021-00869-6.

70. Guzior, D.V.; Quinn, R.A. Review: Microbial Transformations of Human Bile Acids. *Microbiome* **2021**, *9*, 140, doi:10.1186/s40168-021-01101-1.

71. Kemis, J.H.; Linke, V.; Barrett, K.L.; Boehm, F.J.; Traeger, L.L.; Keller, M.P.; Rabaglia, M.E.; Schueler, K.L.; Stapleton, D.S.; Gatti, D.M.; et al. Genetic Determinants of Gut Microbiota Composition and Bile Acid Profiles in Mice. *PLoS Genet* **2019**, *15*, e1008073, doi:10.1371/journal.pgen.1008073.

72. Campbell, C.; McKenney, P.T.; Konstantinovsky, D.; Isaeva, O.I.; Schizas, M.; Verter, J.; Mai, C.; Jin, W.-B.; Guo, C.-J.; Violante, S.; et al. Bacterial Metabolism of Bile Acids Promotes Generation of Peripheral Regulatory T Cells. *Nature* **2020**, *581*, 475–479, doi:10.1038/s41586-020-2193-0.

73. Jones, B.V.; Begley, M.; Hill, C.; Gahan, C.G.M.; Marchesi, J.R. Functional and Comparative Metagenomic Analysis of Bile Salt Hydrolase Activity in the Human Gut Microbiome. *Proceedings of the National Academy of Sciences of the United States of America* **2008**, *105*, 13580–13585, doi:10.1073/pnas.0804437105.

74. Tannock, G.W.; Dashkevicz, M.P.; Feighner, S.D. Lactobacilli and Bile Salt Hydrolase in the Murine Intestinal Tract. *Appl Environ Microbiol* **1989**, *55*, 1848–1851, doi:10.1128/aem.55.7.1848-1851.1989.

75. Marion, S.; Desharnais, L.; Studer, N.; Dong, Y.; Notter, M.D.; Poudel, S.; Menin, L.; Janowczyk, A.; Hettich, R.L.; Hapfelmeier, S.; et al. Biogeography of Microbial Bile Acid Transformations along the Murine Gut. *Journal of Lipid Research* **2020**, *61*, 1450–1463, doi:10.1194/jlr.RA120001021.

76. Bustos, A.Y.; Saavedra, L.; de Valdez, G.F.; Raya, R.R.; Taranto, M.P. Relationship between Bile Salt Hydrolase Activity, Changes in the Internal PH and Tolerance to Bile Acids in Lactic Acid Bacteria. *Biotechnol Lett* **2012**, *34*, 1511–1518, doi:10.1007/s10529-012-0932-5.

77. De Smet, I.; Van Hoorde, L.; Vande Woestyne, M.; Christiaens, H.; Verstraete, W. Significance of Bile Salt Hydrolytic Activities of Lactobacilli. *Journal of Applied Bacteriology* **1995**, *79*, 292–301, doi:10.1111/j.1365-2672.1995.tb03140.x.

78. Tian, Y.; Gui, W.; Koo, I.; Smith, P.B.; Allman, E.L.; Rimal, B.; Cai, J.; Liu, Q.; Patterson, A.D. The Microbiome Modulating Activity of Bile Acids. 19.

79. Grill, J.P.; Perrin, S.; Schneider, F. Bile Salt Toxicity to Some Bifidobacteria Strains: Role of Conjugated Bile Salt Hydrolase and PH. **2000**, *46*, 7.

80. Marteau, P.; Minekus, M.; Havenaar, R.; Huis In't Veld, J.H.J. Survival of Lactic Acid Bacteria in a Dynamic Model of the Stomach and Small Intestine: Validation and the Effects of Bile. *Journal of Dairy Science* **1997**, *80*, 1031–1037, doi:10.3168/jds.S0022-0302(97)76027-2.

81. Foley, M.H.; O'Flaherty, S.; Allen, G.; Rivera, A.J.; Stewart, A.K.; Barrangou, R.; Theriot, C.M. *Lactobacillus* Bile Salt Hydrolase Substrate Specificity Governs Bacterial Fitness and Host Colonization. *Proc Natl Acad Sci USA* **2021**, *118*, e2017709118, doi:10.1073/pnas.2017709118.

82. Liong, M.T.; Shah, N.P. Bile Salt Deconjugation and BSH Activity of Five Bifidobacterial Strains and Their Cholesterol Co-Precipitating Properties. *Food Research International* **2005**, *38*, 135–142, doi:10.1016/j.foodres.2004.08.003.

83. Jones, M.L.; Martoni, C.J.; Prakash, S. Cholesterol Lowering and Inhibition of Sterol Absorption by Lactobacillus Reuteri NCIMB 30242: A Randomized Controlled Trial. *Eur J Clin Nutr* **2012**, *66*, 1234–1241, doi:10.1038/ejcn.2012.126.

84. Wu, Y.; Zhang, Q.; Ren, Y.; Ruan, Z. Effect of Probiotic Lactobacillus on Lipid Profile: A Systematic Review and Meta-Analysis of Randomized, Controlled Trials. *PLoS ONE* **2017**, *12*, e0178868, doi:10.1371/journal.pone.0178868.

85. Anderson, J.W.; Gilliland, S.E. Effect of Fermented Milk (Yogurt) Containing *Lactobacillus Acidophilus* L1 on Serum Cholesterol in Hypercholesterolemic Humans. *Journal of the American College of Nutrition* **1999**, *18*, 43–50, doi:10.1080/07315724.1999.10718826.

86. Fuentes, M.C.; Lajo, T.; Carrión, J.M.; Cuñé, J. Cholesterol-Lowering Efficacy of *Lactobacillus Plantarum* CECT 7527, 7528 and 7529 in Hypercholesterolaemic Adults. *Br J Nutr* **2013**, *109*, 1866–1872, doi:10.1017/S000711451200373X.

87. Zhu, H.; Zhao, F.; Zhang, W.; Xia, W.; Chen, Y.; Liu, Y.; Fan, Z.; Zhang, Y.; Yang, Y. Cholesterol-Lowering Effect of Bile Salt Hydrolase from a *Lactobacillus Johnsonii* Strain Mediated by FXR Pathway Regulation. *Food Funct.* **2022**, *13*, 725–736, doi:10.1039/D1FO03143K.

88. Mouzaki, M.; Wang, A.Y.; Bandsma, R.; Comelli, E.M.; Arendt, B.M.; Zhang, L.; Fung, S.; Fischer, S.E.; McGilvray, I.G.; Allard, J.P. Bile Acids and Dysbiosis in Non-Alcoholic Fatty Liver Disease. *PLoS ONE* **2016**, *11*, e0151829, doi:10.1371/journal.pone.0151829.

89. Jiao, N.; Loomba, R.; Yang, Z.-H.; Wu, D.; Fang, S.; Bettencourt, R.; Lan, P.; Zhu, R.; Zhu, L. *Alterations in Bile Acid Metabolizing Gut Microbiota and Specific Bile Acid Genes as a Precision Medicine to Subclassify NAFLD*; Pathology, 2020;

90. Lee, G.; You, H.J.; Bajaj, J.S.; Joo, S.K.; Yu, J.; Park, S.; Kang, H.; Park, J.H.; Kim, J.H.; Lee, D.H.; et al. Distinct Signatures of Gut Microbiome and Metabolites Associated with Significant Fibrosis in Non-Obese NAFLD. *Nat Commun* **2020**, *11*, 4982, doi:10.1038/s41467-020-18754-5.

91. O'Keefe, S.J.D.; Li, J.V.; Lahti, L.; Ou, J.; Carbonero, F.; Mohammed, K.; Posma, J.M.; Kinross, J.; Wahl, E.; Ruder, E.; et al. Fat, Fibre and Cancer Risk in African Americans and Rural Africans. *Nat Commun* **2015**, *6*, 6342, doi:10.1038/ncomms7342.

92. Anstee, Q.M.; Goldin, R.D. Mouse Models in Non-Alcoholic Fatty Liver Disease and Steatohepatitis Research: Mouse Models in NAFLD and NASH Research. *International Journal of Experimental Pathology* **2006**, *87*, 1–16, doi:10.1111/j.0959-9673.2006.00465.x.

93. Kanuri, G.; Bergheim, I. In Vitro and in Vivo Models of Non-Alcoholic Fatty Liver Disease (NAFLD). *International Journal of Molecular Sciences* **2013**, *14*, 11963–11980, doi:10.3390/ijms140611963.

94. Van Herck, M.; Vonghia, L.; Francque, S. Animal Models of Nonalcoholic Fatty Liver Disease—A Starter's Guide. *Nutrients* **2017**, *9*, 1072, doi:10.3390/nu9101072.

95. Song, Y.; Wu, W.; Sheng, L.; Jiang, B.; Li, X.; Cai, K. Chrysin Ameliorates Hepatic Steatosis Induced by a Diet Deficient in Methionine and Choline by Inducing the Secretion of Hepatocyte Nuclear Factor 4α-dependent Very Low-density Lipoprotein. *J Biochem Mol Toxicol* **2020**, *34*, doi:10.1002/jbt.22497.

96. Yao, Z.M.; Vance, D.E. The Active Synthesis of Phosphatidylcholine Is Required for Very Low Density Lipoprotein Secretion from Rat Hepatocytes. *Journal of Biological Chemistry* **1988**, *263*, 2998–3004, doi:10.1016/S0021-9258(18)69166-5.

97. Fujii, M.; Shibazaki, Y.; Wakamatsu, K.; Honda, Y.; Kawauchi, Y.; Suzuki, K.; Arumugam, S.; Watanabe, K.; Ichida, T.; Asakura, H.; et al. A Murine Model for Non-Alcoholic Steatohepatitis Showing Evidence of Association between Diabetes and Hepatocellular Carcinoma. *Med Mol Morphol* **2013**, *46*, 141–152, doi:10.1007/s00795-013-0016-1.

98. Angrish, M.M.; Dominici, C.Y.; Zacharewski, T.R. TCDD-Elicited Effects on Liver, Serum, and Adipose Lipid Composition in C57BL/6 Mice. *Toxicological Sciences* **2013**, *131*, 108–115, doi:10.1093/toxsci/kfs277.

99. Boverhof, D.R.; Burgoon, L.D.; Tashiro, C.; Chittim, B.; Harkema, J.R.; Jump, D.B.; Zacharewski, T.R. Temporal and Dose-Dependent Hepatic Gene Expression Patterns in Mice Provide New Insights into TCDD-Mediated Hepatotoxicity. *Toxicological Sciences* **2005**, *85*, 1048–1063, doi:10.1093/toxsci/kfi162.

100. Forgacs, A.L.; Dere, E.; Angrish, M.M.; Zacharewski, T.R. Comparative Analysis of Temporal and Dose-Dependent TCDD-Elicited Gene Expression in Human, Mouse, and Rat Primary Hepatocytes. *Toxicological Sciences* **2013**, *133*, 54–66, doi:10.1093/toxsci/kft028.

101. Csanaky, I.L.; Lickteig, A.J.; Klaassen, C.D. Aryl Hydrocarbon Receptor (AhR) Mediated Short-Term Effects of 2,3,7,8-Tetrachlorodibenzo- p -Dioxin (TCDD) on Bile Acid Homeostasis in Mice. *Toxicology and Applied Pharmacology* **2018**, *343*, 48–61, doi:10.1016/j.taap.2018.02.005.

102. Mato, J.M.; Martínez-Chantar, M.L.; Noureddin, M.; Lu, S.C. One-Carbon Metabolism in Liver Health and Disease. In *Liver Pathophysiology*; Elsevier, 2017; pp. 761–765 ISBN 978-0-12-804274-8.

103. Lai, Z.; Chen, J.; Ding, C.; Wong, K.; Chen, X.; Pu, L.; Huang, Q.; Chen, X.; Cheng, Z.; Liu, Y.; et al. Association of Hepatic Global DNA Methylation and Serum One-Carbon Metabolites with Histological Severity in Patients with NAFLD. *Obesity* **2020**, *28*, 197–205, doi:10.1002/oby.22667.

104. Murphy, S.K.; Yang, H.; Moylan, C.A.; Pang, H.; Dellinger, A.; Abdelmalek, M.F.; Garrett, M.E.; Ashley-Koch, A.; Suzuki, A.; Tillmann, H.L.; et al. Relationship Between the

Methylome and Transcriptome in Patients with Non-Alcoholic Fatty Liver Disease: (Functional Methylation in NAFLD)., doi:10.1053/j.gastro.2013.07.047.

105. Chen, P.-M.; Tsai, C.-H.; Huang, C.-C.; Hwang, H.-H.; Li, J.-R.; Liu, C.-C.; Ko, H.-A.; Chiang, E.-P.I. Downregulation of Methionine Cycle Genes MAT1A and GNMT Enriches Protein-Associated Translation Process and Worsens Hepatocellular Carcinoma Prognosis. *IJMS* **2022**, *23*, 481, doi:10.3390/ijms23010481.

106. Corbin, K.D.; Abdelmalek, M.F.; Spencer, M.D.; Da Costa, K.A.; Galanko, J.A.; Sha, W.; Suzuki, A.; Guy, C.D.; Cardona, D.M.; Torquati, A.; et al. Genetic Signatures in Choline and 1-Carbon Metabolism Are Associated with the Severity of Hepatic Steatosis. *FASEB Journal* **2013**, *27*, 1674–1689, doi:10.1096/fj.12-219097.

107. Mart\textasciitilden, A.; Ortiz, P.; Cabrero, C.; Mato, J.M. *S-Adenosyl-L-Methionine Synthetase and Phospholipid Methyltransferase Are Inhibited in Human Cirrhosis*; 1988; pp. 65–68;.

108. Song, J.; Da Costa, K.A.; Fischer, L.M.; Kohlmeier, M.; Kwock, L.; Wang, S.; Zeisel, S.H. Polymorphism of the PEMT Gene and Susceptibility to Nonalcoholic Fatty Liver Disease (NAFLD). *The FASEB Journal* **2005**, *19*, 1266–1271, doi:10.1096/fj.04-3580com.

109. Jin, B.; Gong, Z.; Yang, N.; Huang, Z.; Zeng, S.; Chen, H.; Hu, S.; Pan, G. Downregulation of Betaine Homocysteine Methyltransferase (BHMT) in Hepatocellular Carcinoma Associates with Poor Prognosis. *Tumor Biol.* **2016**, *37*, 5911–5917, doi:10.1007/s13277-015-4443-6.

110. DebRoy, S.; Kramarenko, I.I.; Ghose, S.; Oleinik, N.V.; Krupenko, S.A.; Krupenko, N.I. A Novel Tumor Suppressor Function of Glycine N-Methyltransferase Is Independent of Its Catalytic Activity but Requires Nuclear Localization. *PLoS ONE* **2013**, *8*, e70062, doi:10.1371/journal.pone.0070062.

111. Brosnan, M.E.; Jacobs, R.L.; Brosnan, J.T.; Vance, D.E.; Stabler, S.P.; Wagner, C.; Allen, R.H.; Mudd, S.H. Methyl Balance and Transmethylation Fluxes in Humans. *The American Journal of Clinical Nutrition* **2007**, *85*, 19–25, doi:10.1093/ajcn/85.1.19.

112. Li, Z.; Wang, F.; Liang, B.; Su, Y.; Sun, S.; Xia, S.; Shao, J.; Zhang, Z.; Hong, M.; Zhang, F.; et al. Methionine Metabolism in Chronic Liver Diseases: An Update on Molecular Mechanism and Therapeutic Implication. *Sig Transduct Target Ther* **2020**, *5*, 280, doi:10.1038/s41392-020-00349-7.

113. Pacana, T.; Cazanave, S.; Verdianelli, A.; Patel, V.; Min, H.-K.; Mirshahi, F.; Quinlivan, E.; Sanyal, A.J. Dysregulated Hepatic Methionine Metabolism Drives Homocysteine Elevation in Diet-Induced Nonalcoholic Fatty Liver Disease. *PLOS ONE* **2015**, *10*, e0136822, doi:10.1371/journal.pone.0136822.

114. Ducker, G.S.; Rabinowitz, J.D. One-Carbon Metabolism in Health and Disease. *Cell Metabolism* **2016**, *25*, 27–42, doi:10.1016/j.cmet.2016.08.009.

115. Brosnan, M.E.; MacMillan, L.; Stevens, J.R.; Brosnan, J.T. Division of Labour: How Does Folate Metabolism Partition between One-Carbon Metabolism and Amino Acid Oxidation? *The Biochemical journal* **2015**, *472*, 135–146, doi:10.1042/BJ20150837.

116. Mato, J.M.; Martinez-Chantar, M.L.; Lu, S.C. *S*-Adenosylmethionine Metabolism and Liver Disease. *Annals of hepatology* **2013**, *12*, 183–189, doi:1032614 [pii].

117. Mato, J.M.; Corrales, F.J.; Lu, S.C.; Mati´, M.; Avila, M.A. *S-Adenosylmethionine: A Control Switch That Regulates Liver Function*; 2019;

118. Aspichueta, P.; García-Rodríguez, J.L.; Menor, A.; Lu, S.C.; Mato, J.M.; Aurrekoetxea, I.; Cano, A.; Martínez-Uña, M.; Buqué, X.; Martínez-Chantar, M.L.; et al. Methionine Adenosyltransferase 1A Gene Deletion Disrupts Hepatic Very Low-Density Lipoprotein Assembly in Mice. *Hepatology* **2011**, *54*, 1975–1986, doi:10.1002/hep.24607.

119. Noga, A.A.; Zhao, Y.; Vance, D.E. An Unexpected Requirement for PhosphatidylethanolamineN-Methyltransferase in the Secretion of Very Low Density Lipoproteins. *Journal of Biological Chemistry* **2002**, *277*, 42358–42365, doi:10.1074/jbc.M204542200.

120. Martínez-Chantar, M.L.; Vázquez-Chantada, M.; Ariz, U.; Martínez, N.; Varela, M.; Luka, Z.; Capdevila, A.; Rodríguez, J.; Aransay, A.M.; Matthiesen, R.; et al. Loss of the Glycine N-Methyltransferase Gene Leads to Steatosis and Hepatocellular Carcinoma in Mice. *Hepatology* **2008**, *47*, 1191–1199, doi:10.1002/hep.22159.

121. Hughey, C.C.; Trefts, E.; Bracy, D.P.; James, F.D.; Patrick Donahue, E.; Wasserman, D.H. Glycine N-Methyltransferase Deletion in Mice Diverts Carbon Flux from Gluconeogenesis to Pathways That Utilize Excess Methionine Cycle Intermediates. *Journal of Biological Chemistry* **2018**, *293*, 11944–11954, doi:10.1074/jbc.RA118.002568.

122. Martínez-Chantar, M.L.; Corrales, F.J.; Martínez-Cruz, L.A.; García-Trevijano, E.R.; Huang, Z.Z.; Chen, L.; Kanel, G.; Avila, M.A.; Mato, J.M.; Lu, S.C. Spontaneous Oxidative Stress and Liver Tumors in Mice Lacking Methionine Adenosyltransferase 1A. *The FASEB journal : official publication of the Federation of American Societies for Experimental Biology* **2002**, *16*, 1292–1294, doi:10.1096/fj.02-0078fje.

123. Lu, S.C.; Alvarez, L.; Huang, Z.Z.; Chen, L.; An, W.; Corrales, F.J.; Avila, M.A.; Kanel, G.; Mato, J.M. Methionine Adenosyltransferase 1A Knockout Mice Are Predisposed to Liver Injury and Exhibit Increased Expression of Genes Involved in Proliferation. *Proceedings of the National Academy of Sciences of the United States of America* **2001**, *98*, 5560–5565, doi:10.1073/pnas.091016398.

124. Teng, Y.-W.; Cerdena, I.; Zeisel, S.H. Homocysteinemia in Mice with Genetic Betaine Homocysteine S-Methyltransferase Deficiency Is Independent of Dietary Folate Intake. *The Journal of Nutrition* **2012**, *142*, 1964–1967, doi:10.3945/jn.112.166835.

125. Caballero, F.; Fernández, A.; Matías, N.; Martínez, L.; Fucho, R.; Elena, M.; Caballeria, J.; Morales, A.; Fernández-Checa, J.C.; García-Ruiz, C. Specific Contribution of Methionine and Choline in Nutritional Nonalcoholic Steatohepatitis. *Journal of Biological Chemistry* **2010**, *285*, 18528–18536, doi:10.1074/jbc.M109.099333.

126. Vance, D.E. Phospholipid Methylation in Mammals: From Biochemistry to Physiological Function. *Biochimica et Biophysica Acta - Biomembranes* **2014**, *1838*, 1477–1487, doi:10.1016/j.bbamem.2013.10.018.

127. Vance, D.E. Physiological Roles of Phosphatidylethanolamine N-Methyltransferase. *Biochimica et Biophysica Acta (BBA) - Molecular and Cell Biology of Lipids* **2013**, *1831*, 626–632, doi:10.1016/j.bbalip.2012.07.017.

128. Sehayek, E.; Wang, R.; Ono, J.G.; Zinchuk, V.S.; Duncan, E.M.; Shefer, S.; Vance, D.E.; Ananthanarayanan, M.; Chait, B.T.; Breslow, J.L.; et al. Localization of the PE Methylation Pathway and SR-BI to the Canalicular Membrane: Evidence for Apical PC Biosynthesis That May Promote Biliary Excretion of Phospholipid and Cholesterol. *Journal of Lipid Research* **2003**, *44*, doi:10.1194/jlr.M200488-JLR200.

129. Wan, S.; Kuipers, F.; Havinga, R.; Ando, H.; Vance, D.E.; Jacobs, R.L.; van der Veen, J.N. Impaired Hepatic Phosphatidylcholine Synthesis Leads to Cholestasis in Mice Challenged With a High-Fat Diet: Hepatology Communications. *Hepatol Commun* **2019**, *3*, 262–276, doi:10.1002/hep4.1302.

130. Li, Z.; Agellon, L.B.; Vance, D.E. Phosphatidylcholine Homeostasis and Liver Failure. *Journal of Biological Chemistry* **2005**, *280*, 37798–37802, doi:10.1074/jbc.M508575200.

131. Walkey, C.J.; Yu, L.; Agellon, L.B.; Vance, D.E. Biochemical and Evolutionary Significance of Phospholipid Methylation. *Journal of Biological Chemistry* **1998**, *273*, 27043–27046, doi:10.1074/jbc.273.42.27043.

132. Pynn, C.J.; Henderson, N.G.; Clark, H.; Koster, G.; Bernhard, W.; Postle, A.D. Specificity and Rate of Human and Mouse Liver and Plasma Phosphatidylcholine Synthesis Analyzed in Vivo. *Journal of Lipid Research* **2011**, *52*, 399–407, doi:10.1194/jlr.D011916.

133. Watkins, S.M.; Zhu, X.; Zeisel, S.H. Phosphatidylethanolamine-N-Methyltransferase Activity and Dietary Choline Regulate Liver-Plasma Lipid Flux and Essential Fatty Acid Metabolism in Mice. *The Journal of nutrition* **2003**, *133*, 3386–3391, doi:10.1093/jn/133.11.3386.

134. Choudhary, N.S.; Duseja, A. Genetic and Epigenetic Disease Modifiers: Non-Alcoholic Fatty Liver Disease (NAFLD) and Alcoholic Liver Disease (ALD). *Transl Gastroenterol Hepatol* **2021**, *6*, 2–2, doi:10.21037/tgh.2019.09.06.

135. Pirazzi, C.; Adiels, M.; Burza, M.A.; Mancina, R.M.; Levin, M.; Ståhlman, M.; Taskinen, M.-R.; Orho-Melander, M.; Perman, J.; Pujia, A.; et al. Patatin-like Phospholipase Domain-Containing 3 (PNPLA3) I148M (Rs738409) Affects Hepatic VLDL Secretion in Humans and in Vitro. *Journal of Hepatology* **2012**, *57*, 1276–1282, doi:10.1016/j.jhep.2012.07.030.

136. Gunn, P.J.; Green, C.J.; Pramfalk, C.; Hodson, L. In Vitro Cellular Models of Human Hepatic Fatty Acid Metabolism: Differences between Huh7 and HepG2 Cell Lines in Human and Fetal Bovine Culturing Serum. *Physiol Rep* **2017**, *5*, e13532, doi:10.14814/phy2.13532.

137. Dong, H.; Wang, J.; Li, C.; Hirose, A.; Nozaki, Y.; Takahashi, M.; Ono, M.; Akisawa, N.; Iwasaki, S.; Saibara, T.; et al. The Phosphatidylethanolamine N-Methyltransferase Gene V175M Single Nucleotide Polymorphism Confers the Susceptibility to NASH in Japanese Population. *Journal of Hepatology* **2007**, *46*, 915–920, doi:10.1016/j.jhep.2006.12.012.

138. Sun, M.-Y.; Zhang, L.; Shi, S.-L.; Lin, J.-N. Associations between Methylenetetrahydrofolate Reductase (MTHFR) Polymorphisms and Non-Alcoholic Fatty

Liver Disease (NAFLD) Risk: A Meta-Analysis. *PLoS ONE* **2016**, *11*, e0154337, doi:10.1371/journal.pone.0154337.

139. Calvisi, D.F.; Simile, M.M.; Ladu, S.; Pellegrino, R.; De Murtas, V.; Pinna, F.; Tomasi, M.L.; Frau, M.; Virdis, P.; De Miglio, M.R.; et al. Altered Methionine Metabolism and Global DNA Methylation in Liver Cancer: Relationship with Genomic Instability and Prognosis. *International Journal of Cancer* **2007**, *121*, 2410–2420, doi:10.1002/ijc.22940.

140. Pascale, R.M.; Peitta, G.; Simile, M.M.; Feo, F. Alterations of Methionine Metabolism as Potential Targets for the Prevention and Therapy of Hepatocellular Carcinoma. *Medicina (Lithuania)* **2019**, *55*, 1–24, doi:10.3390/medicina55060296.

141. Frau, M.; Simile, M.M.; Tomasi, M.L.; Demartis, M.I.; Daino, L.; Seddaiu, M.A.; Brozzetti, S.; Feo, C.F.; Massarelli, G.; Solinas, G.; et al. An Expression Signature of Phenotypic Resistance to Hepatocellular Carcinoma Identified by Cross-Species Gene Expression Analysis. *Cellular Oncology* **2012**, *35*, 163–173, doi:10.1007/s13402-011-0067-z.

142. Frau, M.; Tomasi, M.L.; Simile, M.M.; Demartis, M.I.; Salis, F.; Latte, G.; Calvisi, D.F.; Seddaiu, M.A.; Daino, L.; Feo, C.F.; et al. Role of Transcriptional and Posttranscriptional Regulation of Methionine Adenosyltransferases in Liver Cancer Progression. *Hepatology* **2012**, *56*, 165–175, doi:10.1002/hep.25643.

143. Frau, M.; Feo, F.; Pascale, R.M. Pleiotropic Effects of Methionine Adenosyltransferases Deregulation as Determinants of Liver Cancer Progression and Prognosis. *Journal of Hepatology* **2013**, *59*, 830–841, doi:10.1016/j.jhep.2013.04.031.

144. Pascale, R.M.; Simile, M.M.; Calvisi, D.F.; Feo, C.F.; Feo, F. *S*-Adenosylmethionine: From the Discovery of Its Inhibition of Tumorigenesis to Its Use as a Therapeutic Agent. *Cells* **2022**, *11*, 409, doi:10.3390/cells11030409.

145. Anstee, Q.M.; Day, C.P. *S*-Adenosylmethionine (SAMe) Therapy in Liver Disease: A Review of Current Evidence and Clinical Utility. *Journal of Hepatology* **2012**, *57*, 1097–1109, doi:10.1016/j.jhep.2012.04.041.

146. Xu, D.; Shao, F.; Bian, X.; Meng, Y.; Liang, T.; Lu, Z. The Evolving Landscape of Noncanonical Functions of Metabolic Enzymes in Cancer and Other Pathologies. *Cell Metabolism* **2021**, *33*, 33–50, doi:10.1016/j.cmet.2020.12.015.

147. Yang, M.-H.; Liao, C.-C.; Hung, J.-H.; Lai, X.-T.; Yen, C.-H.; Chen, Y.-M.A. Utilizing Proteomic Approach to Identify Nuclear Translocation Related Serine Kinase Phosphorylation Site of GNMT as Downstream Effector for Benzo[a]Pyrene. *Journal of Food and Drug Analysis* **2019**, *27*, 603–609, doi:10.1016/j.jfda.2018.12.007.

148. Raha, A.; Reddy, V.; Houser, W.; Bresnick, E. Binding Characteristics of 4s PAH-binding Protein and *Ah* Receptor from Rats and Mice. *Journal of Toxicology and Environmental Health* **1990**, *29*, 339–355, doi:10.1080/15287399009531397.

149. SImile, M.M.; Feo, C.F.; Calvisi, D.F.; Pascale, R.M.; Feo, F. GNMT: A Multifaceted Suppressor of Hepatocarcinogenesis. *HR* **2021**, doi:10.20517/2394-5079.2020.162.

150. Bae, D.H.; Lane, D.J.R.; Jansson, P.J.; Richardson, D.R. The Old and New Biochemistry of Polyamines. *Biochimica et Biophysica Acta - General Subjects* **2018**, *1862*, 2053–2068, doi:10.1016/j.bbagen.2018.06.004.

151. Bekebrede, A.F.; Keijer, J.; Gerrits, W.J.J.; Boer, V.C.J. de The Molecular and Physiological Effects of Protein-Derived Polyamines in the Intestine. *Nutrients* **2020**, *12*, 197, doi:10.3390/nu12010197.

152. Bachmann, A.S.; Geerts, D. Polyamine Synthesis as a Target of MYC Oncogenes. *Journal of Biological Chemistry* **2018**, *293*, 18757–18769, doi:10.1074/jbc.TM118.003336.

153. Nebert, D.W.; Jensen, N.M.; Perry, J.W.; Oka, T. Association between Ornithine Decarboxylase Induction and the Ah Locus in Mice Treated with Polycyclic Aromatic Compounds. *Journal of Biological Chemistry* **1980**, *255*, 6836–6842.

154. Farrell, K.; Safe, S. 2,3,7,8-Tetrachlorodibenzo-p-Dioxin: Relationship between Toxicity and the Induction of Aryl Hydrocarbon Hydroxylase and Ornithine Decarboxylase. *Chemosphere* **1986**, *15*, 1971–1976, doi:10.1016/0045-6535(86)90494-7.

155. Raunio, H.; Pelkonen, O. *Effect of Polycyclic Aromatic Compounds and Phorbol Esters on Ornithine Decarboxylase and Aryl Hydrocarbon Hydroxylase Activities in Mouse Liver 1*; 1983; pp. 782–786;.

156. Potter, C.L.; Glenn Sipes, I.; Russell, D.H. Inhibition of Ornithine Decarboxylase Activity by 2,3,7,8-Tetrachlorodibenzo-p-Dioxin. *Biochemical Pharmacology* **1982**, *31*, 3367–3371, doi:10.1016/0006-2952(82)90613-X.

157. Thomas, T.; MacKenzie, S.A.; Gallo, M.A. Regulation of Polyamine Biosynthesis by 2,3,7,8-Tetrachlorodibenzo-p-Dioxin (TCDD). *Toxicology Letters* **1990**, *53*, 315–325, doi:10.1016/0378-4274(90)90236-F.

158. Bianchi-Smiraglia, A.; Bagati, A.; Fink, E.E.; Affronti, H.C.; Lipchick, B.C.; Moparthy, S.; Long, M.D.; Rosario, S.R.; Lightman, S.M.; Moparthy, K.; et al. Inhibition of the Aryl Hydrocarbon Receptor/Polyamine Biosynthesis Axis Suppresses Multiple Myeloma. *The Journal of Clinical Investigation* **2018**, *128*, doi:10.1172/JCI70712.

159. Nault, R.; Fader, K.A.; Lydic, T.A.; Zacharewski, T.R. Lipidomic Evaluation of Aryl Hydrocarbon Receptor-Mediated Hepatic Steatosis in Male and Female Mice Elicited by 2,3,7,8- Tetrachlorodibenzo-p-dioxin., doi:10.1021/acs.chemrestox.6b00430.

160. Birnbaum, L.S.; Mcdonald, M.M.; Blair, P.C.; Clark, A.M.; Harris, M.W. Differential Toxicity of 2,3,7,8-Tetrachlorodibenzo-p-Dioxin (TCDD) in C57BL/6J Mice Congenic at the Ah Locus. *Toxicological Sciences* **1990**, *15*, 186–200, doi:10.1093/toxsci/15.1.186.

161. Jones, G.; Greig, J.B. Pathological Changes in the Liver of Mice given 2,3,7,8-Tetrachlorodibenzo-p-Dioxin. *Experientia* **1975**, *31*, 1315–1317, doi:10.1007/BF01945801.

162. Fader, K.A.; Nault, R.; Ammendolia, D.A.; Harkema, J.R.; Williams, K.J.; Crawford, R.B.; Kaminski, N.E.; Potter, D.; Sharratt, B.; Zacharewski, T.R. 2,3,7,8-Tetrachlorodibenzo-p-Dioxin Alters Lipid Metabolism and Depletes Immune Cell Populations in the Jejunum of C57BL/6 Mice. *Toxicological Sciences* **2015**, *148*, 567–580, doi:10.1093/toxsci/kfv206.

163. Fader, K.A.; Nault, R.; Zhang, C.; Kumagai, K.; Harkema, J.R.; Zacharewski, T.R. 2,3,7,8-Tetrachlorodibenzo-p-Dioxin (TCDD)-Elicited Effects on Bile Acid Homeostasis: Alterations in Biosynthesis, Enterohepatic Circulation, and Microbial Metabolism. *Scientific Reports* **2017**, *7*, 5921, doi:10.1038/s41598-017-05656-8.

164. Fader, K.A.; Nault, R.; Kirby, M.P.; Markous, G.; Matthews, J.; Zacharewski, T.R. Convergence of Hepcidin Deficiency, Systemic Iron Overloading, Heme Accumulation, and REV-ERBα/β Activation in Aryl Hydrocarbon Receptor-Elicited Hepatotoxicity. *Toxicology and Applied Pharmacology* **2017**, *321*, 1–17, doi:10.1016/j.taap.2017.02.006.

165. Nault, R.; Fader, K.A.; Kopec, A.K.; Harkema, J.R.; Zacharewski, T.R.; Luyendyk, J.P. From the Cover: Coagulation-Driven Hepatic Fibrosis Requires Protease Activated Receptor-1 (PAR-1) in a Mouse Model of TCDD-Elicited Steatohepatitis. *Toxicological Sciences* **2016**, *154*, 381–391, doi:10.1093/toxsci/kfw175.

166. Ducker, G.S.; Rabinowitz, J.D. One-Carbon Metabolism in Health and Disease. *Cell Metabolism* **2016**, *25*, 27–42, doi:10.1016/j.cmet.2016.08.009.

167. Febbraio, M.A.; Reibe, S.; Shalapour, S.; Ooi, G.J.; Watt, M.J.; Karin, M. Preclinical Models for Studying NASH-Driven HCC: How Useful Are They? *Cell Metabolism* **2018**, *29*, 18–26, doi:10.1016/j.cmet.2018.10.012.

168. Boldyrev, A.A. Molecular Mechanisms of Homocysteine Toxicity. *Biochemistry (Moscow)* **2009**, *74*, 589–598, doi:10.1134/S0006297909060017.

169. Brooks, W.H. Increased Polyamines Alter Chromatin and Stabilize Autoantigens in Autoimmune Diseases. *Frontiers in Immunology* **2013**, *4*, 91, doi:10.3389/fimmu.2013.00091.

170. Pegg, A.E. Mammalian Polyamine Metabolism and Function. *IUBMB life* **2009**, *61*, 880–894, doi:10.1002/iub.230.

171. Mudd, S.H.; Ebert, M.H.; Scriver, C.R. Labile Methyl Group Balances in the Human: The Role of Sarcosine. *Metabolism: Clinical and Experimental* **1980**, *29*, 707–720, doi:10.1016/0026-0495(80)90192-4.

172. Tachikawa, M.; Ikeda, S.; Fujinawa, J.; Hirose, S.; Akanuma, S. ichi; Hosoya, K. ichi Γ-Aminobutyric Acid Transporter 2 Mediates the Hepatic Uptake of Guanidinoacetate, the Creatine Biosynthetic Precursor, in Rats. *PLoS ONE* **2012**, *7*, 32557, doi:10.1371/journal.pone.0032557.

173. Song, J.; Da Costa, K.A.; Fischer, L.M.; Kohlmeier, M.; Kwock, L.; Wang, S.; Zeisel, S.H. Polymorphism of the PEMT Gene and Susceptibility to Nonalcoholic Fatty Liver Disease (NAFLD). *FASEB Journal* **2005**, *19*, 1266–1271, doi:10.1096/fj.04-3580com.

174. Corbin, K.D.; Abdelmalek, M.F.; Spencer, M.D.; Da Costa, K.A.; Galanko, J.A.; Sha, W.; Suzuki, A.; Guy, C.D.; Cardona, D.M.; Torquati, A.; et al. Genetic Signatures in Choline and 1-Carbon Metabolism Are Associated with the Severity of Hepatic Steatosis. *FASEB Journal* **2013**, *27*, 1674–1689, doi:10.1096/fj.12-219097.

175. Kalhan, S.C.; Guo, L.; Edmison, J.; Dasarathy, S.; McCullough, A.J.; Hanson, R.W.; Milburn, M. Plasma Metabolomic Profile in Nonalcoholic Fatty Liver Disease. *Metabolism: Clinical and Experimental* **2011**, *60*, 404–413, doi:10.1016/j.metabol.2010.03.006.

176. Angrish, M.M.; Dominici, C.Y.; Zacharewski, T.R. TCDD-Elicited Effects on Liver, Serum, and Adipose Lipid Composition in C57BL/6 Mice. *Toxicological Sciences* **2013**, *131*, 108–115, doi:10.1093/toxsci/kfs277.

177. Kopec, A.K.; Boverhof, D.R.; Nault, R.; Harkema, J.R.; Tashiro, C.; Potter, D.; Sharratt, B.; Chittim, B.; Zacharewski, T.R. Toxicogenomic Evaluation of Long-Term Hepatic Effects of TCDD in Immature, Ovariectomized C57BL/6 Mice. *Toxicological Sciences* **2013**, *135*, 465–475, doi:10.1093/toxsci/kft156.

178. Birnbaum, L.S. Distribution and Excretion of 2,3,7,8-Tetrachlorodibenzo-p-Dioxin in Congenic Strains of Mice Which Differ at the Ah Locus. *Drug Metabolism and Disposition* **1986**, *14*, 34–40.

179. Nault, R.; Fader, K.A.; Ammendolia, D.A.; Dornbos, P.; Potter, D.; Sharratt, B.; Kumagai, K.; Harkema, J.R.; Lunt, S.Y.; Matthews, J.; et al. Dose-Dependent Metabolic Reprogramming and Differential Gene Expression in TCDD-Elicited Hepatic Fibrosis. *Toxicological Sciences* **2016**, *154*, 253–266, doi:10.1093/toxsci/kfw163.

180. Alcock, R.E.; Behnisch, P.A.; Jones, K.C.; Hagenmaier, H. Dioxin-Like PCBs in the Environment - Human Exposure and the Significance of Sources. *Chemosphere* **1998**, *37*, 1457–1472, doi:10.1016/S0045-6535(99)00137-X.

181. Choi, J.W.; Miyabara, Y.; Hashimoto, S.; Morita, M. Comparison of PCDD/F and Coplanar PCB Concentrations in Japanese Human Adipose Tissue Collected in 1970-1971, 1994-1996 and 2000. *Chemosphere* **2002**, *47*, 591–597, doi:10.1016/S0045-6535(02)00008-5.

182. Masuda, Y.; Schecter, A.; Päpke, O. Concentrations of PCBs, PCDFs and PCDDs in the Blood of Yusho Patients and Their Toxic Equivalent Contribution. *Chemosphere* **1998**, *37*, 1773–1780, doi:10.1016/S0045-6535(98)00242-2.

183. Päpke, O. PCDD/PCDF: Human Background Data for Germany, a 10-Year Experience. *Environmental Health Perspectives* **1998**, *106*, 723–731, doi:10.1289/ehp.98106723.

184. Shen, H.; Han, J.; Tie, X.; Xu, W.; Ren, Y.; Ye, C. Polychlorinated Dibenzo-p-Dioxins/Furans and Polychlorinated Biphenyls in Human Adipose Tissue from Zhejiang Province, China. *Chemosphere* **2009**, *74*, 384–388, doi:10.1016/j.chemosphere.2008.09.094.

185. Zober, A.; Päpke, O. Concentrations of PCDDs and PCDFs in Human Tissue 36 Years after Accidental Dioxin Exposure. *Chemosphere* **1993**, *27*, 413–418, doi:10.1016/0045-6535(93)90321-U.

186. Fader, K.A.; Nault, R.; Doskey, C.M.; Fling, R.R.; Zacharewski, T.R. 2,3,7,8-Tetrachlorodibenzo-p-Dioxin Abolishes Circadian Regulation of Hepatic Metabolic Activity in Mice. *Scientific Reports* **2019**, *9*, 1–18, doi:10.1038/s41598-019-42760-3.

187. Yan, J.; Tung, H.C.; Li, S.; Niu, Y.; Garbacz, W.G.; Lu, P.; Bi, Y.; Li, Y.; He, J.; Xu, M.; et al. Aryl Hydrocarbon Receptor Signaling Prevents Activation of Hepatic Stellate Cells and Liver Fibrogenesis in Mice. *Gastroenterology* **2019**, *157*, 793-806.e14, doi:10.1053/j.gastro.2019.05.066.

188. Lee, J.H.; Wada, T.; Febbraio, M.; He, J.; Matsubara, T.; Lee, M.J.; Gonzalez, F.J.; Xie, W. A Novel Role for the Dioxin Receptor in Fatty Acid Metabolism and Hepatic Steatosis. *Gastroenterology* **2010**, *139*, 653–663, doi:10.1053/J.GASTRO.2010.03.033.

189. Matsubara, T.; Tanaka, N.; Krausz, K.W.; Manna, S.K.; Kang, D.W.; Anderson, E.R.; Luecke, H.; Patterson, A.D.; Shah, Y.M.; Gonzalez, F.J. Metabolomics Identifies an Inflammatory Cascade Involved in Dioxin- and Diet-Induced Steatohepatitis. *Cell Metabolism* **2012**, *16*, 634–644, doi:10.1016/j.cmet.2012.10.006.

190. Kopec, A.K.; Burgoon, L.D.; Ibrahim-Aibo, D.; Burg, A.R.; Lee, A.W.; Tashiro, C.; Potter, D.; Sharratt, B.; Harkema, J.R.; Rowlands, J.C.; et al. Automated Dose-Response Analysis and Comparative Toxicogenomic Evaluation of the Hepatic Effects Elicited by TCDD, TCDF, and PCB126 in C57BL/6 Mice. *Toxicological Sciences* **2010**, *118*, 286–297, doi:10.1093/toxsci/kfq236.

191. Vance, D.E. Phospholipid Methylation in Mammals: From Biochemistry to Physiological Function. *Biochimica et Biophysica Acta - Biomembranes* **2014**, *1838*, 1477–1487, doi:10.1016/j.bbamem.2013.10.018.

192. Nault, R.; Fader, K.A.; Harkema, J.R.; Zacharewski, T. Loss of Liver-Specific and Sexually Dimorphic Gene Expression by Aryl Hydrocarbon Receptor Activation in C57BL/6 Mice. *PLoS ONE* **2017**, *12*, e0184842, doi:10.1371/journal.pone.0184842.

193. Carretero, M.V.; Latasa, M.U.; Garcia-Trevijano, E.R.; Corrales, F.J.; Wagner, C.; Mato, J.M.; Avila, M.A. Inhibition of Liver Methionine Adenosyltransferase Gene Expression by 3-Methylcolanthrene: Protective Effect of *S*-Adenosylmethionine. *Biochemical Pharmacology* **2001**, *61*, 1119–1128, doi:10.1016/S0006-2952(01)00590-1.

194. Luka, Z.; Mudd, S.H.; Wagner, C. Glycine N-Methyltransferase and Regulation of *S*-Adenosylmethionine Levels. *Journal of Biological Chemistry* **2009**, *284*, 22507–22511, doi:10.1074/jbc.R109.019273.

195. Frau, M.; Tomasi, M.L.; Simile, M.M.; Demartis, M.I.; Salis, F.; Latte, G.; Calvisi, D.F.; Seddaiu, M.A.; Daino, L.; Feo, C.F.; et al. Role of Transcriptional and Posttranscriptional Regulation of Methionine Adenosyltransferases in Liver Cancer Progression. *Hepatology* **2012**, *56*, 165–175, doi:10.1002/hep.25643.

196. Frau, M.; Feo, F.; Pascale, R.M. Pleiotropic Effects of Methionine Adenosyltransferases Deregulation as Determinants of Liver Cancer Progression and Prognosis. *Journal of Hepatology* **2013**, *59*, 830–841, doi:10.1016/j.jhep.2013.04.031.

197. Calvisi, D.F.; Simile, M.M.; Ladu, S.; Pellegrino, R.; De Murtas, V.; Pinna, F.; Tomasi, M.L.; Frau, M.; Virdis, P.; De Miglio, M.R.; et al. Altered Methionine Metabolism and Global DNA Methylation in Liver Cancer: Relationship with Genomic Instability and Prognosis. *International Journal of Cancer* **2007**, *121*, 2410–2420, doi:10.1002/ijc.22940.

198. Murray, B.; Barbier-Torres, L.; Fan, W.; Mato, J.M.; Lu, S.C. Methionine Adenosyltransferases in Liver Cancer. *World Journal of Gastroenterology* **2019**, *25*, 4300–4319, doi:10.3748/wjg.v25.i31.4300.

199. Pascale, R.M.; Peitta, G.; Simile, M.M.; Feo, F. Alterations of Methionine Metabolism as Potential Targets for the Prevention and Therapy of Hepatocellular Carcinoma. *Medicina (Lithuania)* **2019**, *55*, 1–24, doi:10.3390/medicina55060296.

200. Barić, I.; Fumić, K.; Glenn, B.; Ćuk, M.; Schulze, A.; Finkelstein, J.D.; James, S.J.; Mejaški-Bošnjak, V.; Pažanin, L.; Pogribny, I.P.; et al. *S*-Adenosylhomocysteine Hydrolase Deficiency in a Human: A Genetic Disorder of Methionine Metabolism. *Proceedings of the National Academy of Sciences of the United States of America* **2004**, *101*, 4234–4239, doi:10.1073/pnas.0400658101.

201. Teng, Y.-W.; Cerdena, I.; Zeisel, S.H. Homocysteinemia in Mice with Genetic Betaine Homocysteine S-Methyltransferase Deficiency Is Independent of Dietary Folate Intake. *The Journal of Nutrition* **2012**, *142*, 1964–1967, doi:10.3945/jn.112.166835.

202. Nault, R.; Fader, K.A.; Kirby, M.P.; Ahmed, S.; Matthews, J.; Jones, A.D.; Lunt, S.Y.; Zacharewski, T.R. Pyruvate Kinase Isoform Switching and Hepatic Metabolic Reprogramming by the Environmental Contaminant 2,3,7,8-Tetrachlorodibenzo-p-Dioxin. *Toxicological Sciences* **2016**, *149*, 358–371, doi:10.1093/toxsci/kfv245.

203. Mosharov, E.; Cranford, M.R.; Banerjee, R. The Quantitatively Important Relationship between Homocysteine Metabolism and Glutathione Synthesis by the Transsulfuration Pathway and Its Regulation by Redox Changes. *Biochemistry* **2000**, *39*, 13005–13011, doi:10.1021/bi001088w.

204. Finkelstein, J.D. Metabolic Regulatory Properties of *S*-Adenosylmethionine and *S*-Adenosylhomocysteine. *Clinical Chemistry and Laboratory Medicine* **2007**, *45*, 1694–1699, doi:10.1515/CCLM.2007.341.

205. Mudd, S.H.; Poole, J.R. Labile Methyl Balances for Normal Humans on Various Dietary Regimens. *Metabolism* **1975**, *24*, 721–735, doi:10.1016/0026-0495(75)90040-2.

206. Farrell, K.; Safe, S. 2,3,7,8-Tetrachlorodibenzo-p-Dioxin: Relationship between Toxicity and the Induction of Aryl Hydrocarbon Hydroxylase and Ornithine Decarboxylase. *Chemosphere* **1986**, *15*, 1971–1976, doi:10.1016/0045-6535(86)90494-7.

207. Nebert, D.W.; Jensen, N.M.; Perry, J.W.; Oka, T. Association between Ornithine Decarboxylase Induction and the Ah Locus in Mice Treated with Polycyclic Aromatic Compounds. *Journal of Biological Chemistry* **1980**, *255*, 6836–6842.

208. Raunio, H.; Pelkonen, O. Effect of Polycyclic Aromatic Compounds and Phorbol Esters on Ornithine Decarboxylase and Aryl Hydrocarbon Hydroxylase Activities in Mouse Liver. *Cancer Research* **1983**, *43*, 782–786.

209. Ruiz-Aracama, A.; Peijnenburg, A.; Kleinjans, J.; Jennen, D.; van Delft, J.; Hellfrisch, C.; Lommen, A. An Untargeted Multi-Technique Metabolomics Approach to Studying Intracellular Metabolites of HepG2 Cells Exposed to 2,3,7,8-Tetrachlorodibenzo-p-Dioxin. *BMC Genomics* **2011**, *12*, 251, doi:10.1186/1471-2164-12-251.

210. Jennen, D.; Ruiz-Aracama, A.; Magkoufopoulou, C.; Piejnenburg, A.; Lommen, A.; van Delft, J.; Kleinjans, J. Integrating Transcriptomics and Metabonomics to Unravel Modes-of-Action of 2,3,7,8- Tetrachlorodibenzo-p-Dioxin (TCDD) in HepG2 Cells. *BMC systems biology* **2011**, *5*, 1–13.

211. Thomas, T.; MacKenzie, S.A.; Gallo, M.A. Regulation of Polyamine Biosynthesis by 2,3,7,8-Tetrachlorodibenzo-p-Dioxin (TCDD). *Toxicology Letters* **1990**, *53*, 315–325, doi:10.1016/0378-4274(90)90236-F.

212. O'Brien, T.G.; Diamond, L. Ornithine Decarboxylase Induction and DNA Synthesis in Hamster Embryo Cell Cultures Treated with Tumor-Promoting Phorbol Diesters1. *Cancer Research* **1977**, *37*, 3895–3900.

213. Tamori, A.; Shuhei, N.; Tetsuo, K.; Shucihi, S.; Kobayshi, K.; Hiroaki, K.; Shuzo, O. Relationship of Ornithine Decarboxylase Activity and Histological Findings in Human Hepatocellular Carcinoma. *Japanese Journal of Clinical Oncology* **1994**, *20*, 1179–1187, doi:10.1093/oxfordjournals.jjco.a039694.

214. Stevens, A.P.; Dettmer, K.; Kirovski, G.; Samejima, K.; Hellerbrand, C.; Bosserhoff, A.K.; Oefner, P.J. Quantification of Intermediates of the Methionine and Polyamine Metabolism by Liquid Chromatography-Tandem Mass Spectrometry in Cultured Tumor Cells and Liver Biopsies. *Journal of Chromatography A* **2010**, *1217*, 3282–3288, doi:10.1016/j.chroma.2010.01.025.

215. Wyss, M.; Kaddurah-Daouk, R. Creatine and Creatinine Metabolism. *Physiological reviews* **2000**, *80*, 1107–1213, doi:10.1016/S1286-0115(06)74505-2.

216. Schmidt, A.; Marescau, B.; Boehm, E.A.; Jan Renema, W.K.; Peco, R.; Das, A.; Steinfeld, R.; Chan, S.; Wallis, J.; Davidoff, M.; et al. Severely Altered Guanidino Compound Levels, Disturbed Body Weight Homeostasis and Impaired Fertility in a Mouse Model of Guanidinoacetate N-Methyltrasferase (GAMT) Deficiency. *Human Molecular Genetics* **2004**, *13*, 905–921, doi:10.1093/hmg/ddh112.

217. Stöckler, S.; Marescau, B.; De Deyn, P.P.; Trijbels, J.M.F.; Hanefeld, F. Guanidino Compounds in Guanidinoacetate Methyltransferase Deficiency, a New Inborn Error of Creatine Synthesis. *Metabolism: Clinical and Experimental* **1997**, *46*, 1189–1193, doi:10.1016/S0026-0495(97)90215-8.

218. Liu, Q.; Cai, J.; Nichols, R.G.; Tian, Y.; Zhang, J.; Smith, P.B.; Wang, Y.; Yan, C.; Patterson, A.D. A Quantitative HILIC–MS/MS Assay of the Metabolic Response of Huh-7 Cells Exposed to 2,3,7,8-Tetrachlorodibenzo-p-Dioxin. *Metabolites* **2019**, *9*.

219. Beischlag, T. V; Luis Morales, J.; Hollingshead, B.D.; Perdew, G.H. The Aryl Hydrocarbon Receptor Complex and the Control of Gene Expression. *Critical reviews in eukaryotic gene expression* **2008**, *18*, 207–250.

220. Huang, G.; Elferink, C.J. A Novel Nonconsensus Xenobiotic Response Element Capable of Mediating Aryl Hydrocarbon Receptor-Dependent Gene Expression. *Molecular Pharmacology* **2012**, *81*, 338–347, doi:10.1124/mol.111.075952.

221. Muku, G.E.; Kusnadi, A.; Kuzu, G.; Tanos, R.; Murray, I.A.; Gowda, K.; Amin, S.; Perdew, G.H. Selective Ah Receptor Modulators Attenuate NPC1L1-Mediated Cholesterol Uptake through Repression of SREBP-2 Transcriptional Activity. *Laboratory Investigation* **2020**, *100*, 250–264, doi:10.1038/s41374-019-0306-x.

222. Tanos, R.; Patel, R.D.; Murray, I.A.; Smith, P.B.; Patterson, A.D.; Perdew, G.H. Aryl Hydrocarbon Receptor Regulates the Cholesterol Biosynthetic Pathway in a Dioxin Response Element-Independent Manner. *Hepatology* **2012**, *55*, 1994–2004, doi:10.1002/hep.25571.

223. Nault, R.; Doskey, C.M.; Fader, K.A.; Rockwell, C.E.; Zacharewski, T. Comparison of Hepatic NRF2 and Aryl Hydrocarbon Receptor Binding in 2,3,7,8-Tetrachlorodibenzo-p-Dioxin–Treated Mice Demonstrates NRF2-Independent PKM2 Induction. *Molecular Pharmacology* **2018**, *94*, 876–884, doi:10.1124/mol.118.112144.

224. Shen, D.; Dalton, T.P.; Nebert, D.W.; Shertzer, H.G. Glutathione Redox State Regulates Mitochondrial Reactive Oxygen Production. Journal of Biological Chemistry 2005, 280, 25305–25312, doi:10.1074/jbc.M500095200.

225. Pascale, R.M.; Feo, C.F.; Calvisi, D.F.; Feo, F. Deregulation of Methionine Metabolism as Determinant of Progression and Prognosis of Hepatocellular Carcinoma. Translational gastroenterology and hepatology 2018, 3, 36, doi:10.21037/tgh.2018.06.04.

CHAPTER 2: 2,3,7,8-TETRACHOLORDIBENZO-*P*-DIOXIN (TCDD) DYSREGULATES HEPATIC ONE CARBON METABOLISM DURING THE PROGRESSION OF STEATOSIS TO STEATOHEPATITIS WITH FIBROSIS IN MICE

Fling, R.R.; Doskey, C.M.; Fader, K.A.; Nault, R.; Zacharewski, T.R. 2,3,7,8-Tetrachlorodibenzo-p-Dioxin (TCDD) Dysregulates Hepatic One Carbon Metabolism during the Progression of Steatosis to Steatohepatitis with Fibrosis in Mice. *Sci Rep* **2020**, *10*, 14831, doi:10.1038/s41598-020-71795-0.

ABSTRACT

2,3,7,8-Tetrachlorodibenzo-*p*-dioxin (TCDD), a persistent environmental contaminant, induces steatosis that can progress to steatohepatitis with fibrosis, pathologies that parallel stages in the development of non-alcoholic fatty liver disease (NAFLD). Coincidently, one carbon metabolism (OCM) gene expression and metabolites are often altered during NAFLD progression. In this study, the time- and dose-dependent effects of TCDD were examined on hepatic OCM in mice. Despite AhR ChIP-seq enrichment at 2 hrs, OCM gene expression was not changed within 72 hrs following a bolus dose of TCDD. Dose-dependent repression of methionine adenosyltransferase 1A (*Mat1a*), adenosylhomocysteinase (*Achy*) and betaine-homocysteine S-methyltransferase (*Bhmt*) mRNA and protein levels following repeated treatments were greater at 28 days compared to 8 days. Accordingly, levels of methionine, betaine, and homocysteic acid were dose-dependently increased, while *S*-adenosylmethionine, *S*-adenosylhomocysteine, and cystathionine exhibited non-monotonic dose-dependent responses consistent with regulation by OCM intermediates and repression of glycine N-methyltransferase (*Gnmt*). However, the dose-dependent effects on SAM-dependent metabolism of polyamines and creatine could not be directly attributed to alterations in SAM levels. Collectively, these results demonstrate persistent AhR activation disrupts hepatic OCM metabolism at the transcript, protein, and metabolite levels within context of TCDD-elicited progression of steatosis to steatohepatitis with fibrosis.

INTRODUCTION

One carbon metabolism (OCM) comprises the interlinking methionine and folate cycles to provide one carbon units for biosynthetic reactions [1]. This includes the biosynthesis of *S*-adenosylmethionine (SAM), the primary cellular methyl donor for methyltransferase reactions, and the second most utilized enzymatic cofactor after ATP [2]. SAM is essential for the biosynthesis of several products required for maintaining and regulating cell structure and function

including creatine for ATP regeneration, phospholipids such as phosphatidylcholine for membrane integrity and lipid transport, and epigenetic gene regulation via the methylation of histones, DNA, and RNA [3,4]. In addition, decarboxylated SAM serves as the source of aminopropyl groups for polyamine biosynthesis which is important for cell growth, survival and proliferation [5].

Alterations in the levels of SAM, as well as related OCM metabolites, can have profound effects on cell growth, differentiation, response to injury, and tissue regeneration [1]. For example, SAM decreases homocysteine re-methylation by allosterically inhibiting betaine homocysteine methyltransferase (BHMT) in the methionine cycle and methylenetetrahydrofolate reductase (MTHFR) in the folate cycle while activating *S*-adenosylmethionine synthase isoform type-1 (MAT1A) and cystathionine β-synthase (CBS) in the transsulfuration pathway [6]. SAM also activates glycine N-methyltransferase (GNMT), a highly expressed hepatic enzyme that converts excess SAM levels to sarcosine to maintain methionine homeostasis [6]. Furthermore, methyltransferases are inhibited by the de-methylated product of SAM, *S*-adenosylhomocysteine (SAH). This includes GNMT which is regulated post-transcriptionally by phosphorylation and allosterically by 5-methyltetrahydrofolate [7]. Inhibition or reduction of OCM-related gene expression in humans or rodent models, as well as prolonged treatment of rodents with high fat diets, alcohol, or carbon tetrachloride, alter OCM metabolite levels during the development of chronic liver diseases comprising non-alcoholic fatty liver disease (NAFLD), cirrhosis, and hepatocellular carcinoma [8,9]. Interestingly, the severity of histopathological lesions in these disease models is alleviated following administration of SAM, betaine or creatine [10–12]. BHMT[13], GNMT [14], and MAT1A [15] knockout models exhibit NAFLD phenotypes with steatosis often progressing towards fibrosis and hepatocellular carcinoma. Phosphatidylethanolamine N-methyltransferase (PEMT) knockout mice have altered phosphatidylcholine levels and steatosis as well as compromised very low density lipoprotein (VLDL) assembly and impaired secretion [16,17]. Phosphatidylcholine biosynthesis via PEMT is

critical for hepatic lipid homeostasis for triglyceride packaging and VLDL particle assembly prior to export.

NAFLD, defined as a spectrum of hepatic disorders, begins as simple steatosis that may progress to steatohepatitis with cirrhosis. Underlying NAFLD increases the risk for more complex metabolic diseases including metabolic syndrome, diabetes, cardiovascular disease, and hepatocellular carcinoma. NAFLD is estimated to affect ~35% of the U.S. population and has emerged as a leading cause for liver transplant [18–21]. In addition to genetics, age, lifestyle, diet and circadian dysregulation, accumulating evidence suggests environmental contaminants may play an underappreciated role in NAFLD development and progression. For instance, 2,3,7,8-tetrachlorodibenzo-*p*-dioxin (TCDD) and related compounds dose-dependently induce the progression of steatosis to steatohepatitis with fibrosis in mice [22–24]. Exposure to TCDD and related compounds is also associated with dyslipidemia and altered glucose homeostasis and liver function in human epidemiological studies [25–28]. These effects are mediated by the aryl hydrocarbon receptor (AhR), a ligand activated basic helix-loop-helix/Per-Arnt-Sim transcription factor. Interestingly, the severity of NAFLD associated histopathologies is absent in AhR-null (*Ahr* $^{-/-}$) models and reduced in heterozygous (*Ahr* $^{+/-}$) models, as well as in mice expressing the weaker ligand binding *Ahr*^{d} allele [29–32].

Previous studies have shown TCDD alters the hepatic expression of genes associated with dyslipidemia, inflammation, and fibrosis as well as the regulation of the circadian clock [22,23,33]. However, there are a paucity of reports investigating the effects of TCDD on OCM. In this study, we tested the hypothesis that TCDD would elicit dose-dependent changes in OCM gene expression, protein levels, and metabolite levels consistent with the progression of NAFLD pathologies in mice. Our results show TCDD dose-dependently altered OCM metabolism and the SAM/SAH ratio, but effects on polyamine and creatine associated gene expression and metabolites levels could not be directly attributed to impacts on cellular methylation potential.

MATERIALS & METHODS

Animal treatment

Postnatal day 25 (PND25) male C57BL/6 mice weighing within 10% of each other were obtained from Charles River Laboratories (Kingston, NY) and housed and treated as previously described [22]. Briefly, mice were housed in Innovive Innocages (San Diego, CA) containing ALPHA-dri bedding (Shepherd Specialty Papers, Chicago, IL) in a 23°C environment with 30–40% humidity and a 12 hr/12 hr light/dark cycle. Aquavive water (Innovive) and Harlan Teklad 22/5 Rodent Diet 8940 (Madison, WI) were provided ad libitum. The rodent diet is a fixed formula complete diet with an energy density of 3.0 kcal/g and a nutrient ingredient composition including 22% protein, 5.5% fat, and 40.6% carbohydrate. Mice (PND29) were orally gavaged at the beginning of the light cycle with 0.1 ml sesame oil vehicle (Sigma-Aldrich, St. Louis, MO) or 0.01, 0.03, 0.1, 0.3, 1, 3, 10, and 30 µg/kg body weight TCDD (AccuStandard, New Haven, CT) every 4 days for either 2 (n=5) or 7 exposures (n=8). The first gavage was administered on day 0 of the study, while the final gavage was on day 4 and day 24 for the 8- and 28-day studies, respectively. On day 8 or day 28, vehicle- and TCDD-treated mice (fasted for 6 hr with access to water) were weighed and euthanized. For time course work, male mice were orally gavaged with a single bolus dose of 30 µg/kg TCDD and samples collected at 0, 2, 4, 8, 12, 24 and 72 hours (n=5). Upon collection, liver samples were immediately flash frozen in liquid nitrogen. Collected tissues were stored at -80°C until analysis. All animal handling procedures were performed with the approval of the Michigan State University (MSU) Institutional Animal Care and Use Committee, in accordance with ethical guidelines and regulations.

Metabolite standards

S-adenosylmethionine-$^{13}C_5$ (#A291533)**,** N1-acetylspermidine (#A187845**)**, putrescine-d_8 (#D416027), spermidine-d_6 (#S680407), spermine-d_{20} (#S680512) were purchased from Toronto Research Chemicals (Toronto, Ontario, Canada). *S*-Adenosylhomocysteine-d_4 (#13603),

spermidine (#14918) and spermine (#18041) were purchased from Cayman Chemical (Ann Arbor, MI). Putrescine (D13208), homocysteic acid (#44925), N,N-dimethylglycine (#05022), amino acid standards solution (A9906), and the cell free amino acid mixture-^{13}C,^{15}N (#767964) were purchased from Sigma-Aldrich. Standard calibration curves between 0.01-10 µM were constructed using serially diluted unlabeled standards with internal standards at 2 µM.

Metabolite extraction and sample processing

Metabolites were extracted from frozen liver samples using methods optimized for the specific metabolites of interest. SAM, SAH and one carbon metabolites (betaine, cystathionine, homocysteic acid, L-methionine, and N,N-dimethylglycine) were extracted from frozen liver using perchloric acid (PCA). Briefly, ~25 mg liver tissue was added to ice cold 0.4 M PCA containing internal standards (SAM-$^{13}C_5$, SAH-d_4, and cell free amino acid mixture-^{13}C,^{15}N) and homogenized for 15 seconds using a Polytron PT2100 homogenizer (Kinematica AG, Luzern, CH). The mixture was centrifuged for 10 min at 13,000 x g, after which the supernatant was removed, and the protein pellet was saved for protein quantification. Supersaturated potassium bicarbonate was added to the supernatant and centrifuged at 13,000 x g at 4° C. Half of the supernatant was removed (335 µl) for SAM & SAH quantification and diluted with perfluoroheptanoic acid to a final solution of 10 mM perfluoroheptanoic acid. The remaining supernatant was diluted with acetonitrile (AcN) to make a final 70:30 AcN:H_20 solution for one carbon metabolite analysis. A modified extraction and derivatization protocol was used for polyamine analysis [34]. Briefly, frozen samples (~25 mg) were homogenized using a Mixer Mill 300 tissue homogenizer with a metal bead in 600 µl of ice cold 0.4 M PCA spiked with putrescine-d_8, spermidine-d_6 and spermine-d_{20} internal standards. The mixture was centrifuged at 13,000 g for 10 min at 4° C. Supernatant (15 µl) was derivatized by adding 6% benzoyl chloride in AcN and vortexed every 15 min for 1 hr at room temperature. Potassium hydroxide (2M, KOH) was added to the tube along with 3.2 M formic acid for analysis. For creatine analysis, frozen liver samples

(~50 mg) were homogenized using a Mixer Mill 300 tissue homogenizer with 1000 µl of 70:30 methanol:water spiked with creatine-d_5, creatinine-d_3, and guanidinoacetate-d_2 and a metal bead in a 2 ml polypropylene tube and centrifuged for 10 min at 13,000 x g. The supernatant (100 µl) was dried down with nitrogen, reconstituted in 50 µl water, and added to 950 µl AcN. For extraction in serum or urine, 2 µl was added to 998 µl 95:5 AcN:water spiked with internal standards, centrifuged for 10 minutes at 13,000 x g, and the supernatant was used for further analysis.

Liquid chromatography tandem mass spectrometry

SAM and SAH were analyzed on a Waters Quattro Micro triple quadrupole mass spectrometer run in positive ionization mode with multiple reaction monitoring (MRM) attached to a Waters Acquity ultra-performance liquid chromatography (UPLC) system (Waters, Milford, MA) using a Waters Acquity HSS T3 column (1.8 µm particle size, 2.1x100mm, Waters, Milford, MA) at 40°C. Mobile phases consisted of 10 mM PFHA (solution A) and AcN (solution B). Additional OCM metabolites (betaine, cystathionine, homocysteic acid, L-methionine, and N,N-dimethylglycine) were measured on a Waters TQD triple quadrupole mass spectrometer run in positive ionization mode attached to a Waters Acquity UPLC system equipped with a Waters Acquity UPLC BEH amide column (1.7 µm particle size, 2.1x100mm, Waters, Milford, MA) held at 40 °C. Mobile phases consisted of 10 mM ammonium formate + 0.1% formic acid (solution A) and AcN (solution B). Creatine and derivatized polyamine extractions were analyzed on a Waters Xevo G2-XS QTof attached to a Waters Acquity UPLC using exact mass and retention times for identification and quantification of metabolites. Extracts were separated using a Waters Acuity UPLC BEH amide column (1.7 µm particle size, 2.1x100mm) held at 40°C. Mobile phases consisted of 10 mM ammonium formate (solution A) and AcN (solution B). The QTof was run in positive ionization mode with continuum data acquisition and leucine enkephalin used as the lockspray reference compound. The MS total useful signal (MSTUS) method was used to normalize urine samples [35]. Progenesis QI software (Waters, Milford, MA) was used to

determine total useful signal for each sample by summing metabolite peak areas common to all samples. Derivatized polyamine extracts were separated with a Waters Acquity UPLC BEH C18 column (1.7 µm particle size, 2.1x100mm) held at 30°C. The mobile phases were water containing 0.1% formic acid (solution A) and AcN (solution B). The QTof was run in positive ionization mode with continuum data acquisition and leucine enkephalin used as the lockspray reference compound. Liver extracts were normalized to total protein of each sample.

Protein quantification and capillary electrophoresis protein analysis.

Protein quantification and electrophoresis protein analysis were performed as previously published with slight modifications [33]. Briefly, Dried protein pellets from metabolic extractions were resuspended in 0.1 M KOH and quantified using a standard curve made with bovine serum albumin and the bicinchoninic acid (BCA) assay (Sigma-Aldrich). For OCM protein analysis, liver samples were homogenized in RIPA buffer supplemented with a protease inhibitor cocktail (Sigma-Aldrich) using a Polytron PT2100 homogenizer (Kinematica, Lucerne, Switzerland) and homogenized on ice. Samples were centrifuged and concentration measured using the BCA assay. The WES capillary electrophoresis system (ProteinSimple, San Jose, CA) was used with the following antibodies and dilutions from Abclonal (Cambridge, MA): AHCY (#A5300; 1:130), BHMT (#A6357; 1:300), CBS (#A1427; 1:100), GNMT (#A6608; 1:130), and MAT1A (#A6650; 1:200). Primary antibodies were detected using a polyclonal anti-rabbit secondary antibody conjugated to horseradish peroxidase. Chemiluminescence signal raw data was analyzed with the Compass Software (ProteinSimple, San Jose, CA). Target protein levels were normalized to total protein levels.

Gene Expression Analysis.

Hepatic RNA-seq data sets were previously published [22]**.** Genes were considered differentially expressed when |fold-change| ≥ 1.5 and posterior probability values (P1(t)) ≥ 0.8 as

determined by an empirical Bayes approach [36,37]. For figures, relative transcript counts represents the maximum raw number of aligned reads to each transcript across all treatments indicating the potential level of hepatic expression, where low level of expression ≤ 500 reads, and higher level of expression ≥ 10,000 reads. Sequencing data for the 72 hr time course and 28 day dose response study are available at the Gene Expression Omnibus (GEO; GSE109863 and GSE87519, respectively).

Hepatic gene expression in the 8-day study and renal gene expression in the 28 day study were assessed using quantitative real-time polymerase chain reaction (qRT-PCR). Total RNA was reverse transcribed by SuperScript II (Invitrogen) using oligo dT primer according to the manufacturer's protocol. PCR amplification was conducted on a Bio-Rad CFX Connect Real-Time PCR Detection System. Gene expression relative to vehicle control was calculated using the $2^{-\Delta\Delta CT}$ method. Liver samples were normalized to the housekeeping genes *ActB*, *Hprt*, and *Gapdh*. Kidney samples were normalized to *Gapdh*. Primer sequences are provided in Supplementary Table S1. BMD Express 2.0 [38] was used for benchmark dose response modeling to calculate benchmark dose lower confidence limits (BMDL) using parameters defined by Yang et al [39]. If the best fit model was sigmoidal, the ED_{50} value was calculated from sigmodal parameters used for the model fit.

ChIP and putative DRE identification

The AhR ChIP-seq data and computationally identified putative dioxin response elements (pDREs) were previously published [40]. Significant AhR ChIP-seq binding used a false discovery rate (FDR) ≤ 0.05. pDREs were considered functional with a matrix similarity score (MSS) ≥ 0.856. ChIP-seq data is available in the Gene Expression Omnibus (GSE97634).

RESULTS

TCDD elicited dose-dependent effects on OCM

AhR activation following acute or repeated treatment with TCDD elicits NAFLD pathologies in mice that include dose-dependent hepatic lipid accumulation, immune cell infiltration, and periportal fibrosis with bile duct proliferation occurring only in males [22,40–45]. Dysregulation of OCM, most notably SAM and SAH levels, is reported in human NAFLD and rodent models [2,9]. Gene expression, protein levels, and metabolite levels were integrated to further investigate the time and dose-dependent effects of TCDD on OCM including the SAM-dependent creatine and polyamine biosynthesis pathways.

To assess the effects of TCDD on SAM biosynthesis and metabolism (Figure 8a), gene expression, protein levels, and metabolite levels were analyzed in liver samples after mice were orally gavaged every 4 days for 8 or 28 days. At 8 days, TCDD elicited a dose-dependent decrease in the SAM/SAH ratio (Figure 8b). By 28 days, the SAM/SAH ratio exhibited a non-monotonic dose-response, with a decreasing trend between 0.3-10 µg/kg TCDD (Figure 8c). The effects on SAM and the SAM/SAH ratio are consistent with changes in OCM gene expression and protein levels. At 8 days, TCDD dose-dependently repressed *Mat1a* (BMDL 0.5 µg/kg; Figure 8c). At 28 days, TCDD repressed *Mat1a* 4.5-fold (BMDL 0.1 µg/kg). However, at 30 µg/kg TCDD, *Mat2a* was induced 2.1-fold while repressing highly expressed *Gnmt* (12.1-fold), a known regulator of SAM levels, and *Sardh* (19.6-fold), which catalyzes the oxidative demethylation of sarcosine back to glycine (Figure 8c). The dose-dependent decreases in MAT1A and GNMT protein levels were in agreement with respective gene repression (Figure 8d). In addition, other highly expressed SAM-dependent methyltransferases including guanidinoacetate N-methyltransferase (*Gamt*), indolethylamine N-methyltransferase (*Inmt)*, nicotinamide N-methyltransferase (*Nnmt*), and phosphatidylethanolamine N-methyltransferase (*Pemt*) were repressed 2.0-, 636.4-, 2.9- and 3.7-fold, respectively at 28 days (Figure 8c). The non-monotonic dose-response for the SAM/SAH ratio at 28 days likely involves dysregulation of *Mat1a* and *Mat2a*

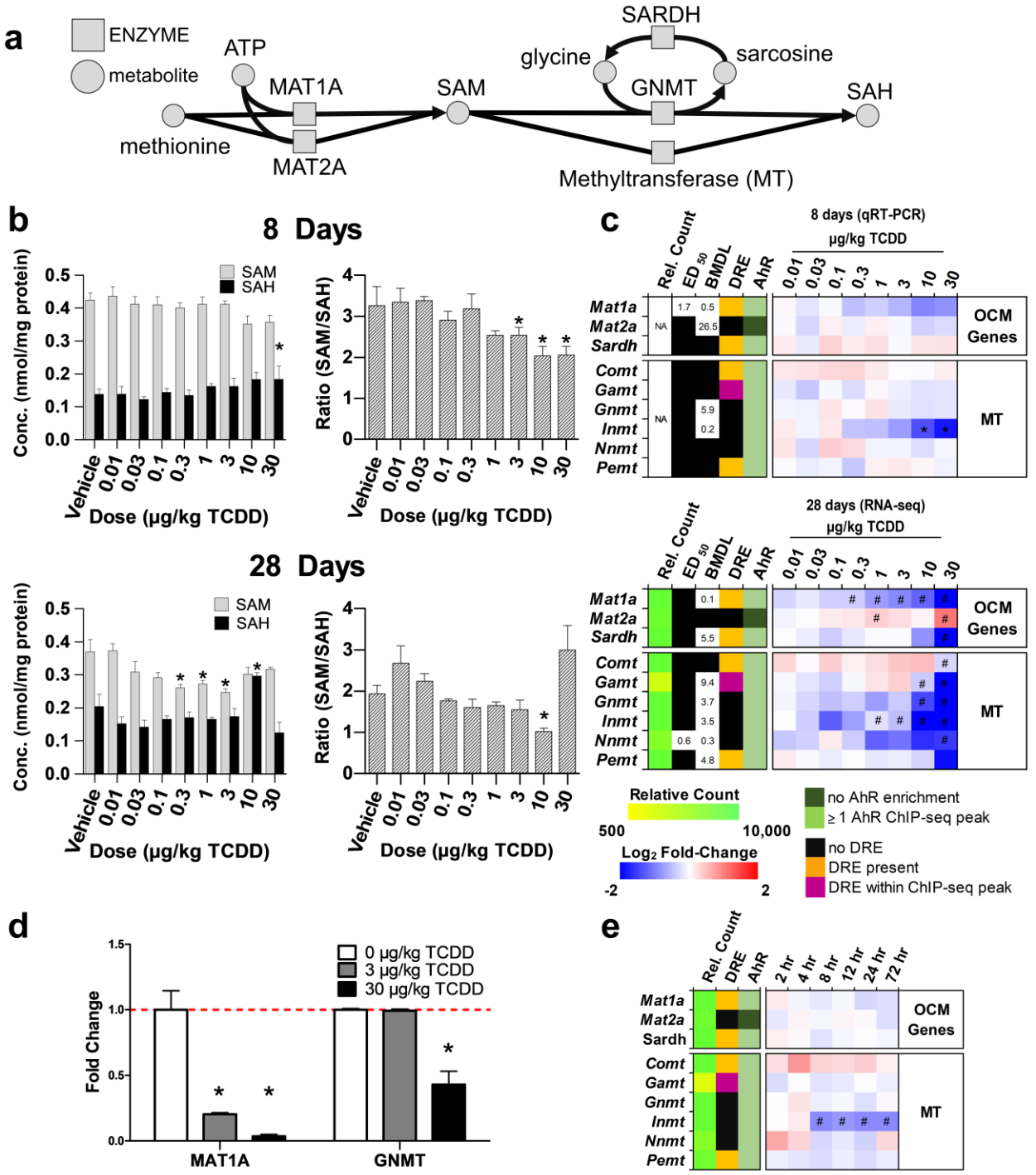

FIGURE 8. TCDD-ELICITED REPRESSION OF SAM BIOSYNTHESIS AND METHYLTRANSFERASE GENE EXPRESSION

a) Schematic pathway depicting enzymes (☐) and metabolites (○) associated with SAM biosynthesis and utilization by methyltransferases (MT). b) Hepatic levels of SAM and SAH were

FIGURE 8. (cont'd)

determined by LC-MS/MS (mean ± s.e.m., n=5-6) at 8 and 28 days of repeated TCDD exposure and c) hepatic gene expression of genes involved in the biosynthesis, regulation, and utilization of SAM and SAH were assessed at 8 and 28 days by RT-qPCR or RNA-seq, respectively (n=8). d) Fold change for hepatic MAT1A and GNMT protein levels after 28 days measured by the WES capillary electrophoresis system (mean ± s.e.m., n=4). e) Hepatic gene expression associated with SAM metabolism was determined by RNA-seq for a time-course after a bolus dose of 30 µg/kg TCDD (n=5). For the heatmaps, the median effective dose (ED_{50}) and benchmark dose lower limit (BMDL) and relative transcript count (rel. count,) are denoted. The red/blue color scale represents the log2(fold change) for differential gene expression. Orange represents the presence of putative dioxin response elements (pDREs). AhR enrichment peaks (FDR ≤ 0.05) are denoted by light green. pDREs found within AHR ChIP-seq enrichment peaks are denoted by garnet. Asterisks (*) denote $p < 0.05$ determined by one-way ANOVA with a Dunnett's post-hoc test. Pound signs (#) denote posterior probabilities P1(t) ≥ 0.80 compared to vehicle. *Official gene name and symbol, and metabolite abbreviations: catechol-O-methyltransferase (Comt), guanidinoacetate N-methyltransferase (Gamt), glycine N-methyltransferase (Gnmt), indolethylamine N-transferase (Inmt), S-adenosylmethionine synthase isoform 1a or 2a (Mat1a, Mat2a), nicotinamide N-methyltransferase (Nnmt), phosphatidylethanolamine N-methyltransferase (Pemt), sarcosine dehydrogenase (Sardh), S-adenosylmethionine (SAM), S-adenosylhomocysteine (SAH)*

expression, as well as the repression of *Gnmt*, in addition to the repression of SAM-dependent *Gamt*, *Inmt*, *Nnmt,* and *Pemt* methylation reactions (Figure 8b & c). Despite pDRE-independent AhR enrichment at 2 hrs for most of these genes, there was negligible gene repression within the first 72 hrs following treatment with 30 µg/kg TCDD (Figure 8e). Moreover, repression of the above genes was greater at 28 days compared to 8 days.

Other metabolites of the OCM and transsulfuration pathways (Figure 9) are important for methylation and were also affected by TCDD. Homocysteine is the product of SAH catabolism catalyzed by adenosylhomocysteine (AHCY) which was dose-dependently repressed by TCDD at the mRNA and protein levels in the absence of AhR enrichment (Figure 9b). Under normal conditions, BHMT uses betaine as a donor to methylate homocysteine in the re-synthesis of methionine, producing N,N-dimethylglycine as a byproduct. At 28 days, *Bhmt* mRNA and protein levels were dose-dependently repressed by TCDD (Figure 9b & c). Accordingly, there was a 2.6-fold increase in betaine and a non-significant 1.4-fold decrease in N,N-dimethylglycine (Figure 9d). Alternatively, homocysteine can enter the transsulfuration pathway. However, cystathionine β-synthase (*Cbs*) mRNA and protein levels were also dose-dependently repressed with a corresponding decrease in cystathionine levels (Figure 9b, c & e). At 28 days, cystathionine levels recovered following treatment with 10 and 30 µg/kg TCDD which may be due the allosteric activation of CBS by increasing SAM levels. Repression of BHMT in the methionine cycle and CBS in the transsulfuration pathway is consistent with the dose-dependent increase in homocysteic acid (Figure 9e), produced as a result of the spontaneous oxidation of accumulating homocysteine [46]. Collectively, these changes would be expected to reduce hepatic methionine levels, but they were increased 5.8-fold (Figure 9e). This may be due to increased methionine import with the induction of *Slcs 1a5*, *7a5*, *7a7*, *7a8*, *38a1*, *38a2* and *43a2*. *Slc3a2*, the heavy chain heterodimeric partner for many amino acid transporters, was also dose-dependently induced by TCDD and contained a ChIP-seq peak with a pDRE (Figure 9f).

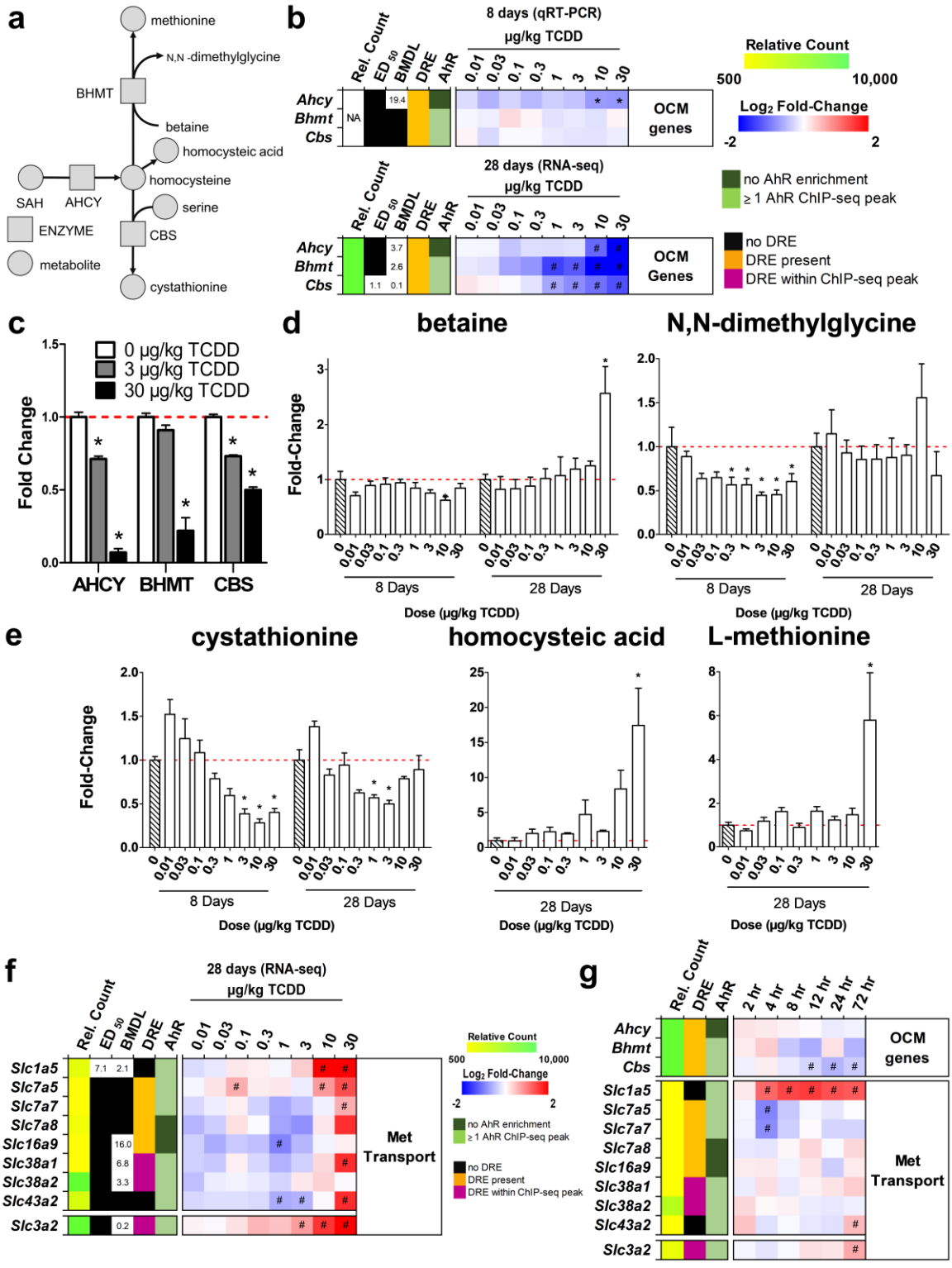

FIGURE 9. TCDD ELICITED EFFECTS ON THE HEPATIC METABOLISM OF HOMOCYSTEINE

FIGURE 9. (cont'd)

a) Schematic of pathway depicting enzymes and metabolites associated with homocysteine metabolism. Boxes represent enzymes and circles represent metabolites. b) Hepatic gene expression associated with homocysteine metabolism was measured at 8 or 28 days by qRT-PCR and RNA-seq, respectively (n=8). c) Hepatic protein levels (mean ± s.e.m.) were determined by capillary electrophoresis for AHCY, BHMT, and CBS in male mice at 28 days (n=4). d) Metabolite fold change at 8 days (mean ± s.e.m., n=3-6) or 28 days (mean ± s.e.m., n=4-5) were determined by LC-MS/MS for betaine, N,N-dimethylglycine and e) cystathionine (8 and 28 days), or methionine and homocysteic acid (28 days only). f) Hepatic gene expression of methionine transporters at 28 days (n=8). g) Hepatic gene expression associated with homocysteine metabolism was determined by RNA-seq for a time-course after a bolus dose of 30 µg/kg TCDD (n=5). For the heatmaps, the effective dose (ED_{50}), benchmark dose lower limit (BMDL), and relative transcript counts (rel. count) are denoted. The red/blue color scale represents the log2(fold change) for differential gene expression. Orange represents the presence of putative dioxin response elements (pDREs). AhR enrichment peaks (FDR ≤ 0.05) are denoted by light green. pDREs found within AHR ChIP-seq enrichment peaks are denoted by garnet. Asterisks (*) denote $p < 0.05$ determined by one-way ANOVA with a Dunnett's post-hoc test. Pound signs (#) denote posterior probabilities P1(t) ≥ 0.80 compared to vehicle. *Official gene name and symbol: adenosylhomocysteinase (Ahcy), betaine homocysteine methyltransferase (Bhmt), cystathionine beta-synthetase (Cbs)*

As observed with *Mat1a*, *Mat2a*, *Gnmt*, *Gamt*, *Inmt* and *Pemt*, the repression of *Ahcy* and *Bhmt* and *Cbs* was also negligible within the first 72 hrs following treatment with 30 µg/kg TCDD (Figure 9g). *Bhmt*, *Cbs, Slc1a5, 3a1, 7a5, 7a7, 7a8, 16a9,* and *43a2* also exhibited pDRE-independent AhR enrichment at 2hrs, while the ChIP-seq peaks for *Slc38a1* and *Slc38a2* did contain a pDRE within the enriched AhR bound region.

TCDD-elicited effects on polyamine metabolism

To further investigate the effects of TCDD-elicited alterations in the SAM/SAH ratio, subsequent effects on SAM-dependent pathways were examined. Polyamines are ubiquitous polycationic alkylamines that are crucial for a broad range of cellular functions including cell cycle modulation, scavenging reactive oxygen species, and the control of gene expression. *S*-adenosylmethionine decarboxylase (Amd1), which was modestly induced (1.6-fold at 3 µg/kg TCDD, Figure 10a), catalyzes the decarboxylation of SAM to produce decarboxylated SAM. The donation of the propylamine group from decarboxylated SAM to putrescine is catalyzed by spermine synthase (Srm) which was induced 2.5-fold at 30 µg/kg TCDD (Figure 10a). Surprisingly, putrescine levels, which are typically kept low within cells [47], were increased 8.0-fold at 30 µg/kg TCDD (Figure 10b), possibly due to the 1.9-fold induction of ornithine decarboxylase (Odc1), and the 2.3-fold repression of ornithine decarboxylase antizyme (Oaz1), which promotes ODC1 degradation (Figure 10a) [5]. There were also 1.6- and 2.2-fold increases in spermidine and N1-acetylspermidine at 30 µg/kg TCDD, respectively (Figure 10b). The 4.9-fold induction of the polyamine transporter, Slc22a3, and the 3.9-fold induction of spermine oxidase (Smox) at 30 µg/kg TCDD, which oxidizes spermine to spermidine, may also contribute to putrescine accumulation (Figure 10a). Like methionine and homocysteine metabolism, polyamine associated gene expression exhibited only moderate changes in the first 72 hours following a bolus dose of 30 µg/kg TCDD (Figure 10c). Collectively, TCDD dysregulated polyamine biosynthesis and transport, consistent with increased putrescine, spermidine and

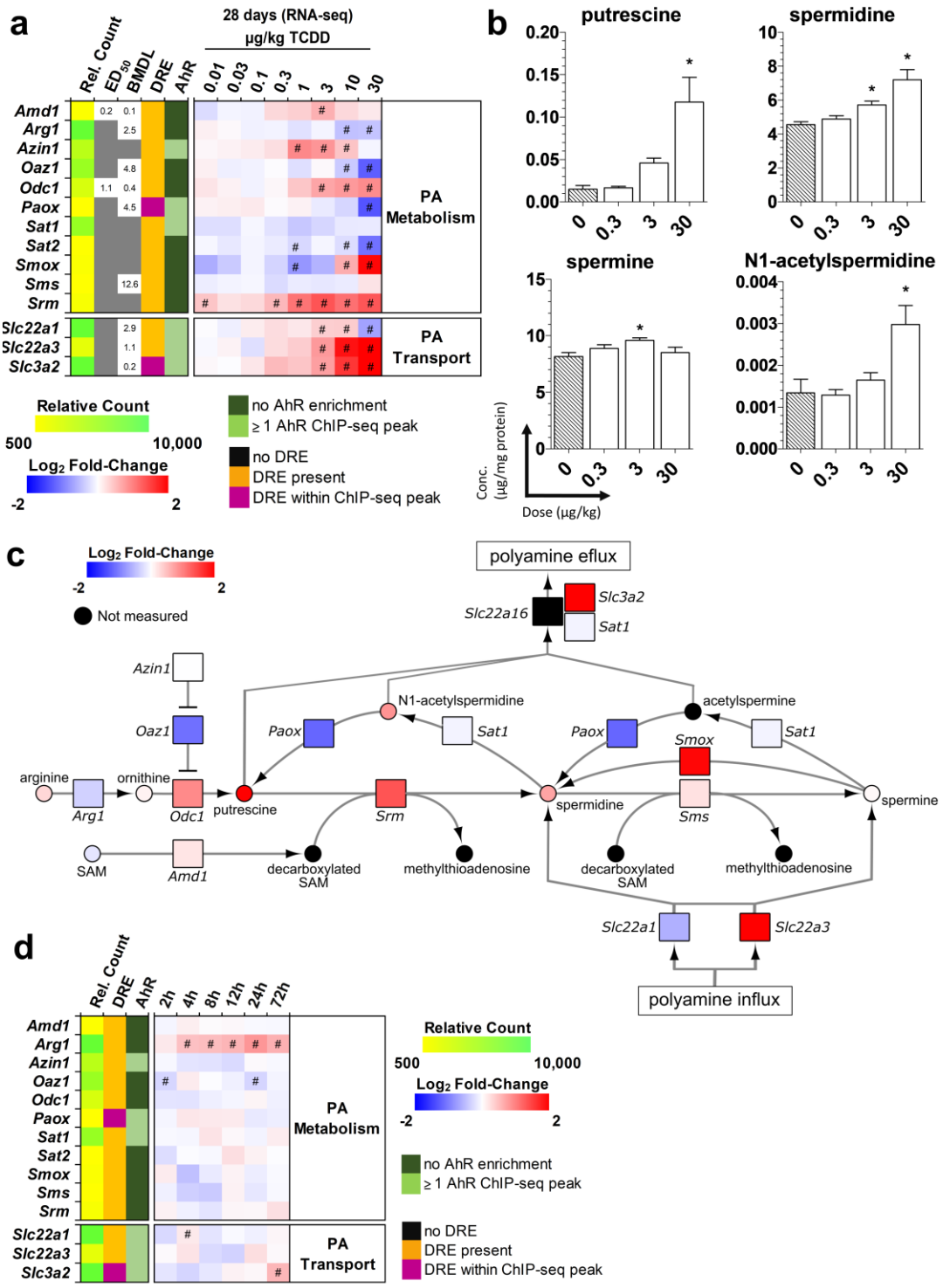

FIGURE 10. TCDD-ELICITED EFFECTS ON POLYAMINE (PA) BIOSYNTHESIS

a) Hepatic gene expression associated with PA metabolism was examined using RNA-seq at 28 days repeated TCDD exposure (n=8). b) Hepatic PA levels were determined by LC-MS/MS at 28

F**igure 10. (cont'd)**

days repeated TCDD exposure (mean ± s.e.m. n=5). c) Hepatic gene expression associated with polyamine metabolism was determined by RNA-seq for a time-course after a bolus dose of 30 µg/kg TCDD. d) Schematic pathway of hepatic polyamine biosynthesis incorporating fold changes of metabolites (◯) and gene expression (□) in male mice orally gavaged with sesame oil vehicle or 30 µg/kg TCDD every 4 days for 28 days. Fold changes of metabolites and gene expression were determined by LC-MS/MS or RNA-seq, respectively. For the heatmaps, the effective dose (ED_{50}), benchmark dose lower limit (BMDL), and relative transcript count (Rel. Count) are denoted. The red/blue color scale represents the log2(fold change) for differential gene expression. Orange represents the presence of putative dioxin response elements (pDREs). AhR enrichment peaks (FDR ≤ 0.05) are denoted by light green. pDREs found within AHR ChIP-seq enrichment peaks are denoted by garnet. Asterisks (*) denote *$p < 0.05$ determined by one-way ANOVA with a Dunnett's post-hoc test. Pound signs (#) denote posterior probabilities $P1(t) \geq 0.80$ compared to vehicle.). *Official gene name and symbol, and metabolite abbreviations: S-adenosylmethionine decarboxylase (Amd1), antizyme inhibitor 1 (Azin1), ornithine decarboxylase antizyme 1 (Oaz1), ornithine decarboxylase (Odc1), L-ornithine (ORN), peroxisomal N1-acetyl-spermine/spermidine oxidase (Paox), polyamine (PA), spermine/spermidine acetyltransferase (Sat1 & 2), 4F2 cell-surface antigen heavy chain (Slc3a2), spermidine synthase (Srm), spermine synthase (Sms), spermine oxidase (Smox), S-adenosylmethionine (SAM), decarboxylated SAM (Decarbox-SAM), methylthioadenosine (MTA)*

N1-acetylspermidine levels (Figure 10d).

TCDD elicited effects on creatine metabolism

The consequences of OCM dysregulation on SAM-dependent creatine biosynthesis were also assessed. Creatine biosynthesis begins in the kidneys where mitochondrial glycine amidinotransferase (Gatm aka Agat) transfers a guanidino group from arginine (ARG) to glycine (GLY) to produce guanidinoacetate (GAA) (Figure 11a). In the liver, GAA is methylated to form creatine by guanidinoacetate N-methyltransferase (Gamt) which is reported to consume 60% of hepatic SAM [48]. At 28 days, TCDD increased renal Gatm (1.8-fold) and decreased hepatic Slc6a13 (6.3-fold), a guanidinoacetate transporter [49], and hepatic Gamt (20.0-fold) (Figure 11a & b). This coincided with increases in serum GAA levels (Figure 11c). The modest 1.3-fold increase in hepatic creatine levels was accompanied by a 3.0-fold increase in the creatine importer Slc6a8 (ED_{50}: 3.4 µg/kg TCDD, 3.0-fold), while urinary creatinine decreased 1.5-fold (trending). Despite DRE-dependent AhR enrichment in Gamt, no changes in gene expression were observed up to 72 hr following treatment (Figure 11d). These results suggest TCDD-elicited repression of Gamt caused systemic increases in GAA levels at 28 days.

DISCUSSION

Alterations in OCM, including human polymorphisms, correlate with NAFLD progression and severity [50–52]. Previous work has shown that persistent AhR activation by TCDD induces a NAFLD-like phenotype that includes hepatic fat accumulation, inflammation, and mild fibrosis in mice [22,41,45,53]. However, the effects of TCDD on OCM within the context of this NAFLD model have not been comprehensively investigated. Herein, we show TCDD dose-dependently alters

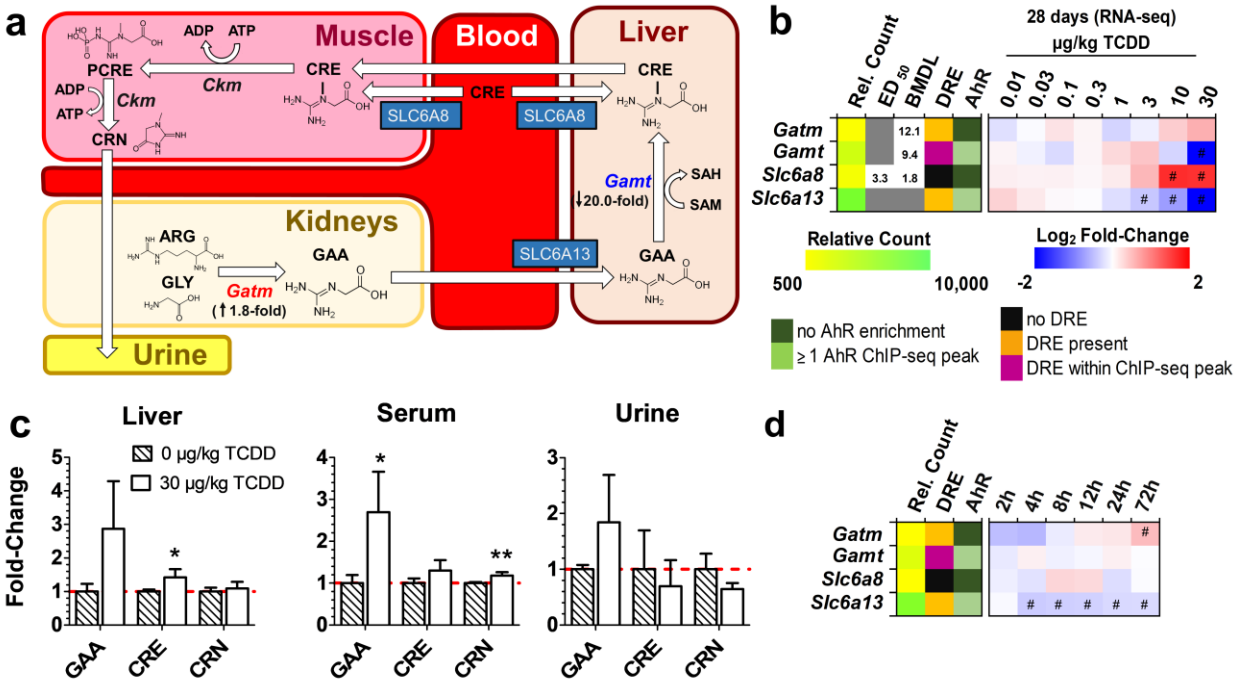

FIGURE 11. TCDD-ELICITED DOSE-DEPENDENT EFFECTS ON CREATINE BIOSYNTHESIS.

a) Schematic of systemic creatine biosynthesis and transport. For 30 µg/kg TCDD treatment groups, renal Gatm expression and hepatic Gamt fold-changes from vehicle are denoted. b) Hepatic gene expression associated with creatine metabolism at 8 or 28 days following repeated TCDD exposure. c) Guanidinoacetate (GAA)-, creatine (CRE)-, and creatinine (CRN)-fold changes determined by LC-MS/MS in male mice orally gavaged with sesame oil vehicle or 30 µg/kg TCDD every 4 days for 28 days (mean ± s.e.m., n=5). d) Hepatic expression associated with creatine metabolism in male mice orally gavaged with a bolus dose of 30 µg/kg TCDD (n=8). For the heatmaps, the effective dose (ED_{50}), benchmark dose lower limit (BMDL), and relative transcript count (Rel. Count) are denoted. The red/blue color scale represents the log2(fold change) for differential gene expression. Orange represents the presence of putative dioxin response elements (pDREs) with a matrix similarity scores (MSS) ≥ 0.856. AhR enrichment peaks (FDR ≤ 0.05) denoted by light green were determined by ChIP-seq. pDREs found within AHR ChIP-seq enrichment peaks are denoted by garnet. Asterisks denote (*) $p < 0.05$ or (**) $p < 0.01$ determined by one-way ANOVA with a Dunnett's post-hoc test. Pound signs (#) denote posterior

Figure 11. (cont'd)

probabilities P1(t) ≥ 0.80 compared to vehicle. *Official gene name and symbol, and metabolite abbreviations: guanidinoacetate N-methyltransferase (Gamt), glycine amidinotransferase, mitochondrial (Gatm), creatine kinase M-type (Ckm), arginine (ARG), glycine (GLY), guanidinoacetate (GAA),creatine (CRE), and creatinine (CRN), phosphocreatine (PCRE)*

OCM at the transcript, protein, and metabolite levels. The SAM/SAH ratio, an indicator of methylation potential, and creatine and polyamine biosynthesis pathways were altered.

In this study, TCDD is used as a surrogate for the cumulative burden of all AhR ligands. Mice were orally gavaged with 0.01 – 30 µg/kg TCDD starting at post-natal day 28 with TCDD every 4 days for 8 and 28 days to approach steady state levels due to the 8-12 day half-life of TCDD in mice [24,54]. Using this dosing regimen, oral gavage of 30 µg/kg TCDD resulted in mouse hepatic tissue levels comparable to serum levels reported in Viktor Yushchenko following intentional poisoning, while 0.01 µg/kg TCDD increased hepatic levels compared to background levels in control mouse liver, and were comparable to the level of dioxin-like compounds in the serum of US, German, Spanish and United Kingdom populations [23,55–60]. Similar doses and/or treatment regimens have been used in previous studies from this lab as well as other groups [33,44,61–63]. Although there was an increase in serum ALT levels following oral gavage with 30 µg/kg TCDD every 4 days for 28 days for a total of 7 treatments, there was no evidence of overt toxicity, no body weight loss >15%, no significant change in food consumption, and no histopathological evidence of necrosis or apoptosis [23,33,64]. Consequently, the dose-dependent effects of TCDD on OCM, the SAM/SAH ratio and the biosynthesis of polyamines and creatine cannot be attributed to overt toxicity.

Mat1a is highly expressed in the adult liver making it the major site of SAM biosynthesis. As the primary methyl group donor for methyltransferase reactions, hepatic SAM and SAH levels are maintained in a narrow range with increases or decreases the SAM/SAH ratio outside this window potentially affecting numerous cell functions [2,65]. Our studies show TCDD dose-dependently repressed *Mat1a* mRNA and protein levels (Figure 8c & d), as previously reported with other AhR ligands [66,67]. TCDD also altered the SAM/SAH ratio with trends suggesting SAM levels decreased while SAH levels increased at higher doses at 8 days (Figure 8b). A similar trend was observed at 28 days, except for a reproducible increase in the SAM/SAH ratio at 30

μg/kg TCDD (Figure 8b) that coincided with the induction of *Mat2a* and the repression of several highly expressed methyl transferases including GNMT (Figure 12a). GNMT is the most abundant hepatic methyltransferase that acts as a sink by transferring methyl groups from SAM to glycine to reduce SAM levels in order to regulate methionine consumption and SAM levels [7]. Interestingly, repression of *Mat1a* with the induction of *Mat2a*, which is usually only expressed during liver development, is characteristic of NAFLD and aggressive hepatocellular carcinoma progression [68–72].

SAH is a potent competitive methyltransferase inhibitor [73]. It is readily metabolized by AHCY to adenosine and homocysteine (not measured in our analysis) to allow OCM to proceed. However, AHCY mRNA and protein levels were dose-dependently repressed by TCDD (Figure 9b & c). Homocysteine can be re-methylated back to methionine by BHMT or MTR which catalyzes the transfer of a methyl group from betaine or 5-methyltetrahydrofolate, respectively. In mice, BHMT is highly expressed in the liver and is the primary methionine biosynthesis pathway [74]. TCDD dose-dependently repressed BHMT coincident with an increase in betaine and decrease in N,N-dimethylglycine (Figure 9c & d). An alternative pathway to re-methylation, homocysteine can be converted to cystathionine by CBS, which would undergo further metabolism by cystathionine gamma-lyase to produce cysteine and support glutathione biosynthesis. However, TCDD dose-dependently repressed *Cbs* mRNA and protein levels, and reduced cystathionine levels (Figure 9b, c & e). CBS activity may also be further allosterically repressed by TCDD induced oxidative stress [75,76]. The partial recovery of cystathionine levels at higher TCDD doses is consistent with *Mat2a* induction with increased SAM levels allosterically activating CBS [6]. Consequently, homocysteine is not consumed in the transsulfuration pathway or by re-methylation to methionine, and undergoes oxidation as indicated by the increase in homocysteic acid levels, the spontaneous oxidation product of homocysteine (Figure 9e). Despite BHMT transcriptional repression and inhibition by SAM, hepatic methionine levels increased due

to the induction of transporters, and the repression of *Mat1a* and major methyltransferases that consume SAM (Figure 12).

Given TCDD affected OCM, we next examined the potential consequences of an altered SAM/SAH ratio on polyamine and creatine biosynthesis. Polyamines are low molecular weight aliphatic polycations present in all living cells. *De novo* synthesis, interconversion, degradation and transport ensure levels of putrescine, spermidine and spermine are maintained in a narrow range since low levels inhibit cell proliferation and high levels or catabolic byproducts are toxic [5,47]. Approximately 5% of hepatic SAM is used to produce polyamines [48,77]. Consistent with previous reports that TCDD increases ODC activity, our results showed TCDD increased *Odc* expression and disrupted polyamine biosynthesis [78–80], in contrast to short term studies that reported TCDD decreased polyamine levels [81–83]. Adaptive compensatory responses such as increased *Smox* expression, catalyzing the interconversion of spermine to spermidine, and the differential expression of transporters, may partially explain the different effects of TCDD on polyamine levels we observed after 28 days of treatment (Figure 10). The increase in putrescine by TCDD is comparable to levels induced by 12-O-tetradecanoylpphorbol-13-acetate (TPA), an inducer of ODC activity [84–86]. Putrescine levels are normally low when demand for polyamines are low due to multiple levels of ODC activity regulation and the allosteric activation of SAM decarboxylase (AMD1) [5]. Yet, putrescine levels increased despite the TCDD-elicited dose-dependent induction of *Odc* and spermidine synthase (*Srm*) suggesting decarboxylated SAM may be limiting (Figure 10a & b). Paradoxically, there was an increase in spermidine and N1-acetylspermidine levels with negligible effects on spermine levels possibly due to interconversion and/or transport to maintain cellular polyamine homeostasis.

Phosphocreatine is an important phosphate donor that can quickly regenerate ATP via substrate level phosphorylation reactions. As much as 70% of hepatic SAM is consumed in creatine biosynthesis, although hepatic levels are low with >90% of creatine stored in muscle [87].

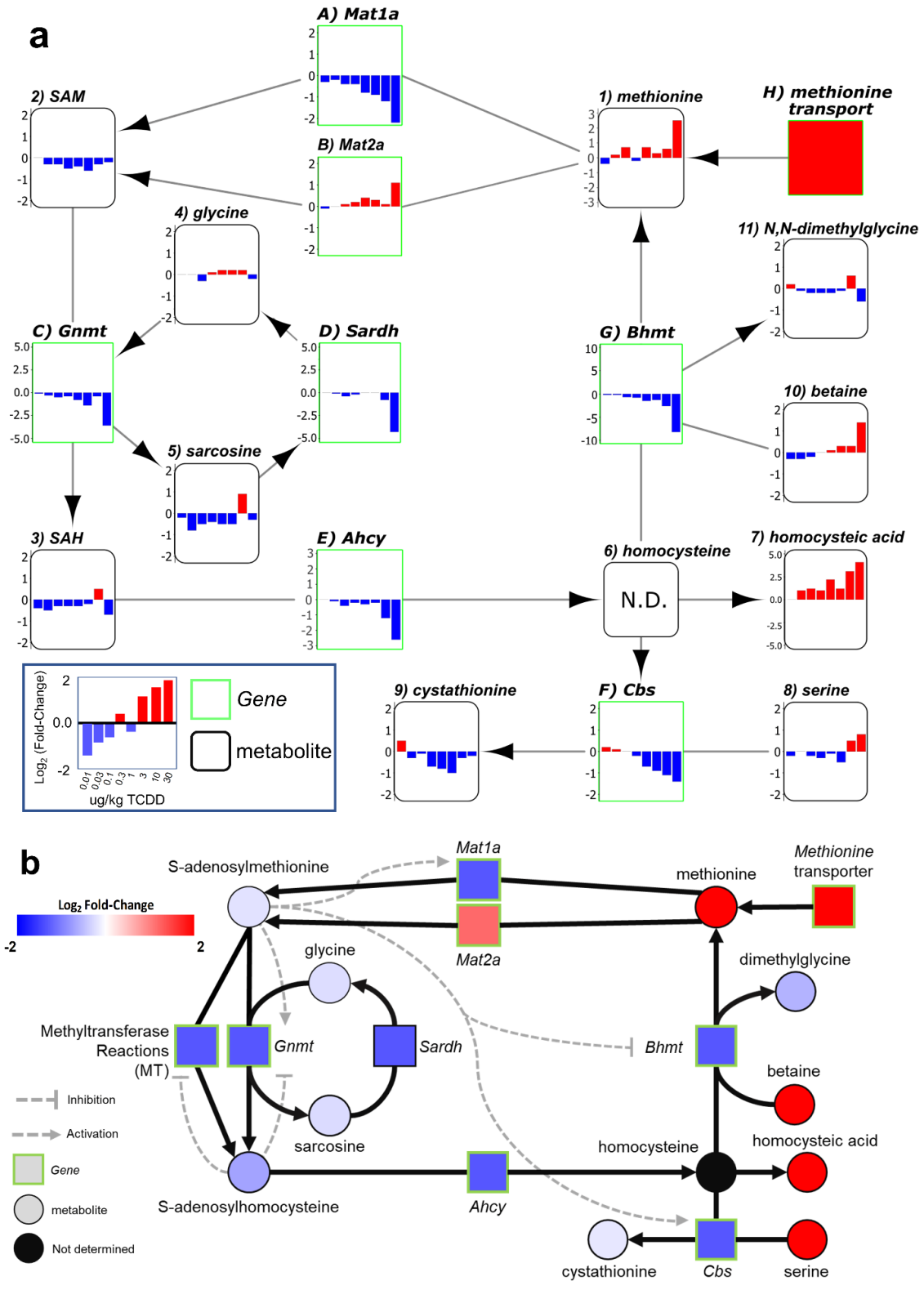

FIGURE 12. SUMMARY OF EFFECTS OF TCDD ON OCM GENE EXPRESSION AND METABOLITES

FIGURE 12. (cont'd)

a) OCM pathway schematic depicting dose response effects of TCDD on gene expression (green rectangles labelled A-H) and metabolite levels (black rounded rectangles labelled 1-11) in male C57BL/6 mice at 28 days repeated TCDD exposure. Gene expression and metabolite levels were determined by RNA-seq or LC-MS/MS, respectively. Homocysteine levels were not determined (N.D.). The Log2(fold change) range is denoted on left y-axis of each box and the bar colors represents red as induced and blue as repressed. b) OCM pathway schematic depicting changes in gene expression and metabolite levels in male C57BL/6 mice orally gavaged with sesame oil vehicle or 30 µg/kg TCDD every 4 days for 28 days. Inhibition or activation of enzymes in pathway are indicated by grey dashed lines. Changes in genes expression and metabolite levels were determined by RNA-seq or LC-MS/MS, respectively. Green boxes represent genes and black circles represent metabolites. The Log2(fold change) represents red as induced and blue as repressed. *Official gene name and symbol: a. S-adenosylmethionine synthase isoform 1a (Mat1a), b. S-adenosylmethionine synthase isoform 2a(Mat2a), c. glycine N-methyltransferase (Gnmt), d. sarcosine dehydrogenase (Sardh), e. adenosylhomocysteinase (Ahcy), f. cystathionine beta-synthetase (Cbs), g. betaine homocysteine methyltransferase (Bhmt), h. solute carrier family (Slc1a5, 7a5, 7a7, 7a8, 16a9, 38a1, 38a2, and 43a2)*

TCDD increased renal *Gatm* expression while repressing hepatic *Gamt* with modest effects on the levels of creatine and creatinine despite an increase in serum GAA (Figure 11) comparable to levels reported in GAMT$^{-/-}$ mice and humans deficient in GAMT activity [88,89]. TCDD also decreased creatinine levels in short-term *in vitro* studies [82,90]. Similar to polyamines, adaptive responses following prolonged TCDD exposure may account for the modest changes in hepatic creatine and creatinine levels despite the repression of *Gamt.* For instance, induction of the creatine importer, *Slc6a8,* in the liver was only observed after 28 days of treatment (Figure 11b). Collectively, the SAM-dependent biosynthesis of both creatine and polyamine demonstrated differential gene expression and metabolite levels. Despite disruption of OCM by TCDD, the effects on polyamine and creatine biosynthesis cannot be adequately explained due to alterations on the SAM/SAH ratio alone.

Many genes associated with OCM and the transsulfuration pathway exhibited BMDLs in the sub to low µg/kg range only after 8 and 28 days of treatment. In addition, OCM and transsulfuration pathway disruption was time-dependent with the greatest effects after 28 days, more modest changes at 8 days and modest effects following a single bolus dose. The canonical mechanism of action of TCDD and related compounds involves binding to the cytoplasmic AhR, translocation to the nucleus, and heterodimerization with ARNT. The ligand-bound AhR/ARNT complex then binds to DREs within the promoter region of target genes, leading to recruitment of transcriptional co-regulators and differential gene expression [91]. Numerous studies have also reported differential gene expression following AhR binding within DNA regions lacking a DRE [92–94]. Despite ChIP-seq evidence of AhR enrichment at 2 hrs, only modest changes in OCM gene expression were observed in the first 72 hrs after treatment. In contrast, AhR targets such as *Cyp1a1, Cyp1a2* and *Tiparp* were induced within 2 hrs [95]. Moreover, many differentially expressed OCM genes exhibited AhR genomic enrichment in the absence of a pDRE. Collectively, these results suggest that (i) although AhR activation is required, it in itself is not

sufficient and likely requires unknown additional responses, (ii) TCDD-elicited OCM disruption involves DRE-dependent and –independent changes in gene expression, and (iii) the effects of TCCD are not immediate and require persistent AhR activation.

Given that OCM and transsulfuration pathway enzyme activity is subject to allosteric activation and competitive inhibition by intermediate metabolites (Figure 12b), and are regulated by post-translational modification, more integrative approaches such as tracer studies are required to identify the key steps affected by TCDD that alter the flux of ^{13}C-labelled intermediates through OCM and its associated pathways. Moreover, an examination of other SAM-dependent reactions would expand our understanding of additional OCM mechanisms disrupted by TCDD such as the methylation of histones, DNA, and RNA associated with epigenetic regulation, and the biosynthesis of phosphatidylcholine via the PEMT and Kennedy pathways. Phosphatidylcholine is not only critical for membrane integrity, but also the secretion of very low-density lipoprotein (VLDL) [2,65]. Interestingly, the inhibition of VLDL secretion by TCDD contributes to steatosis in mice [41,53]. Additional studies are required to determine the relevance of these effects in humans due to the species-specific effects of TCDD and related compounds.

REFERENCES

REFERENCES

1. Walker, A.K. 1-Carbon Cycle Metabolites Methylate Their Way to Fatty Liver. Trends in endocrinology and metabolism: TEM 2016, 28, 63–72, doi:10.1016/j.tem.2016.10.004.

2. Ducker, G.S.; Rabinowitz, J.D. One-Carbon Metabolism in Health and Disease. *Cell Metabolism* **2016**, *25*, 27–42, doi:10.1016/j.cmet.2016.08.009.

3. Mentch, S.J.; Mehrmohamadi, M.; Huang, L.; Liu, X.; Gupta, D.; Mattocks, D.; Gomez Padilla, P.; Ables, G.; Bamman, M.M.; Thalacker-Mercer, A.E.; et al. Histone Methylation Dynamics and Gene Regulation Occur through the Sensing of One-Carbon Metabolism. *Cell Metabolism* **2015**, *22*, 861–873, doi:10.1016/j.cmet.2015.08.024.

4. Friso, S.; Udali, S.; De Santis, D.; Choi, S.W. One-Carbon Metabolism and Epigenetics. *Molecular Aspects of Medicine* **2017**, *54*, 28–36, doi:10.1016/j.mam.2016.11.007.

5. Pegg, A.E. Mammalian Polyamine Metabolism and Function. *IUBMB life* **2009**, *61*, 880–894, doi:10.1002/iub.230.

6. Finkelstein, J.D. Metabolic Regulatory Properties of *S*-Adenosylmethionine and *S*-Adenosylhomocysteine. *Clinical Chemistry and Laboratory Medicine* **2007**, *45*, 1694–1699, doi:10.1515/CCLM.2007.341.

7. Luka, Z.; Mudd, S.H.; Wagner, C. Glycine N-Methyltransferase and Regulation of *S*-Adenosylmethionine Levels. *Journal of Biological Chemistry* **2009**, *284*, 22507–22511, doi:10.1074/jbc.R109.019273.

8. Mudd, S.H.; Cerone, R.; Schiaffino, M.C.; Fantasia, A.R.; Minniti, G.; Caruso, U.; Lorini, R.; Watkins, D.; Matiaszuk, N.; Rosenblatt, D.S.; et al. Glycine N-Methyltransferase Deficiency: A Novel Inborn Error Causing Persistent Isolated Hypermethioninaemia. *Journal of Inherited Metabolic Disease* **2001**, *24*, 448–464, doi:10.1023/A:1010577512912.

9. Febbraio, M.A.; Reibe, S.; Shalapour, S.; Ooi, G.J.; Watt, M.J.; Karin, M. Preclinical Models for Studying NASH-Driven HCC: How Useful Are They? *Cell Metabolism* **2018**, *29*, 18–26, doi:10.1016/j.cmet.2018.10.012.

10. Aspichueta, P.; García-Rodríguez, J.L.; Menor, A.; Lu, S.C.; Mato, J.M.; Aurrekoetxea, I.; Cano, A.; Martínez-Uña, M.; Buqué, X.; Martínez-Chantar, M.L.; et al. Methionine Adenosyltransferase 1A Gene Deletion Disrupts Hepatic Very Low-Density Lipoprotein Assembly in Mice. *Hepatology* **2011**, *54*, 1975–1986, doi:10.1002/hep.24607.

11. Deminice, R.; Da Silva, R.P.; Lamarre, S.G.; Kelly, K.B.; Jacobs, R.L.; Brosnan, M.E.; Brosnan, J.T. Betaine Supplementation Prevents Fatty Liver Induced by a High-Fat Diet: Effects on One-Carbon Metabolism. *Amino Acids* **2015**, *47*, 839–846, doi:10.1007/s00726-014-1913-x.

12. Deminice, R.; da Silva, R.P.; Lamarre, S.G.; Brown, C.; Furey, G.N.; McCarter, S.A.; Jordao, A.A.; Kelly, K.B.; King-Jones, K.; Jacobs, R.L.; et al. Creatine Supplementation Prevents the

Accumulation of Fat in the Livers of Rats Fed a High-Fat Diet. *The Journal of Nutrition* **2011**, *141*, 1799–1804, doi:10.3945/jn.111.144857.

13. Teng, Y.-W.; Mehedint, M.G.; Garrow, T.A.; Zeisel, S.H. Deletion of Betaine-Homocysteine S-Methyltransferase in Mice Perturbs Choline and 1-Carbon Metabolism, Resulting in Fatty Liver and Hepatocellular Carcinomas. *The Journal of biological chemistry* **2011**, *286*, 36258–36267, doi:10.1074/jbc.M111.265348.

14. Martínez-Chantar, M.L.; Vázquez-Chantada, M.; Ariz, U.; Martínez, N.; Varela, M.; Luka, Z.; Capdevila, A.; Rodríguez, J.; Aransay, A.M.; Matthiesen, R.; et al. Loss of the Glycine N-Methyltransferase Gene Leads to Steatosis and Hepatocellular Carcinoma in Mice. *Hepatology* **2008**, *47*, 1191–1199, doi:10.1002/hep.22159.

15. Martínez-Chantar, M.L.; Corrales, F.J.; Martínez-Cruz, L.A.; García-Trevijano, E.R.; Huang, Z.Z.; Chen, L.; Kanel, G.; Avila, M.A.; Mato, J.M.; Lu, S.C. Spontaneous Oxidative Stress and Liver Tumors in Mice Lacking Methionine Adenosyltransferase 1A. *The FASEB journal : official publication of the Federation of American Societies for Experimental Biology* **2002**, *16*, 1292–1294.

16. Zhu, X.; Song, J.; Mar, M.-H.; Edwards, L.J.; Zeisel, S.H. Phosphatidylethanolamine N-Methyltransferase (PEMT) Knockout Mice Have Hepatic Steatosis and Abnormal Hepatic Choline Metabolite Concentrations despite Ingesting a Recommended Dietary Intake of Choline. *Biochem. J* **2003**, *370*, 987–993, doi:10.1042/BJ20021523.

17. Li, Z.; Agellon, L.B.; Allen, T.M.; Umeda, M.; Jewell, L.; Mason, A.; Vance, D.E. The Ratio of Phosphatidylcholine to Phosphatidylethanolamine Influences Membrane Integrity and Steatohepatitis. *Cell Metabolism* **2006**, *3*, 321–331, doi:10.1016/j.cmet.2006.03.007.

18. Pitsavos, C.; Panagiotakos, D.; Weinem, M.; Stefanadis, C. Diet, Exercise and the Metabolic Syndrome. *The Review of Diabetic Studies* **2006**, *3*, 118–118, doi:10.1900/rds.2006.3.118.

19. Unger, R.H.; Clark, G.O.; Scherer, P.E.; Orci, L. Lipid Homeostasis, Lipotoxicity and the Metabolic Syndrome. *Biochimica et Biophysica Acta - Molecular and Cell Biology of Lipids* **2010**, *1801*, 209–214, doi:10.1016/j.bbalip.2009.10.006.

20. Unger, R.H.; Scherer, P.E. Gluttony, Sloth and the Metabolic Syndrome: A Roadmap to Lipotoxicity. *Trends in Endocrinology and Metabolism* **2010**, *21*, 345–352, doi:10.1016/j.tem.2010.01.009.

21. Wong, R.J.; Aguilar, M.; Cheung, R.; Perumpail, R.B.; Harrison, S.A.; Younossi, Z.M.; Ahmed, A. Nonalcoholic Steatohepatitis Is the Second Leading Etiology of Liver Disease among Adults Awaiting Liver Transplantation in the United States. *Gastroenterology* **2015**, *148*, 547–555, doi:10.1053/j.gastro.2014.11.039.

22. Fader, K.A.; Nault, R.; Ammendolia, D.A.; Harkema, J.R.; Williams, K.J.; Crawford, R.B.; Kaminski, N.E.; Potter, D.; Sharratt, B.; Zacharewski, T.R. 2,3,7,8-Tetrachlorodibenzo-p-Dioxin Alters Lipid Metabolism and Depletes Immune Cell Populations in the Jejunum of C57BL/6 Mice. *Toxicological Sciences* **2015**, *148*, 567–580, doi:10.1093/toxsci/kfv206.

23. Nault, R.; Fader, K.A.; Ammendolia, D.A.; Dornbos, P.; Potter, D.; Sharratt, B.; Kumagai, K.; Harkema, J.R.; Lunt, S.Y.; Matthews, J.; et al. Dose-Dependent Metabolic Reprogramming

and Differential Gene Expression in TCDD-Elicited Hepatic Fibrosis. *Toxicological Sciences* **2016**, *154*, 253–266, doi:10.1093/toxsci/kfw163.

24. Kopec, A.K.; Boverhof, D.R.; Nault, R.; Harkema, J.R.; Tashiro, C.; Potter, D.; Sharratt, B.; Chittim, B.; Zacharewski, T.R. Toxicogenomic Evaluation of Long-Term Hepatic Effects of TCDD in Immature, Ovariectomized C57BL/6 Mice. *Toxicological Sciences* **2013**, *135*, 465–475, doi:10.1093/toxsci/kft156.

25. Kumar, J.; Lind, L.; Salihovic, S.; van Bavel, B.; Ingelsson, E.; Lind, P.M. Persistent Organic Pollutants and Liver Dysfunction Biomarkers in a Population-Based Human Sample of Men and Women. *Environmental Research* **2014**, *134*, 251–256, doi:10.1016/j.envres.2014.07.023.

26. Taylor, K.W.; Novak, R.F.; Anderson, H.A.; Birnbaum, L.S.; Blystone, C.; De Vito, M.; Jacobs, D.; Köhrle, J.; Lee, D.H.; Rylander, L.; et al. Evaluation of the Association between Persistent Organic Pollutants (POPs) and Diabetes in Epidemiological Studies: A National Toxicology Program Workshop Review. *Environmental Health Perspectives* **2013**, *121*, 774–783, doi:10.1289/ehp.1205502.

27. Casals-Casas, C.; Desvergne, B. Endocrine Disruptors: From Endocrine to Metabolic Disruption. *Annual Review of Physiology* **2011**, *73*, 135–162, doi:10.1146/annurev-physiol-012110-142200.

28. Grün, F.; Blumberg, B. Endocrine Disrupters as Obesogens. *Molecular and Cellular Endocrinology* **2009**, *304*, 19–29, doi:10.1016/j.mce.2009.02.018.

29. Fernandez-Salguero, P.M.; Hllbert, D.M.; Rudikoff, S.; Ward, J.M.; Gonzalez, F.J. Aryl-Hydrocarbon Receptor-Deficient Mice Are Resistant to 2,3,7,8-Tetrachlorodibenzo-p-Dioxin-Induced Toxicity. *Toxicology and Applied Pharmacology* **1996**, *140*, 173–179, doi:10.1006/taap.1996.0210.

30. Kerley-Hamilton, J.S.; Trask, H.W.; Ridley, C.J.A.; Dufour, E.; Ringelberg, C.S.; Nurinova, N.; Wong, D.; Moodie, K.L.; Shipman, S.L.; Moore, J.H.; et al. Obesity Is Mediated by Differential Aryl Hydrocarbon Receptor Signaling in Mice Fed a Western Diet. *Environmental Health Perspectives* **2012**, *120*, 1252–1259, doi:10.1289/ehp.1205003.

31. Jaeger, C.; Xu, C.; Sun, M.; Krager, S.; Tischkau, S.A. Aryl Hydrocarbon Receptor-Deficient Mice Are Protected from High Fat Diet-Induced Changes in Metabolic Rhythms. *Chronobiology International* **2017**, *34*, 318–336, doi:10.1080/07420528.2016.1256298.

32. Xu, C.X.; Wang, C.; Zhang, Z.M.; Jaeger, C.D.; Krager, S.L.; Bottum, K.M.; Liu, J.; Liao, D.F.; Tischkau, S.A. Aryl Hydrocarbon Receptor Deficiency Protects Mice from Diet-Induced Adiposity and Metabolic Disorders through Increased Energy Expenditure. *International Journal of Obesity* **2015**, *39*, 1300–1309, doi:10.1038/ijo.2015.63.

33. Fader, K.A.; Nault, R.; Doskey, C.M.; Fling, R.R.; Zacharewski, T.R. 2,3,7,8-Tetrachlorodibenzo-p-Dioxin Abolishes Circadian Regulation of Hepatic Metabolic Activity in Mice. *Scientific Reports* **2019**, *9*, 1–18, doi:10.1038/s41598-019-42760-3.

34. Liu, R.; Bi, K.; Jia, Y.; Wang, Q.; Yin, R.; Li, Q. Determination of Polyamines in Human Plasma by High-Performance Liquid Chromatography Coupled with Q-TOF Mass Spectrometry. *Journal of Mass Spectrometry* **2012**, *47*, 1341–1346, doi:10.1002/jms.3084.

35. Warrack, B.M.; Hnatyshyn, S.; Ott, K.-H.; Reily, M.D.; Sanders, M.; Zhang, H.; Drexler, D.M. Normalization Strategies for Metabonomic Analysis of Urine Samples. *Journal of Chromatography B* **2009**, *877*, 547–552, doi:10.1016/j.jchromb.2009.01.007.

36. Nault, R.; Fader, K.A.; Zacharewski, T. RNA-Seq versus Oligonucleotide Array Assessment of Dose-Dependent TCDD-Elicited Hepatic Gene Expression in Mice. *BMC genomics* **2015**, *16*, 373, doi:10.1186/s12864-015-1527-z.

37. Eckel, J.E.; Gennings, C.; Chinchilli, V.M.; Burgoon, L.D.; Zacharewski, T.R. Empirical Bayes Gene Screening Tool for Time-Course or Dose-Response Microarray Data. *Journal of Biopharmaceutical Statistics* **2004**, *14*, 647–670, doi:10.1081/BIP-200025656.

38. Phillips, J.R.; Svoboda, D.L.; Tandon, A.; Patel, S.; Sedykh, A.; Mav, D.; Kuo, B.; Yauk, C.L.; Yang, L.; Thomas, R.S.; et al. BMDExpress 2: Enhanced Transcriptomic Dose-Response Analysis Workflow. *Bioinformatics* **2018**, 1–3, doi:10.1093/bioinformatics/bty878.

39. Yang, L.; Allen, B.C.; Thomas, R.S. BMDExpress: A Software Tool for the Benchmark Dose Analyses of Genomic Data. *BMC Genomics* **2007**, *8*, 387, doi:10.1186/1471-2164-8-387.

40. Fader, K.A.; Nault, R.; Kirby, M.P.; Markous, G.; Matthews, J.; Zacharewski, T.R. Convergence of Hepcidin Deficiency, Systemic Iron Overloading, Heme Accumulation, and REV-ERBα/β Activation in Aryl Hydrocarbon Receptor-Elicited Hepatotoxicity. *Toxicology and Applied Pharmacology* **2017**, *321*, 1–17, doi:10.1016/j.taap.2017.02.006.

41. Nault, R.; Fader, K.A.; Lydic, T.A.; Zacharewski, T.R. Lipidomic Evaluation of Aryl Hydrocarbon Receptor-Mediated Hepatic Steatosis in Male and Female Mice Elicited by 2,3,7,8- Tetrachlorodibenzo-p-dioxin., doi:10.1021/acs.chemrestox.6b00430.

42. Birnbaum, L.S.; Mcdonald, M.M.; Blair, P.C.; Clark, A.M.; Harris, M.W. Differential Toxicity of 2,3,7,8-Tetrachlorodibenzo-p-Dioxin (TCDD) in C57BL/6J Mice Congenic at the Ah Locus. *Toxicological Sciences* **1990**, *15*, 186–200, doi:10.1093/toxsci/15.1.186.

43. Jones, G.; Greig, J.B. Pathological Changes in the Liver of Mice given 2,3,7,8-Tetrachlorodibenzo-p-Dioxin. *Experientia* **1975**, *31*, 1315–1317, doi:10.1007/BF01945801.

44. Fader, K.A.; Nault, R.; Zhang, C.; Kumagai, K.; Harkema, J.R.; Zacharewski, T.R. 2,3,7,8-Tetrachlorodibenzo-p-Dioxin (TCDD)-Elicited Effects on Bile Acid Homeostasis: Alterations in Biosynthesis, Enterohepatic Circulation, and Microbial Metabolism. *Scientific Reports* **2017**, *7*, 5921, doi:10.1038/s41598-017-05656-8.

45. Nault, R.; Fader, K.A.; Kopec, A.K.; Harkema, J.R.; Zacharewski, T.R.; Luyendyk, J.P. From the Cover: Coagulation-Driven Hepatic Fibrosis Requires Protease Activated Receptor-1 (PAR-1) in a Mouse Model of TCDD-Elicited Steatohepatitis. *Toxicological Sciences* **2016**, *154*, 381–391, doi:10.1093/toxsci/kfw175.

46. Boldyrev, A.A. Molecular Mechanisms of Homocysteine Toxicity. *Biochemistry (Moscow)* **2009**, *74*, 589–598, doi:10.1134/S0006297909060017.

47. Brooks, W.H. Increased Polyamines Alter Chromatin and Stabilize Autoantigens in Autoimmune Diseases. *Frontiers in Immunology* **2013**, *4*, 91, doi:10.3389/fimmu.2013.00091.

48. Mudd, S.H.; Ebert, M.H.; Scriver, C.R. Labile Methyl Group Balances in the Human: The Role of Sarcosine. *Metabolism: Clinical and Experimental* **1980**, *29*, 707–720, doi:10.1016/0026-0495(80)90192-4.

49. Tachikawa, M.; Ikeda, S.; Fujinawa, J.; Hirose, S.; Akanuma, S. ichi; Hosoya, K. ichi Γ-Aminobutyric Acid Transporter 2 Mediates the Hepatic Uptake of Guanidinoacetate, the Creatine Biosynthetic Precursor, in Rats. *PLoS ONE* **2012**, *7*, 32557, doi:10.1371/journal.pone.0032557.

50. Song, J.; Da Costa, K.A.; Fischer, L.M.; Kohlmeier, M.; Kwock, L.; Wang, S.; Zeisel, S.H. Polymorphism of the PEMT Gene and Susceptibility to Nonalcoholic Fatty Liver Disease (NAFLD). *FASEB Journal* **2005**, *19*, 1266–1271, doi:10.1096/fj.04-3580com.

51. Corbin, K.D.; Abdelmalek, M.F.; Spencer, M.D.; Da Costa, K.A.; Galanko, J.A.; Sha, W.; Suzuki, A.; Guy, C.D.; Cardona, D.M.; Torquati, A.; et al. Genetic Signatures in Choline and 1-Carbon Metabolism Are Associated with the Severity of Hepatic Steatosis. *FASEB Journal* **2013**, *27*, 1674–1689, doi:10.1096/fj.12-219097.

52. Kalhan, S.C.; Guo, L.; Edmison, J.; Dasarathy, S.; McCullough, A.J.; Hanson, R.W.; Milburn, M. Plasma Metabolomic Profile in Nonalcoholic Fatty Liver Disease. *Metabolism: Clinical and Experimental* **2011**, *60*, 404–413, doi:10.1016/j.metabol.2010.03.006.

53. Angrish, M.M.; Dominici, C.Y.; Zacharewski, T.R. TCDD-Elicited Effects on Liver, Serum, and Adipose Lipid Composition in C57BL/6 Mice. *Toxicological Sciences* **2013**, *131*, 108–115, doi:10.1093/toxsci/kfs277.

54. Birnbaum, L.S. Distribution and Excretion of 2,3,7,8-Tetrachlorodibenzo-p-Dioxin in Congenic Strains of Mice Which Differ at the Ah Locus. *Drug Metabolism and Disposition* **1986**, *14*, 34–40.

55. Alcock, R.E.; Behnisch, P.A.; Jones, K.C.; Hagenmaier, H. Dioxin-Like PCBs in the Environment - Human Exposure and the Significance of Sources. *Chemosphere* **1998**, *37*, 1457–1472, doi:10.1016/S0045-6535(99)00137-X.

56. Choi, J.W.; Miyabara, Y.; Hashimoto, S.; Morita, M. Comparison of PCDD/F and Coplanar PCB Concentrations in Japanese Human Adipose Tissue Collected in 1970-1971, 1994-1996 and 2000. *Chemosphere* **2002**, *47*, 591–597, doi:10.1016/S0045-6535(02)00008-5.

57. Masuda, Y.; Schecter, A.; Päpke, O. Concentrations of PCBs, PCDFs and PCDDs in the Blood of Yusho Patients and Their Toxic Equivalent Contribution. *Chemosphere* **1998**, *37*, 1773–1780, doi:10.1016/S0045-6535(98)00242-2.

58. Päpke, O. PCDD/PCDF: Human Background Data for Germany, a 10-Year Experience. *Environmental Health Perspectives* **1998**, *106*, 723–731, doi:10.1289/ehp.98106723.

59. Shen, H.; Han, J.; Tie, X.; Xu, W.; Ren, Y.; Ye, C. Polychlorinated Dibenzo-p-Dioxins/Furans and Polychlorinated Biphenyls in Human Adipose Tissue from Zhejiang Province, China. *Chemosphere* **2009**, *74*, 384–388, doi:10.1016/j.chemosphere.2008.09.094.

60. Zober, A.; Päpke, O. Concentrations of PCDDs and PCDFs in Human Tissue 36 Years after Accidental Dioxin Exposure. *Chemosphere* **1993**, *27*, 413–418, doi:10.1016/0045-6535(93)90321-U.

61. Yan, J.; Tung, H.C.; Li, S.; Niu, Y.; Garbacz, W.G.; Lu, P.; Bi, Y.; Li, Y.; He, J.; Xu, M.; et al. Aryl Hydrocarbon Receptor Signaling Prevents Activation of Hepatic Stellate Cells and Liver Fibrogenesis in Mice. *Gastroenterology* **2019**, *157*, 793-806.e14, doi:10.1053/j.gastro.2019.05.066.

62. Lee, J.H.; Wada, T.; Febbraio, M.; He, J.; Matsubara, T.; Lee, M.J.; Gonzalez, F.J.; Xie, W. A Novel Role for the Dioxin Receptor in Fatty Acid Metabolism and Hepatic Steatosis. *Gastroenterology* **2010**, *139*, 653–663, doi:10.1053/J.GASTRO.2010.03.033.

63. Matsubara, T.; Tanaka, N.; Krausz, K.W.; Manna, S.K.; Kang, D.W.; Anderson, E.R.; Luecke, H.; Patterson, A.D.; Shah, Y.M.; Gonzalez, F.J. Metabolomics Identifies an Inflammatory Cascade Involved in Dioxin- and Diet-Induced Steatohepatitis. *Cell Metabolism* **2012**, *16*, 634–644, doi:10.1016/j.cmet.2012.10.006.

64. Kopec, A.K.; Burgoon, L.D.; Ibrahim-Aibo, D.; Burg, A.R.; Lee, A.W.; Tashiro, C.; Potter, D.; Sharratt, B.; Harkema, J.R.; Rowlands, J.C.; et al. Automated Dose-Response Analysis and Comparative Toxicogenomic Evaluation of the Hepatic Effects Elicited by TCDD, TCDF, and PCB126 in C57BL/6 Mice. *Toxicological Sciences* **2010**, *118*, 286–297, doi:10.1093/toxsci/kfq236.

65. Vance, D.E. Phospholipid Methylation in Mammals: From Biochemistry to Physiological Function. *Biochimica et Biophysica Acta - Biomembranes* **2014**, *1838*, 1477–1487, doi:10.1016/j.bbamem.2013.10.018.

66. Nault, R.; Fader, K.A.; Harkema, J.R.; Zacharewski, T. Loss of Liver-Specific and Sexually Dimorphic Gene Expression by Aryl Hydrocarbon Receptor Activation in C57BL/6 Mice. *PLoS ONE* **2017**, *12*, e0184842, doi:10.1371/journal.pone.0184842.

67. Carretero, M.V.; Latasa, M.U.; Garcia-Trevijano, E.R.; Corrales, F.J.; Wagner, C.; Mato, J.M.; Avila, M.A. Inhibition of Liver Methionine Adenosyltransferase Gene Expression by 3-Methylcolanthrene: Protective Effect of *S*-Adenosylmethionine. *Biochemical Pharmacology* **2001**, *61*, 1119–1128, doi:10.1016/S0006-2952(01)00590-1.

68. Frau, M.; Tomasi, M.L.; Simile, M.M.; Demartis, M.I.; Salis, F.; Latte, G.; Calvisi, D.F.; Seddaiu, M.A.; Daino, L.; Feo, C.F.; et al. Role of Transcriptional and Posttranscriptional Regulation of Methionine Adenosyltransferases in Liver Cancer Progression. *Hepatology* **2012**, *56*, 165–175, doi:10.1002/hep.25643.

69. Frau, M.; Feo, F.; Pascale, R.M. Pleiotropic Effects of Methionine Adenosyltransferases Deregulation as Determinants of Liver Cancer Progression and Prognosis. *Journal of Hepatology* **2013**, *59*, 830–841, doi:10.1016/j.jhep.2013.04.031.

70. Calvisi, D.F.; Simile, M.M.; Ladu, S.; Pellegrino, R.; De Murtas, V.; Pinna, F.; Tomasi, M.L.; Frau, M.; Virdis, P.; De Miglio, M.R.; et al. Altered Methionine Metabolism and Global DNA Methylation in Liver Cancer: Relationship with Genomic Instability and Prognosis. *International Journal of Cancer* **2007**, *121*, 2410–2420, doi:10.1002/ijc.22940.

71. Murray, B.; Barbier-Torres, L.; Fan, W.; Mato, J.M.; Lu, S.C. Methionine Adenosyltransferases in Liver Cancer. *World Journal of Gastroenterology* **2019**, *25*, 4300–4319, doi:10.3748/wjg.v25.i31.4300.

72. Pascale, R.M.; Peitta, G.; Simile, M.M.; Feo, F. Alterations of Methionine Metabolism as Potential Targets for the Prevention and Therapy of Hepatocellular Carcinoma. *Medicina (Lithuania)* **2019**, *55*, 1–24, doi:10.3390/medicina55060296.

73. Barić, I.; Fumić, K.; Glenn, B.; Ćuk, M.; Schulze, A.; Finkelstein, J.D.; James, S.J.; Mejaški-Bošnjak, V.; Pažanin, L.; Pogribny, I.P.; et al. *S*-Adenosylhomocysteine Hydrolase Deficiency in a Human: A Genetic Disorder of Methionine Metabolism. *Proceedings of the National Academy of Sciences of the United States of America* **2004**, *101*, 4234–4239, doi:10.1073/pnas.0400658101.

74. Teng, Y.-W.; Cerdena, I.; Zeisel, S.H. Homocysteinemia in Mice with Genetic Betaine Homocysteine S-Methyltransferase Deficiency Is Independent of Dietary Folate Intake. *The Journal of Nutrition* **2012**, *142*, 1964–1967, doi:10.3945/jn.112.166835.

75. Nault, R.; Fader, K.A.; Kirby, M.P.; Ahmed, S.; Matthews, J.; Jones, A.D.; Lunt, S.Y.; Zacharewski, T.R. Pyruvate Kinase Isoform Switching and Hepatic Metabolic Reprogramming by the Environmental Contaminant 2,3,7,8-Tetrachlorodibenzo-p-Dioxin. *Toxicological Sciences* **2016**, *149*, 358–371, doi:10.1093/toxsci/kfv245.

76. Mosharov, E.; Cranford, M.R.; Banerjee, R. The Quantitatively Important Relationship between Homocysteine Metabolism and Glutathione Synthesis by the Transsulfuration Pathway and Its Regulation by Redox Changes. *Biochemistry* **2000**, *39*, 13005–13011, doi:10.1021/bi001088w.

77. Mudd, S.H.; Poole, J.R. Labile Methyl Balances for Normal Humans on Various Dietary Regimens. *Metabolism* **1975**, *24*, 721–735, doi:10.1016/0026-0495(75)90040-2.

78. Farrell, K.; Safe, S. 2,3,7,8-Tetrachlorodibenzo-p-Dioxin: Relationship between Toxicity and the Induction of Aryl Hydrocarbon Hydroxylase and Ornithine Decarboxylase. *Chemosphere* **1986**, *15*, 1971–1976, doi:10.1016/0045-6535(86)90494-7.

79. Nebert, D.W.; Jensen, N.M.; Perry, J.W.; Oka, T. Association between Ornithine Decarboxylase Induction and the Ah Locus in Mice Treated with Polycyclic Aromatic Compounds. *Journal of Biological Chemistry* **1980**, *255*, 6836–6842.

80. Raunio, H.; Pelkonen, O. Effect of Polycyclic Aromatic Compounds and Phorbol Esters on Ornithine Decarboxylase and Aryl Hydrocarbon Hydroxylase Activities in Mouse Liver. *Cancer Research* **1983**, *43*, 782–786.

81. Ruiz-Aracama, A.; Peijnenburg, A.; Kleinjans, J.; Jennen, D.; van Delft, J.; Hellfrisch, C.; Lommen, A. An Untargeted Multi-Technique Metabolomics Approach to Studying

Intracellular Metabolites of HepG2 Cells Exposed to 2,3,7,8-Tetrachlorodibenzo-p-Dioxin. *BMC Genomics* **2011**, *12*, 251, doi:10.1186/1471-2164-12-251.

82. Jennen, D.; Ruiz-Aracama, A.; Magkoufopoulou, C.; Piejnenburg, A.; Lommen, A.; van Delft, J.; Kleinjans, J. Integrating Transcriptomics and Metabonomics to Unravel Modes-of-Action of 2,3,7,8- Tetrachlorodibenzo-p-Dioxin (TCDD) in HepG2 Cells. *BMC systems biology* **2011**, *5*, 1–13.

83. Thomas, T.; MacKenzie, S.A.; Gallo, M.A. Regulation of Polyamine Biosynthesis by 2,3,7,8-Tetrachlorodibenzo-p-Dioxin (TCDD). *Toxicology Letters* **1990**, *53*, 315–325, doi:10.1016/0378-4274(90)90236-F.

84. O'Brien, T.G.; Diamond, L. Ornithine Decarboxylase Induction and DNA Synthesis in Hamster Embryo Cell Cultures Treated with Tumor-Promoting Phorbol Diesters1. *Cancer Research* **1977**, *37*, 3895–3900.

85. Tamori, A.; Shuhei, N.; Tetsuo, K.; Shucihi, S.; Kobayshi, K.; Hiroaki, K.; Shuzo, O. Relationship of Ornithine Decarboxylase Activity and Histological Findings in Human Hepatocellular Carcinoma. *Japanese Journal of Clinical Oncology* **1994**, *20*, 1179–1187, doi:10.1093/oxfordjournals.jjco.a039694.

86. Stevens, A.P.; Dettmer, K.; Kirovski, G.; Samejima, K.; Hellerbrand, C.; Bosserhoff, A.K.; Oefner, P.J. Quantification of Intermediates of the Methionine and Polyamine Metabolism by Liquid Chromatography-Tandem Mass Spectrometry in Cultured Tumor Cells and Liver Biopsies. *Journal of Chromatography A* **2010**, *1217*, 3282–3288, doi:10.1016/j.chroma.2010.01.025.

87. Wyss, M.; Kaddurah-Daouk, R. Creatine and Creatinine Metabolism. *Physiological reviews* **2000**, *80*, 1107–1213, doi:10.1016/S1286-0115(06)74505-2.

88. Schmidt, A.; Marescau, B.; Boehm, E.A.; Jan Renema, W.K.; Peco, R.; Das, A.; Steinfeld, R.; Chan, S.; Wallis, J.; Davidoff, M.; et al. Severely Altered Guanidino Compound Levels, Disturbed Body Weight Homeostasis and Impaired Fertility in a Mouse Model of Guanidinoacetate N-Methyltrasferase (GAMT) Deficiency. *Human Molecular Genetics* **2004**, *13*, 905–921, doi:10.1093/hmg/ddh112.

89. Stöckler, S.; Marescau, B.; De Deyn, P.P.; Trijbels, J.M.F.; Hanefeld, F. Guanidino Compounds in Guanidinoacetate Methyltransferase Deficiency, a New Inborn Error of Creatine Synthesis. *Metabolism: Clinical and Experimental* **1997**, *46*, 1189–1193, doi:10.1016/S0026-0495(97)90215-8.

90. Liu, Q.; Cai, J.; Nichols, R.G.; Tian, Y.; Zhang, J.; Smith, P.B.; Wang, Y.; Yan, C.; Patterson, A.D. A Quantitative HILIC–MS/MS Assay of the Metabolic Response of Huh-7 Cells Exposed to 2,3,7,8-Tetrachlorodibenzo-p-Dioxin. *Metabolites* **2019**, *9*.

91. Beischlag, T. V; Luis Morales, J.; Hollingshead, B.D.; Perdew, G.H. The Aryl Hydrocarbon Receptor Complex and the Control of Gene Expression. *Critical reviews in eukaryotic gene expression* **2008**, *18*, 207–250.

92. Huang, G.; Elferink, C.J. A Novel Nonconsensus Xenobiotic Response Element Capable of Mediating Aryl Hydrocarbon Receptor-Dependent Gene Expression. *Molecular Pharmacology* **2012**, *81*, 338–347, doi:10.1124/mol.111.075952.

93. Muku, G.E.; Kusnadi, A.; Kuzu, G.; Tanos, R.; Murray, I.A.; Gowda, K.; Amin, S.; Perdew, G.H. Selective Ah Receptor Modulators Attenuate NPC1L1-Mediated Cholesterol Uptake through Repression of SREBP-2 Transcriptional Activity. *Laboratory Investigation* **2020**, *100*, 250–264, doi:10.1038/s41374-019-0306-x.

94. Tanos, R.; Patel, R.D.; Murray, I.A.; Smith, P.B.; Patterson, A.D.; Perdew, G.H. Aryl Hydrocarbon Receptor Regulates the Cholesterol Biosynthetic Pathway in a Dioxin Response Element-Independent Manner. *Hepatology* **2012**, *55*, 1994–2004, doi:10.1002/hep.25571.

95. Nault, R.; Doskey, C.M.; Fader, K.A.; Rockwell, C.E.; Zacharewski, T. Comparison of Hepatic NRF2 and Aryl Hydrocarbon Receptor Binding in 2,3,7,8-Tetrachlorodibenzo-p-Dioxin–Treated Mice Demonstrates NRF2-Independent PKM2 Induction. *Molecular Pharmacology* **2018**, *94*, 876–884, doi:10.1124/mol.118.112144.

CHAPTER 3: ARYL HYDROCARBON RECEPTOR (AHR) ACTIVATION BY 2,3,7,8-TETRACHLORODIBENZO-P-DIOXIN (TCDD) DOSE-DEPENDENTLY SHIFTS THE GUT MICROBIOME CONSISTENT WITH THE PROGRESSION OF NON-ALCOHOLIC FATTY LIVER DISEASE

Fling, R.R.; Zacharewski, T.R. Aryl Hydrocarbon Receptor (AhR) Activation by 2,3,7,8-Tetrachlorodibenzo-p-Dioxin (TCDD) Dose-Dependently Shifts the Gut Microbiome Consistent with the Progression of Non-Alcoholic Fatty Liver Disease. *IJMS* **2021**, *22*, 12431, doi:10.3390/ijms222212431.

ABSTRACT

Gut dysbiosis with disrupted enterohepatic bile acid metabolism is commonly associated with non-alcoholic fatty liver disease (NAFLD) and recapitulated in a NAFLD-phenotype elicited by 2,3,7,8-tetrachlorodibenzo-*p*-dioxin (TCDD) in mice. TCDD induces hepatic fat accumulation and increases levels of secondary bile acids, including taurolithocholic acid and deoxycholic acid (microbial modified bile acids involved in host bile acid regulation signaling pathways). To investigate the effects of TCDD on the gut microbiota, the cecum contents of male C57BL/6 mice orally gavaged with sesame oil vehicle or 0.3, 3, or 30 µg/kg TCDD were examined using shotgun metagenomic sequencing. Taxonomic analysis identified dose-dependent increases in Lactobacillus species (i.e., *Lactobacillus reuteri*). Increased species were also associated with dose-dependent increases in bile salt hydrolase sequences, responsible for deconjugation reactions in secondary bile acid metabolism. Increased *L. reuteri* levels were further associated with mevalonate-dependent isopentenyl diphosphate (IPP) biosynthesis and *O*-succinylbenzoate synthase, a menaquinone biosynthesis associated gene. Analysis of the gut microbiomes from cirrhosis patients identified an increased abundance of genes from mevalonate-dependent IPP biosynthesis as well as several other menaquinone biosynthesis genes, including *O*-succinylbenzoate synthase. These results extend the association of lactobacilli with the AhR/intestinal axis in NAFLD progression and highlight the similarities between TCDD-elicited phenotypes in mice to human NAFLD.

INTRODUCTION

Non-alcoholic fatty liver disease (NAFLD) is estimated to affect ~25% of the global population and is defined as a spectrum of progressive pathologies, including steatosis, immune cell infiltration/inflammation, fibrosis, and cirrhosis. It is associated with increased risk for hepatocellular carcinoma and is the second leading cause of liver transplants in the USA [1]. Other pathologies, including obesity, type 2 diabetes (T2D), and coronary heart disease,

demonstrate a high co-occurrence with NAFLD, e.g., ~40–70% in T2D patients and ~90% in obese patients [2]. A multi-hit hypothesis for NAFLD proposes several contributing factors to development and progression, including disruptions in the immune system, adipose tissue metabolism, and the gut microbiome [3].

Emerging evidence also suggests that environmental contaminants may play an underappreciated role in gut dysbiosis and NAFLD development [4–11]. Specifically, 2,3,7,8-tetrachlorodibenzo-*p*-dioxin (TCDD), a persistent environmental organochloride pollutant, induces steatosis and the progression to steatohepatitis with fibrosis in mice resembling human NAFLD development [9,12–14]. TCDD-induced dyslipidemia also exhibits other similar NAFLD characteristics, such as decreased VLDL secretion, free fatty acid accumulation, inhibition of β-oxidation, and disrupted cholesterol and bile acid metabolism [9,12,15–17].

The effects of TCDD and other related polychlorinated dibenzo-*p*-dioxins (PCDDs), polychlorinated dibenzofurans (PCDFs), and polychlorinated coplanar biphenyls (PCBs) as well as polyaromatic hydrocarbons (PAHs), are mediated through activation of the aryl hydrocarbon receptor (AhR), a basic helix-loop-helix/Per-Arnt-Sim transcription factor typically associated with xenobiotic metabolism [18]. In addition, the AhR plays an essential role in gut homeostasis through regulation of the immune system and bile acid metabolism [9,12,19,20] with endogenous and xenobiotic AhR ligands affecting the gut microbiome congruent with NAFLD-like pathology [8–10]. Moreover, gut dysbiosis is commonly reported in NAFLD, making the gut microbiome an attractive target for non-invasive diagnostic tools and a potential target for intervention [21,22].

Although the AhR exhibits promiscuous binding activity for a wide variety of structurally diverse xenobiotics, natural products, and endogenous metabolites, its endogenous role remains unknown [23]. Upon ligand binding, the cytosolic AhR translocates to the nucleus where it disassociates from its chaperone proteins and dimerizes with the AhR nuclear transporter (ARNT). The AhR/ARNT heterodimer complex then binds to dioxin response elements located throughout the genome, affecting gene expression [24].

Endobiotic ligands for the AhR include host-derived metabolites, such as tryptophan catabolites (e.g., L-kynurenine), microbial-produced indole derivatives (e.g., indole-3-aldehyde produced by *Lactobacillus reuteri*), and compounds derived from fruits and cruciferous vegetables (e.g., indole-3-carbinol) [23]. Microbially produced indoles activate AhR in the intestine, affecting barrier function and homeostasis by regulating the intestinal immune system through $CD4^+$ T-cell differentiation and the induction of interleukin (IL)-22 and IL-10 cytokine production [24]. AhR-dependent IL-22 production subsequently increases antimicrobial peptide expression in intestinal epithelial cells, thus, inhibiting pathogen infection and inflammation [24–26].

Knockout models and/or treatment with endogenous and xenobiotic AhR ligands results in shifts in the gut microbiome with diverse effects depending on the model and ligand [8,11,26–28]. Shifts in the Firmicutes/Bacteroidetes ratio can differ between AhR ligands, e.g., 2,3,7,8-tetrachlorodibenzofuran decreased the ratio [8] whereas TCDD increases it [11]. However, responses in various AhR models are in agreement regarding increased secondary bile acids [8,9] and effects on segmented filamentous bacteria [8,11,27]. AhR knockout models, and treatment with TCDD or other endogenous compounds also demonstrate strong correlations between AhR activation and enrichment of Lactobacillus species i.e., *L. reuteri* [26–30]. Tryptophan catabolism to AhR ligands by Lactobacillus species is a proposed mechanism for gut microbial regulation of AhR signaling that modulates intestinal and gut microbiome homeostasis [26].

Bile acids also affect the gut microbiome by exerting antimicrobial activity [31]. Conversely, the gut microbiota play critical roles in host bile acid homeostasis through microbial metabolism that qualitatively and quantitatively impact bile acid composition with consequences for bile acid activated signaling pathways in the host. The gut microbiome performs the first step of bile acid deconjugation with subsequent oxidation, reduction, or dehydroxylation reactions to produce diverse secondary bile acid molecular species [32].

Select secondary bile acids, e.g., glycodeoxycholic acid (GDCA), demonstrate higher inhibition of bacterial growth compared to other primary and secondary bile acids [33]. In regard to the host, some secondary bile acids e.g., lithocholic acid (LCA) and deoxycholic acid (DCA), exhibit a high affinity for the farnesoid x receptor (FXR) and G protein-coupled bile acid receptor (GPBAR1, a.k.a. TGR5), which regulate glucose, lipid, and bile acid homeostasis [34–36]. In human NAFLD, secondary bile acid metabolism is disrupted with bile acid analogs that target the FXR and GPBAR1 signaling pathways under development for the treatment of liver disease [22,31,37].

Previous work demonstrated that the serum levels of LCA and DCA increased following TCDD treatment suggesting enrichment for the microbial bile acid metabolism [9]. To further explore dose-dependent disruptions in the gut microbiome and microbial metabolism relevant to the progression of NAFLD-like pathologies, shotgun metagenomic analysis was used to examine the dose dependent taxonomic and metabolic disruptions elicited by TCDD.

MATERIALS & METHODS

Animal Treatment

Postnatal day 25 (PND25) male C57BL/6 mice weighing within 10% of each other were obtained from Charles River Laboratories (Kingston, NY, USA) and housed and treated as previously described [9]. Briefly, mice were housed in Innovive Innocages (San Diego, CA, USA) containing ALPHA-dri bedding (Shepherd Specialty Papers, Chicago, IL, USA) in a 23 °C environment with 30–40% humidity and a 12 h/12 h light/dark cycle. Aquavive water (Innovive) and Harlan Teklad 22/5 Rodent Diet 8940 (Madison, WI, USA) were provided *ad libitum*. The rodent diet is a fixed formula complete diet with an energy density of 3.0 kcal/g and a nutrient ingredient composition, including 22% protein, 5.5% fat, and 40.6% carbohydrate. Mice (PND29) were orally gavaged at the beginning of the light cycle (between Zeitgeber time 0–3) with 0.1 mL sesame oil vehicle (Sigma-Aldrich, St. Louis, MO, USA) or 0.3, 3 and 30 µg/kg body weight TCDD

(AccuStandard, New Haven, CT, USA) every 4 days for 7 total exposures (*n* = 3 per treatment group). The study was conducted in three cohorts with mice housed separately among treatment groups for a total of 9 mice per treatment group. In each cohort, three mice were housed per treatment group, and one mouse was randomly selected from each treatment group per cohort (*n* = 3 per treatment group for the metagenomic analysis) to account for coprophagia and ensure reproducibility. The first gavage was administered on day 0 of the study. On day 28, vehicle- and TCDD-treated mice (fasted for 6 h with access to water) were weighed and euthanized by CO_2 inhalation between Zeitgeber time 0–3. Upon collection, cecums were immediately flash frozen in liquid nitrogen and stored at −80 °C until analysis. All animal handling procedures were performed with the approval of the Michigan State University (MSU) Institutional Animal Care and Use Committee.

Metagenomic sequencing

Microbial DNA from cecum contents (~25 mg) was extracted using the FastDNA spin kit for soil (SKU 116560200, MP Biomedicals, Santa Ana, CA, USA). Extracted DNA was submitted to Novogene (Sacramento, CA, USA) for quality control, library preparation, and 150-bp paired-end sequencing at a depth 136–157 million reads using an Illumina NovaSeq 6000. Reads aligning to the C57BL/6 *Mus musculus* genome (https://www.ncbi.nlm.nih.gov/assembly/GCF_000001635.26/, NCBI genome assembly: GRCm38.p6, accessed on 10 October 2020) were identified, flagged, and removed using bowtie2 [88], SamTools [89] and bedtools [90]. For human metagenomic analysis, reads were filtered against the human genome (https://www.ncbi.nlm.nih.gov/assembly/GCF_000001405.13/, NCBI genome assembly: GRCh37/hg19, accessed on 10 January 2021) using the Kneaddata bioinformatics tool developed at the Huttenhower Lab (https://github.com/biobakery/kneaddata, accessed on 10 January 2021).

Metagenomic taxonomic analysis

Kaiju was used for taxonomic analysis of mouse cecum metagenomic dataset. The reference database used was the progenomes database downloaded from the kaiju webserver (https://kaiju.binf.ku.dk/database/kaiju_db_progenomes_2020-05-25.tgz, accessed on 15 October 2020). Multivariate association between dose and taxonomy relative abundances used Maaslin2 (https://github.com/biobakery/Maaslin2, accessed on 15 October 2020)[91] with the following default settings used: normalization (total sum scaling), analysis method (general linear model), and Benjamini-Hochberg multiple test correction. Adjusted *p*-values for Maaslin2 analysis used dose (sesame oil vehicle (0), 0.3, 3, or 30 µg/kg TCDD) as the fixed effect, which was treated as continuous variable and the vehicle set for reference. For comparison of taxonomy between vehicle and 30 µg/kg TCDD treatment groups, DeSeq2 was used to determine adjusted *p*-values using default settings [92].

Metagenomic functional analysis

The HUMAnN 3.0 bioinformatic pipeline [93] was used with default settings to classify reads to UniRef90 protein identifications using UniProt's UniRef90 protein data base (January 2019, accessed on 15 January 2021). Reads aligned to UniRef90 identifications were mapped to enzyme commission (EC) number entries using the human_regroup_table tool. Read abundance was normalized to gene copies per million reads (CPM) using the human_renorm_table tool. Multivariate association between dose and enzyme commission number relative abundance used Maaslin2 with same settings used for taxonomy analysis.

Xander (a gene-targeted assembler, https://github.com/rdpstaff/Xander_assembler, accessed on 5 February 2021) was used to annotate and quantify bile salt hydrolase sequences with the following settings: k-mer size = 45, filter size = 35, minimum assembled contig bit score = 50, and minimum assembled protein contigs = 100 [94]. Reference DNA and protein *bsh* sequences used for Xander were downloaded from FunGenes Gene Repository and are listed in

supplementary material (Tables S9 and S10) [95]. For RefSeq *bsh* sequence analysis, relative abundance was determined by normalizing to total abundance of *rplB* sequences also determined by Xander per sample. Significance was determined with Maaslin2 with the same settings used for taxonomy analysis

Human metagenomic data from the National Center for Biotechnology Information (NCBI) Sequence Read Archive (SRA) under accession number PRJEB6337 (https://www.ncbi.nlm.nih.gov/bioproject/PRJEB6337/, accessed on 25 March 2021) was analyzed using the same HUMAnN 3.0 pipeline as cecum metagenomic data. Fecal shotgun metagenomic samples from Chinese patients were defined as healthy (*n* = 52) or cirrhotic with subclassifications of compensated (*n* = 48) or decompensated (*n* = 44) by the authors [39].

Cirrhosis was diagnosed by either biopsy, clinical evidence of decompensation, or other metrics, including radiological evidence of liver nodularity and intra-abdominal varices in a patient with chronic liver disease [39]. The subclassification was used as fixed effect for analysis with healthy as the reference category. Again, Maaslin2 was used with settings used for mouse functional analysis with diagnosis as a fixed effect with healthy diagnosis as reference to determine adjusted *p*-values for compensated and decompensated patient designations.

RESULTS

TCDD-elicited toxicity enriched for Lactobacillus species

Taxonomic analysis identified significant dose-dependent population shifts among caecum microbiota in response to TCDD. While no significance was observed between treatment groups at the phylum level, a decreasing trend was observed for Bacteroidetes concurrent with increasing trends in Firmicutes abundance (Figure 13A). At the genus level, Turicibacter was enriched by TCDD while Lactobacillus trended towards enrichment (Figure 13B). Interestingly, at the species level, 10 out of 13 enriched species were from the Lactobacillus genus e.g., *L. reuteri* and *Lactobacillus sp. ASF360*, as well as *Turicibacter sanguinis*. Conversely, the most abundant

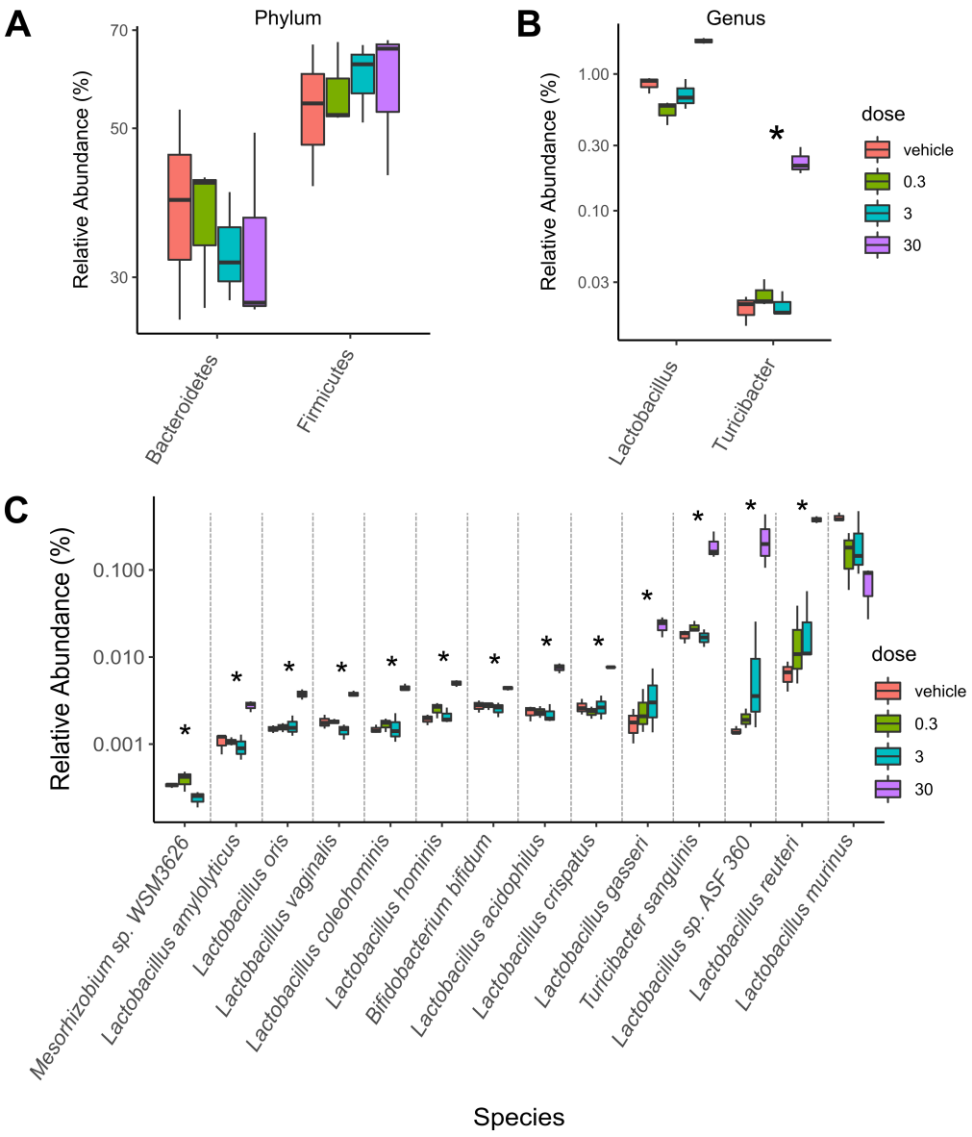

FIGURE 13. TCDD ENRICHED LACTOBACILLUS SPECIES IN THE CECUM MICROBIOTA.

Taxa abundance were assessed in metagenomic cecum samples from male C57BL/6 mice following oral gavage with sesame oil vehicle or 0.3, 3, or 30 µg/kg TCDD every 4 days for 28 days (n = 3). Significant shifts in relative abundances of taxa are presented at the (**A**) phylum, (**B**) genus, (**C**) and species levels. Significance is denoted with an asterisk (*; adjusted p-value < 0.1).

Lactobacillus species in vehicle treated mice, *Lactobacillus murinus*, trended towards a dose-dependent decrease (Figure 13C). The major changes in taxa were observed in the 30 µg/kg TCDD treatment group.

Bile salt hydrolase (Bsh) levels correlated with significantly enriched species

Many Lactobacillus species deconjugate primary conjugated bile acids mediated by bile salt hydrolases (BSH), imparting bile acid tolerance [38]. To further investigate the effect of TCDD on bile acid metabolism, *bsh* sequences were annotated and quantified within metagenomic samples. Annotations to *bsh* were increased by TCDD and associated with enriched species, including *L. reuteri* and *T. sanguinis* (Figures 13C and 14A, and Table S1). Conversely, *L. murinus* associated *bsh* annotations exhibited a dose-dependent decrease consistent with decreasing trends in taxonomic abundance. Although not reaching significance, many *bsh* sequences were also associated with unclassified Lachnospiraceae species, including *Lachnospiraceae bacterium A4*, a community member reaching 5–23% relative abundance in the cecum metagenomic samples (Figure 14A). In contrast, *Lactobacillus gasseri* was enriched but no *bsh* sequences were identified (Figure 14B). To summarize, the top enriched species were also associated with increased abundances in *bsh* levels in the cecum.

TCDD enriched for mevalonate-dependent isoprenoid biosynthesis

To investigate other metabolic pathways imparting competitive advantages to TCDD-elicited gut environmental stresses, functional gene annotations associated with *L. reuteri*, the most enriched species, were assessed. Among enriched uniref90 annotations in the cecum metagenomic dataset was the aromatic amino acid aminotransferase (UniRef90_A0A2S1ENB9) also classified to *L. reuteri* (Table S2). Aromatic amino acid aminotransferase is required for *L. reuteri* production of the tryptophan metabolite, indole-3-aldehyde, a known AhR ligand reported to induce IL-22 *in vivo* [26]. Among 39 enzyme commission (EC) annotations that were enriched

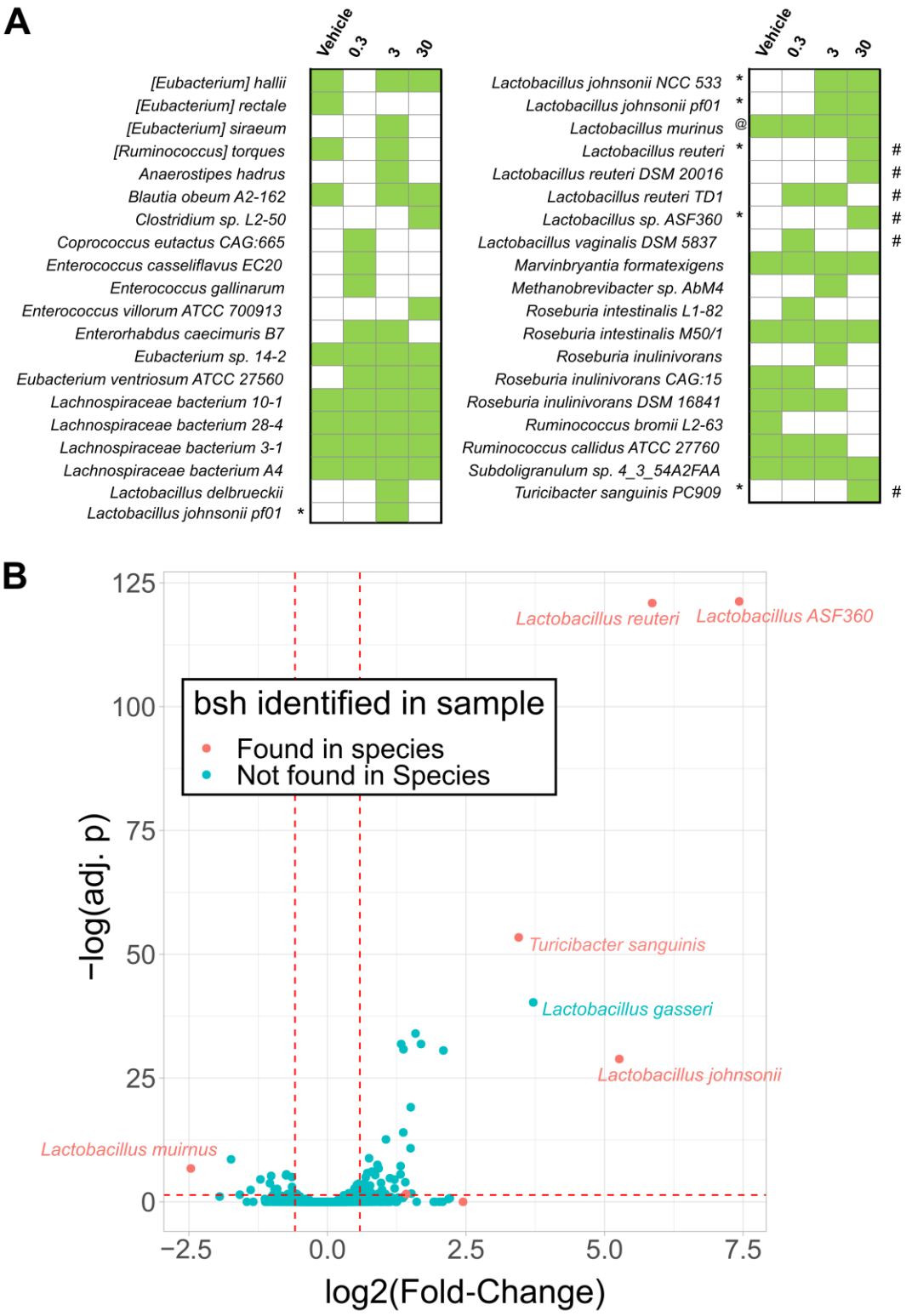

FIGURE 14. TCDD ENRICHED LACTOBACILLUS SPECIES POSSESSING BILE SALT HYDROLASE (BSH).

FIGURE 14 (cont'd)

The presence of *bsh* gene sequences were assessed in metagenomic caecum samples from male C57BL/6 mice following oral gavage with sesame oil vehicle or 0.3, 3, or 30 µg/kg TCDD every 4 days for 28 days using three independent cohorts (n = 3). (**A**) The presence (green boxes) or absence of *bsh* sequences detected in any of the metagenomic samples (n = 3) are denoted within the respective treatment groups. Significant increases (*) or decreases (@) in normalized *bsh* abundances (adj. $p < 0.1$) are denoted. Also denoted is significantly increased species (#) determined by taxonomic analysis that corresponded with respective RefSeq species *bsh* annotations. Significance was determined by Maaslin2 R package. (**B**) Volcano plot displaying $\log_2$(fold-changes) in relative abundance of species between vehicle and 30 µg/kg TCDD treatment groups versus -log(adjusted p-values [adj. p]). Red dots denotes *bsh* sequences detected in 30 µg/kg TCDD treatment group. Significance was determined by the DeSeq2 R package comparing only vehicle and 30 µg/kg TCDD groups. Red dashed lines are reference to −log(0.05) value for the y-axis and −1 and 1 for the x-axis.

and associated with *L. reuteri* were several annotated to the isoprenoid biosynthesis pathway (Figures 15 and S1, and Table S3).

Bacteria biosynthesize isopentenyl diphosphate (IPP) either through the mevalonate-dependent pathway, which is also found in mammals, or the 2-C-methyl-D-erythritol 4-phosphate (MEP)-pathway. Both *L. reuteri* and *Lactobacillus johnsonii* were the major contributors to mevalonate-dependent IPP biosynthesis pathway enrichment with almost all genes in the pathway increased by TCDD; four out of six of the genes significantly increased by TCDD (Figures 3 and S1). Gene enrichment in the alternative MEP-pathway were unchanged by TCDD. For *L. murinus*, only two EC annotations (EC 2.7.1.148, 4-diphosphocytidyl-2-C-methyl-D-erythritol (CDP-ME) kinase, and EC 5.3.3.2, isopentenyl-diphosphate Delta-isomerase) were identified in the MEP pathway also found in *L. reuteri* (Figure S2).

HUMAnN 3.0 analysis of a published metagenomics dataset of fecal samples from human cirrhotic patients (https://www.ncbi.nlm.nih.gov/bioproject/PRJEB6337/, accessed on 25 March 2021) [39] revealed strikingly similar results to our caecum samples from TCDD treated mice. Specifically, increased gene abundance associated with the mevalonate-dependent pathways was also evident in patients with compensated and decompensated liver disease (Figure 16). Compensated cirrhosis is defined as no decrease in liver function while decompensated cirrhosis exhibits decreased liver function. Among decompensated patients with cirrhosis, the mevalonate dependent IPP pathway was increased in 7 out of 8 EC numbers required for de novo IPP biosynthesis (Figure 16). Taxa annotated to genes in the pathway exhibited a wide variety in genera for each EC number in human samples compared to murine cecum samples from this study (Figure S3). Taxonomy classified to a majority of the mevalonate-dependent genes were from the Lactobacillales order, including Enterococcus, Lactobacillus, Streptococcus genera (Figure S3 and Table S5). Lactobacillus and Streptococcus species, including *L. reuteri* and *Streptococcus anginosus*, a known pathogen in liver abscesses [40], were among species classified to the pathway in cirrhosis patients (Tables S4 and S5).

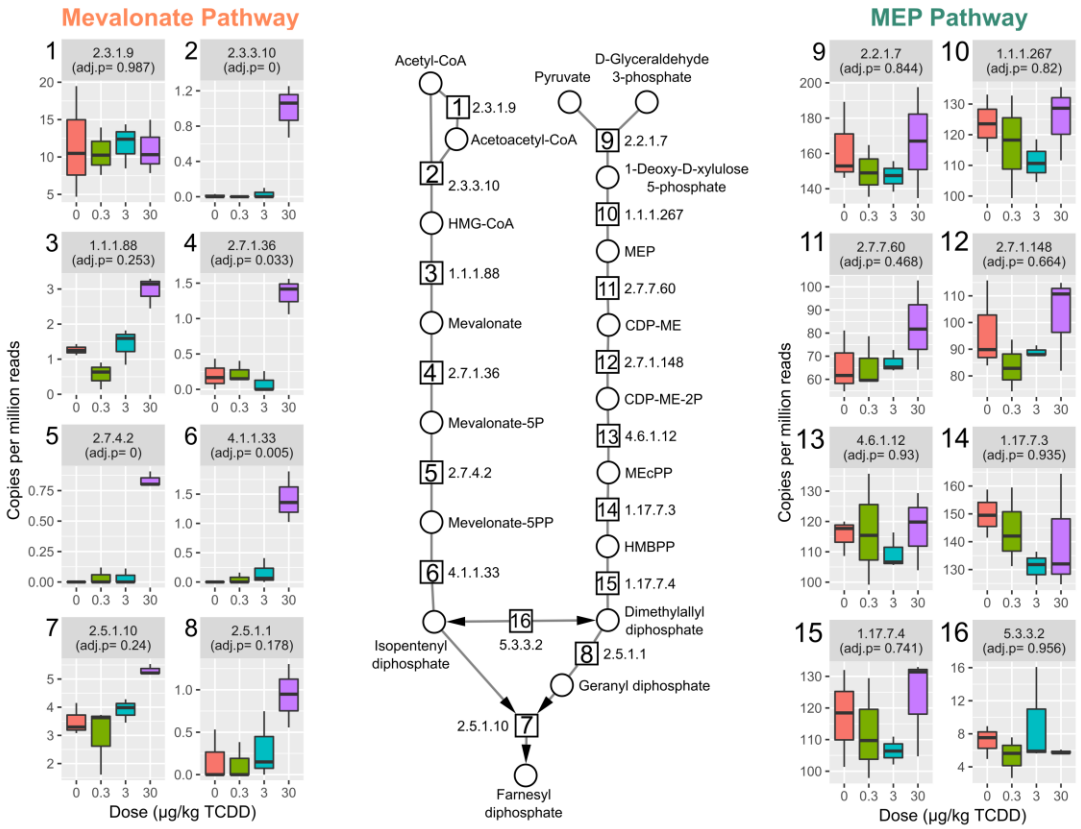

FIGURE 15. TCDD ENRICHED GENES FROM THE MEVALONATE-DEPENDENT ISOPRENOID BIOSYNTHESIS PATHWAY

(a) Relative abundance of genes involved in isoprenoid biosynthesis and grouped by enzyme commission (EC) numbers for the mevalonate dependent and 2-C-methyl-D-erythritol 4-phosphate (MEP) pathways in cecum samples from male C57BL6 mice following oral gavage with sesame oil vehicle or 0.3, 3, or 30 µg/kg TCDD every 4 days for 28 days (*n* = 3). Individual box plots are also numbered with the EC number matching the enzymatic step in pathway schematic. Adjusted *p*-values (adj. *p*) were determined by the Maaslin2 R package. Abbreviations: 3-hydroxyl-3-methyl-glutaryl-CoA (HMG-CoA), (R)-5-phosphomevalonate (mevalonate-5P), (R)-5-diphosphomevalonate (mevalonate-5PP), 2-C-methyl-D-erythritol 4-phosphate (MEP), 4-(cytidine 5'-diphospho)-2-C-methyl-D-erythritol (CDP-ME), 4-(cytidine 5'-diphospho)-2-C-methyl-D-erythritol (DEP-ME-2P), 2-C-Methyl-D-erythritol 2,4-cyclodiphosphate (MEcPP), and 1-hydroxy-2-methyl-2-butenyl 4-diphosphate (HMBPP).

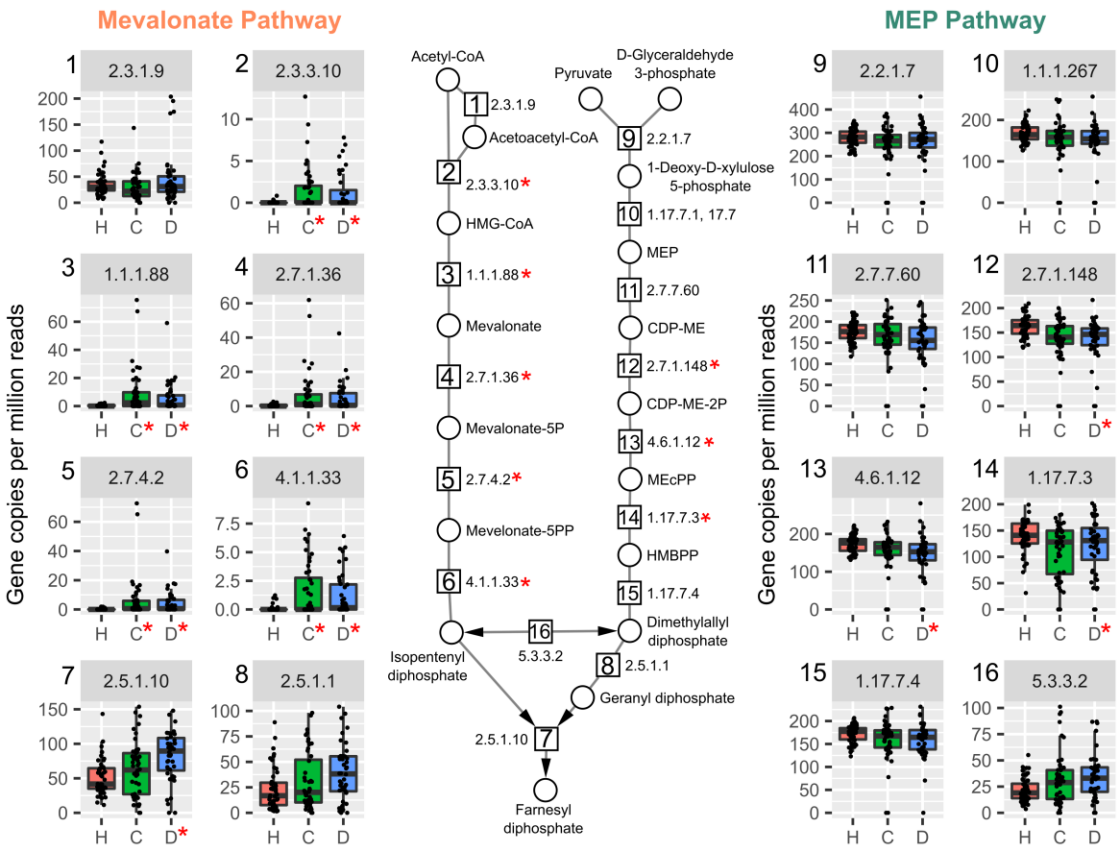

FIGURE 16. MEVALONATE-DEPENDENT IPP BIOSYNTHESIS GENES ARE ENRICHED IN A PUBLISHED METAGENOMICS DATASET OF FECAL SAMPLES FROM CIRRHOSIS PATIENTS.

Humann3 analysis of fecal gut microbiomes in healthy (H, red, *n* = 52), compensated (C, green, *n* = 48), or decompensated (D, blue, *n* = 44) cirrhosis for mevalonate-dependent and methyl-D-erythritol 4-phosphate (MEP) pathways. Individual boxplots are numbered with the EC number matching the enzymatic step in pathway schematic. Significance is denoted with a red asterisk (*, adjusted *p*-values < 0.05) compared to healthy group. Abbreviations.: 3-hydroxyl-3-methyl-glutaryl-CoA (HMG-CoA), (R)-5-phosphomevalonate (mevalonate-5P), (R)-5-diphosphomevalonate (mevalonate-5PP), 2-C-methyl-D-erythritol 4-phosphate (MEP), 4-(cytidine 5'-diphospho)-2-C-methyl-D-erythritol (CDP-ME), 4-(cytidine 5'-diphospho)-2-C- methyl-D-erythritol (DEP-ME-2P), 2-C-methyl-D-erythritol 2,4-cyclodiphosphate (MEcPP), 1-hydroxy-2-methyl-2-butenyl 4-diphosphate (HMBPP).

Vitamin K2 (menaquinone) and peptidoglycan biosynthesis pathways in mouse NAFLD-phenotypes and gut microbiomes of cirrhosis patients

In polyprenol diphosphate biosynthesis, IPP is recursively added to geranyl diphosphate (GPP) or farnesyl diphosphate (FPP) for polyprenol biosynthesis used in vitamin K2 (a.k.a., menaquinone) and peptidoglycan biosynthesis [41,42]. TCDD enriched for heptaprenyl diphosphate synthase (EC 2.5.1.30) with major contributions from *L. reuteri* and *L. johnsonii* (Figure 17). As bacterial cell wall restructuring has been reported in response to bile acids and different levels of isoprenoid biosynthesis pathways were identified, peptidoglycan biosynthesis was also assessed [43]. Most genes encoding enzymes required for peptidoglycan biosynthesis were present in the metagenomic dataset (Figure 18A) with no changes observed following TCDD treatment. However, serine-type D-Ala-D-Ala carboxypeptidase (Figure 18a, EC 3.4.16.4, step 14), responsible for peptidoglycan polymer crosslinking, trended upwards. Additionally, most peptidoglycan biosynthesis EC numbers had annotations to *L. reuteri* (Figure 18B). Overall, TCDD did not alter peptidoglycan synthesis related gene levels.

De novo menaquinone biosynthesis requires chorismate and the addition of a polyprenol diphosphate (i.e., geranyl-geranyl diphosphate) (Figure 19A). Two alternative pathways exist for menaquinone biosynthesis, the *O*-succinylbenzoate or futalosine route [44]. Only a few EC number annotations were detected for the futalosine pathway (EC 4.2.1.151 and EC 2.5.1.120), while all EC numbers were identified for the *O*-succinylbenzoate menaquinone pathway (Figure 19A). In the mouse cecum dataset, species contributing to *O*-succinylbenzoate menaquinone biosynthesis pathway included *Escherichia coli*, several Bacteroides (e.g., *Bacteroides vulgatus* and *Bacteroides caecimuris*), and Lactobacillus species (e.g., *L. reuteri*) (Figure 19B and Table S6). No one species was annotated to the entire set of enzymes needed for de novo biosynthesis from chorismate, however *B. vulgatus* was annotated for 6 out of 9 genes in the pathway (Table S6). *O*-Succinylbenzoate synthase (Figure 18A, EC 4.2.1.113, step 4) was increased by 30 µg/kg

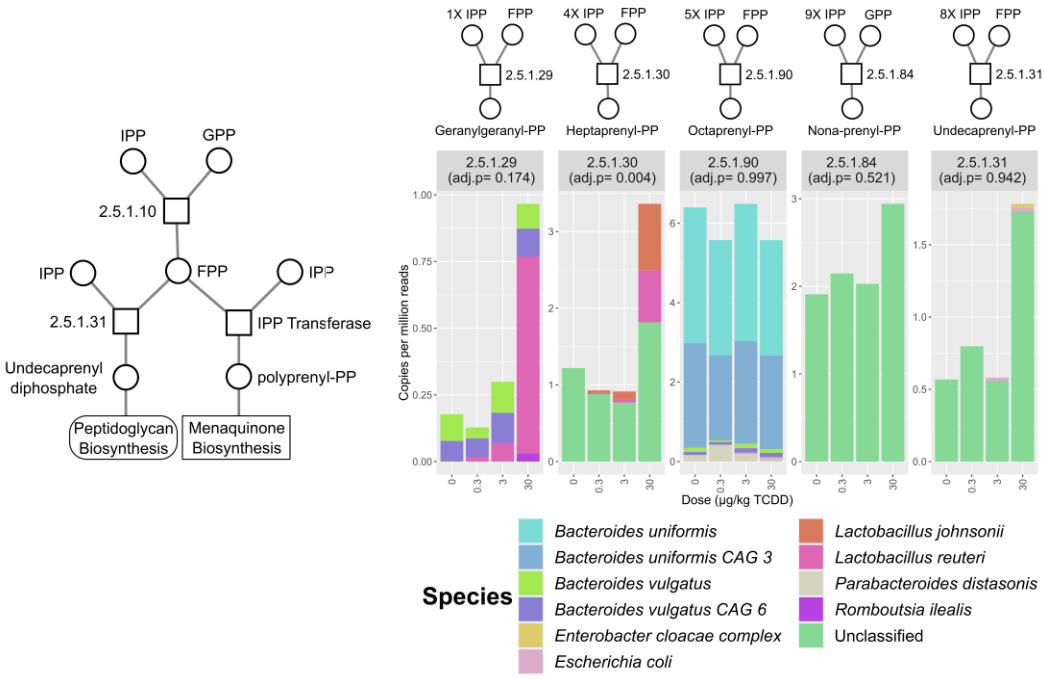

FIGURE 17. RELATIVE ABUNDANCE OF POLYPRENOL TRANSFERASE EC ANNOTATIONS IDENTIFIED IN THE MOUSE CECUM METAGENOMIC DATASET.

Stacked bar plots represent mean relative abundance of grouped EC numbers (*n* = 3) and represent identified species that contributed to mean total abundance for each treatment group. The number of isopentenyl diphosphate (IPP) and farnesyl diphosphate (FPP) molecules used for respective polyprenol biosynthesis are also denoted. Adjusted *p*-values were determined by the Maaslin2 R package. Abbreviations: isopentenyl diphosphate (IPP), geranyl diphosphate (GPP), polyprenyl diphosphate (polyprenyl-PP).

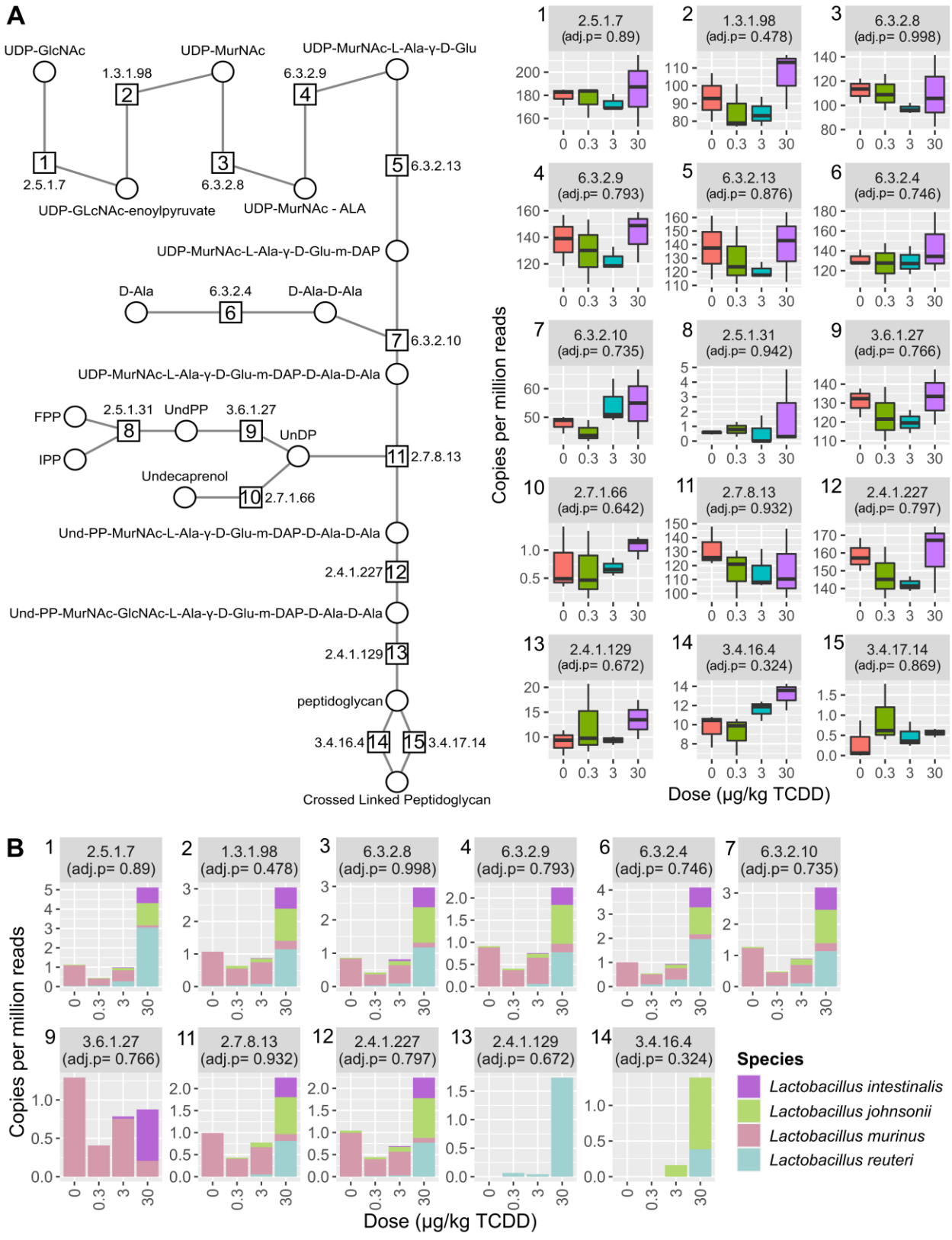

FIGURE 18. PEPTIDOGLYCAN BIOSYNTHESIS WAS UNCHANGED BY TCDD.

FIGURE 18. (cont'd)

(A) Relative abundance of peptidoglycan biosynthesis EC numbers identified in the metagenomic dataset. (B) Relative abundance of only Lactobacillus species classified to peptidoglycan biosynthesis EC numbers. Individual boxplots are numbered with the EC number matching the enzymatic step in pathway schematic. Adjusted *p*-values (adj. *p*) were determined by MAASLIN2. Abbreviations: UDP-N-acetyl-alpha-D-glucosamine (UDP-GlcNac), UDP-N-acetylmuramate (UDP-MurNAc), UDP-N-acetyl-alpha-D-muramoyl-L-alanine (UDP-MurNAc-ALA), UDP-N-acetyl-alpha-D-muramoyl-L-alanyl-D-glutamate(UDP-MurNAc-Ala-D-Glu), UDP-N-acetylmuramoyl-L-alanyl-gamma-D-glutamyl-meso-2,6-diaminopimelate (UDP-MurNAc-Ala-D-Glu-m-DAP), D-Alanyl-D-alanine (D-Ala-D-Ala), UDP-N-acetylmuramoyl-L-alanyl-D-glutamyl-6-carboxy-L-lysyl-D-alanyl-D-alanine (UDP-MurNAc-Ala-D-Glu-m-DAP-D-Ala-D-Ala), Undecaprenyl-diphospho-N-acetylmuramoyl-L-alanyl-D-glutamyl-meso-2,6-diaminopimeloyl-D-alanyl-D-alanine (Und-PP-MurNAc-Ala-D-Glu-m-DAP-D-Ala-D-Ala), Undecaprenyl-diphospho-N-acetylmuramoyl-(N-acetylglucosamine)-L-alanyl-D-glutamyl-meso-2,6-diaminopimeloyl-D-alanyl-D-alanine (Und-PP-MurNAc-GlcNAc-Ala-D-Glu-m-DAP-D-Ala-D-Ala).

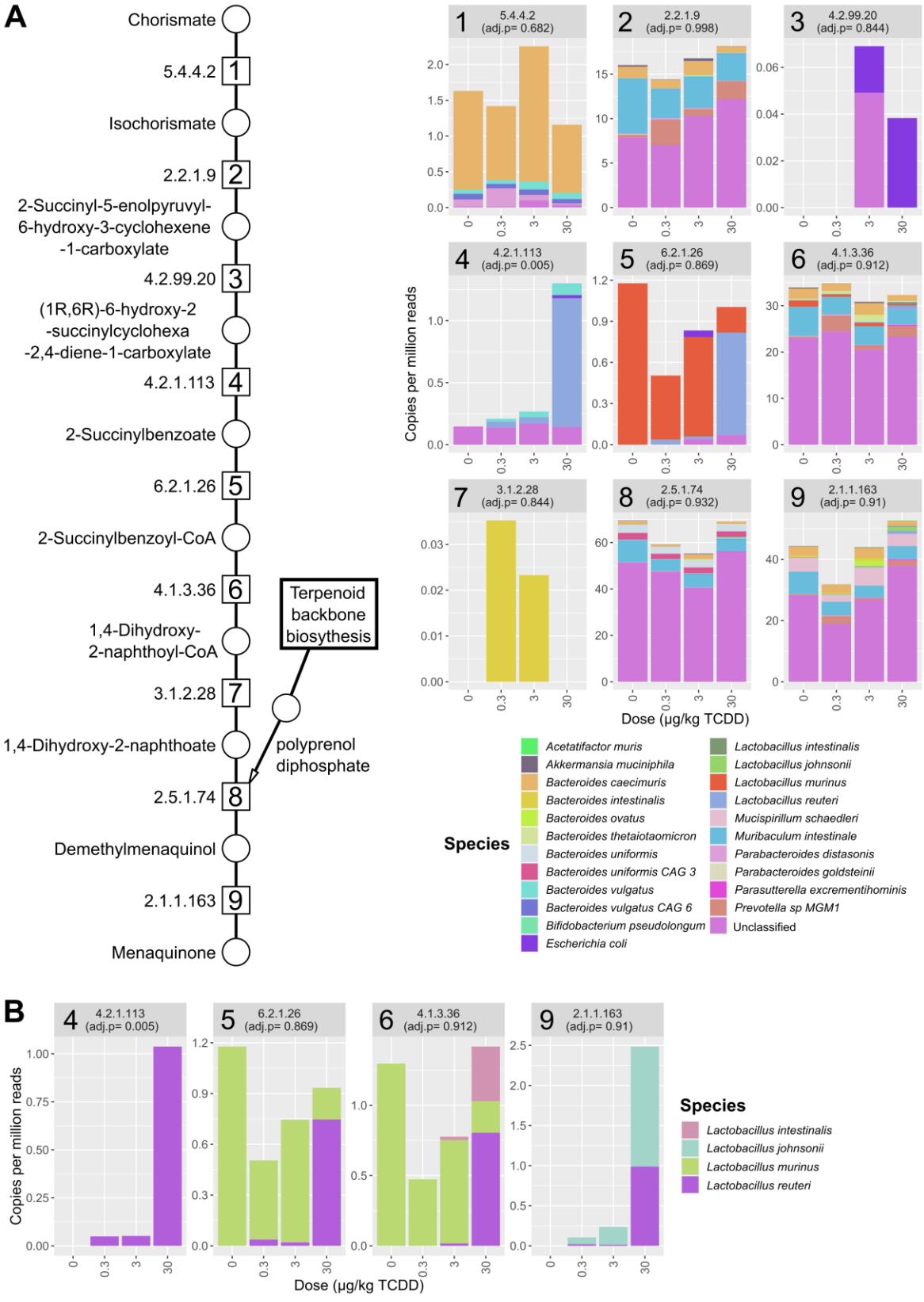

FIGURE 19. TCDD-ELICITED EFFECTS ON MENAQUINONE BIOSYNTHESIS.

FIGURE 19. (cont'd)

(A) Relative abundance of menaquinone biosynthesis EC annotations identified in the metagenomic dataset. Individual stacked bar plots are labeled with the EC number matching the enzymatic step in pathway schematic. Stacked bar plots of annotated EC numbers involved in menaquinone biosynthesis. Values are mean relative abundance (*n* = 3) classified to the respective species and in cecum samples from male C57BL/6 mice following oral gavage with sesame oil vehicle or 0.3, 3, or 30 µg/kg TCDD every 4 days for 28 days. (B) Menaquinone biosynthesis EC numbers classified to Lactobacillus species in the cecum metagenomic datasets. Adjusted *p*-values (adj. *p*) were determined by Maaslin2 R package.

TCDD with *L. reuteri* being the major contributor to relative abundance (Figure 19, step 4).

Lactobacillus species annotated to menaquinone biosynthesis included *L. reuteri*, *L. murinus,* and *L. johnsonii*. Among annotated menaquinone biosynthesis EC numbers, *L. reuteri* was among the identified Lactobacillus species that had the highest relative abundance and most menaquinone EC annotations (Figure 19B). *L. reuteri* also had annotations in samples for EC numbers involved in the final steps of the shikimate pathway responsible for chorismate biosynthesis (Table S7).

In the cirrhosis samples, several EC numbers representing the initial menaquinone biosynthesis steps were also increased in compensated and decompensated patients (Figure 20, steps 1,3,4-5), including *O*-succinylbenzoate synthase (Figure 20, EC 4.2.1.113, step 4). However, *L. reuteri* was not among species classified to this EC number. Species classified to all comprising the complete pathway included *E. coli*, and Klebsiella species, such as *K. pneumoniae* and Citrobacter species. *L. reuteri* was not annotated to any menaquinone biosynthesis genes in healthy or compensated patients, but several EC numbers in the decompensated group (EC 6.2.1.26, 4.1.3.6, and 2.1.1.163), which are involved in later stages of menaquinone biosynthesis (Table S8).

DISCUSSION

Previous studies have reported that TCDD elicited NAFLD-like pathologies, dysregulated bile acid metabolism and gut microbiome dysbiosis [9,11,12,28,30]. This study further elucidated the shifts in the gut microbiota associated with TCDD treatment using shotgun metagenomic sequencing. We show that TCDD dose-dependently shifted the gut microbiota composition by enriching for Lactobacillus species, consistent with hepatic disruption of host and microbial bile acid metabolism. In addition, TCDD enriched for genes involved in mevalonate dependent isoprenoid precursor biosynthesis and menaquinone biosynthesis, crucial for microbial cell growth and survival. Over-representation of these microbial associated pathways were also identified in

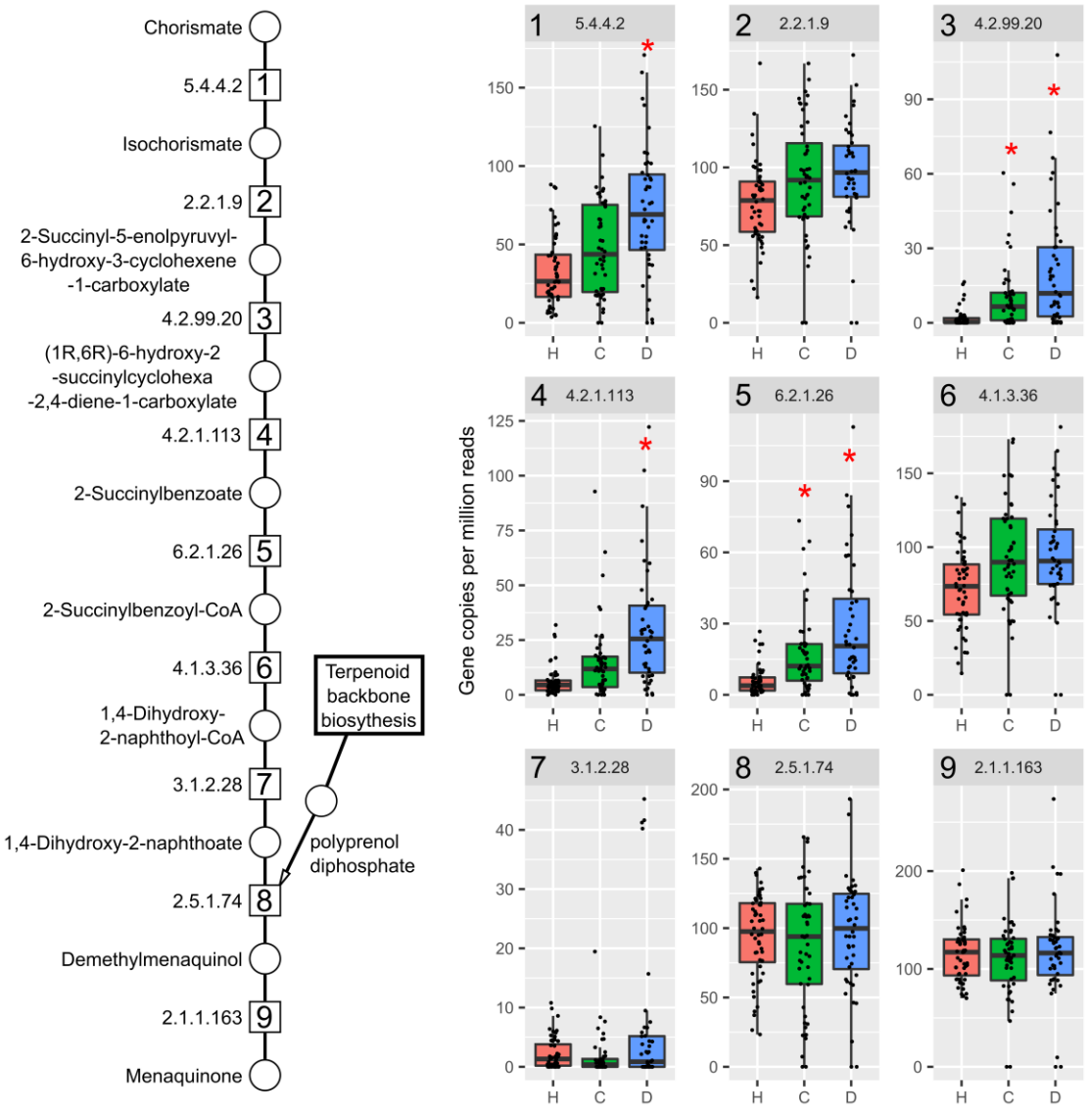

FIGURE 20. MENAQUINONE BIOSYNTHESIS GENES ARE INCREASED IN CIRRHOTIC PATIENTS.

Humann3 analysis of fecal metagenomic dataset of patients with healthy (H, red, *n* = 52), compensated (C, green, *n* = 48), or decompensated (D, blue, *n* = 44) liver cirrhosis diagnosis for EC numbers in menaquinone biosynthesis. Individual box plots are labeled with the EC number matching the enzymatic step in pathway schematic. Significance is denoted with a red asterisk (*; adjusted *p*-values < 0.05) with the healthy group as reference.

human cirrhosis stool metagenomics datasets.

TCDD-elicited gut dysbiosis is in agreement with observed effects in published in vivo studies following treatment with endogenous (i.e., FICZ) and exogenous (i.e., TCDD and TCDF) AhR agonists [8,9,11,28–30]. More specifically, we observed an increased Firmicutes/Bacteroides ratio with dose-dependent increases in Lactobacillus species [28,30]. Lactobacillus species are often associated with NAFLD and with increased abundances in patients with diabetes and liver fibrosis [45]. Probiotic Lactobacillus species, including *L. reuteri* supplementation, have also been reported to alleviate NAFLD pathologies by reducing steatosis [46], fibrosis [47], insulin resistance [48] and serum cholesterol levels [49]. However, Lactobacillus species supplementation may also exacerbate fibrosis [50]. In humans and mice, *L. reuteri* supplementation can modulate the gut microbiota and alter bile acid metabolism. *L. reuteri* enrichment also approached comparable levels compared to samples from humans and mice administered probiotic supplementation [51,52].

We observed a species-specific increase of *L. reuteri* with a concurrent decrease in *L. murinus* suggesting shifts in Lactobacillus composition at the species and/or strain levels. Further, decreased abundance of *L. murinus* has been reported in human NAFLD [53]. Other taxa enriched following treatment included *Turicibacter sanguinis*, an anaerobic gram-positive bacillus commonly found in animals, including humans [54]. Interestingly, *T. sanguinis* has been shown to deconjugate bile acids and metabolize serotonin affecting lipid and steroid metabolism [54,55]. Quantitative trait locus analysis correlated *T. sanguinis* abundance with cholic acid levels and expression of the intestinal bile acid transporter *Slc10a2* [54]. Both cholic acid levels and *Slc10a2* expression are dose-dependently increased by TCDD [9]. Consequently, the dose-dependent taxonomic shift in Lactobacillus and Turicibacter species known to deconjugate conjugated bile acids is consistent with increased levels of secondary bile acids following TCDD treatment.

Some host relevant intestinal health and homeostatic effects can be attributed to Lactobacillus species mediated by bile salt hydrolases (BSHs), which are responsible for

deconjugation reactions, the gateway step for conversion of conjugated primary bile acid to secondary bile acids [56]. A majority of Lactobacillus species possess BSHs, often containing multiple different gene copies within their genome, some with different bile acid substrate preferences [33,38]. However, the presence of *bsh* sequences does not simply infer bile acid tolerance as growth inhibition and reduced fitness is also possible depending on the conjugated or deconjugated bile acids present and/or BSH specificity [33,38,57]. For example, *L. gasseri bsh* knockout mutants exhibit increased fitness compared to wild type strains [38]. Interestingly, *L. gasseri bsh* sequences were not identified despite increased *L. gasseri* abundance following TCDD treatment. Our *bsh* analysis also found TCDD enriched Lactobacillus-associated sequences that may impart bile acid tolerance. For example, the *bsh* sequence enriched by TCDD annotated to *L. johnsonii (*RefSeq ID: EGP12391) (Table S3) exhibited higher substrate specificity for glycine over taurine conjugated bile acids [58]. In a companion study using the dose response and treatment regimen, Fader et al. reported TCDD increased serum DCA levels ~80 fold, with only a ~two-fold increase in serum GDCA levels [9]. In contrast, hepatic taurolithocholic acid (TLCA) levels were increased ~233 fold while serum lithocholic acid increased only four-fold following TCDD treatment.

Moreover, glycine conjugated bile acids, including GDCA, are more toxic towards Lactobacillus species than taurine conjugated bile acids [33,59,60]. Increased levels of BSH with a substrate preference for glycine conjugated bile acid may partially explain select Lactobacillus species enrichment. Further, both TLCA and DCA are potent FXR and GPBAR1 agonists that regulate the lipid, glucose, and bile acid metabolism [61,62]. Consequently, shifts in microbial secondary bile acids by Lactobacillus species may play a role in TCDD elicited gut dysbiosis impacting host regulation of energy homeostasis.

Coincident with increased levels of *bsh* was the dose-dependent increase in genes from the mevalonate-dependent isoprenoid biosynthesis, the pathway also used in mammals for cholesterol biosynthesis. The MEP pathway is the predominant isoprenoid biosynthesis pathway

among gut microbiota while the mevalonate-dependent pathway is only found in select bacteria, including Lactobacillus and Streptococcus species [63]. The output from either pathway is farnesyl diphosphate (FPP) and geranyl diphosphate (GPP), substrates required for polyprenol biosynthesis used in menaquinone and cell wall biosynthesis. Menaquinones are utilized by bacteria for anaerobic/aerobic respiration, providing antioxidant activity with menaquinone supplementation affecting the gut microbiome [64]. In the context of *L. reuteri,* we observed genes annotated to the shikimate pathway, which is responsible for chorismate biosynthesis, a precursor for aromatic amino acids and the naphthoquinone head group of menaquinone, as well as genes involved in *de novo* menaquinone biosynthesis. While the complete biosynthesis pathway was not present in *L. reuteri*, it is consistent with other metagenomic reports of incomplete menaquinone biosynthesis pathways among Lactobacillus species in the gut [44]. It has been proposed that Lactobacillus species may participate in later menaquinone biosynthesis steps through the uptake of intermediates, such as *O*-succinylbenzoate from other bacteria or dietary sources [44]. In addition, the ability to utilize menaquinones for respiration is typically not associated with Lactobacillus species. However, some lactic acid bacteria, including *L. reuteri* strains, demonstrate the ability to respire when menaquinone and heme are supplemented [65,66].

Metagenomic analysis also identified the mevalonate-dependent pathway enrichment in fecal samples from patients with cirrhosis. The mevalonate-dependent pathway is reported to be increased in fibrosis patients with autoimmune pathologies [67]. Isoprenoid biosynthesis pathways are also elevated in the lung microbiome of cystic fibrosis patients, with the MEP pathway enriched rather than the mevalonate route [68]. The association between fibrosis and isoprenoid biosynthesis enrichment warrants further investigation in the context of potential mechanisms contributing to bacterial fitness and/or fibrosis.

Increased abundance of the mevalonate-dependent biosynthesis pathway could also be a biomarker of Lactobacillus and Streptococcus proliferation that is often associated with non-

alcoholic steatohepatitis (NASH)/fibrosis [21,45]. We identified enrichment of the mevalonate-dependent pathway in both mouse and human microbiomes, whereas the complete pathway was primarily annotated to Streptococcus and Lactobacillus species (Table S7). Other factors, such as simvastatin and proton pump inhibitors (PPIs), that are commonly prescribed for NAFLD patients may also impact these microbial pathways. Simvastatin, which is primarily excreted in the feces [69], has been reported to reduce bacterial growth by directly inhibiting bacterial HMG-CoA synthesis while PPIs inhibit Streptococcus species growth [70–72]. These microbiome-drug interactions highlight off target effects that should be considered when investigating novel NAFLD treatments, such as new drug development and/or probiotic interventions.

In addition to increased mevalonate-dependent isoprenoid biosynthesis genes in cirrhotic patients, menaquinone biosynthesis gene abundance was also increased. This suggests taxa with the ability to produce menaquinone may have a competitive advantage when intestinal environmental conditions shift during disease progression. In cirrhosis patients, *E. coli* and *B. vulgatus* were associated with genes providing a majority of the menaquinone biosynthesis capacity. These species are also increased in human NAFLD [73]. Similar to the results in mice exposed to TCDD, *L. reuteri* was associated with several menaquinone biosynthesis genes and only detected in decompensated cirrhosis patients but lacked the complete pathway (Table S10). In cirrhosis patients, it is unclear whether *L. reuteri* is participating in menaquinone metabolism and/or benefiting from increased abundance of species, like *E. coli* that are capable of producing menaquinones.

This study was designed to account for factors affecting gut microbiota analysis, including cage effects, coprophagia, and circadian rhythms [74]. Significant shifts in taxa were observed in Lactobacillus species. However, the small group size (n = 3) following adjustment for multiple testing lacked sufficient power to confirm more subtle shifts, such as the two fold enrichment of *Lachnospiraceae A4*, an abundant community member associated with *bsh* sequences. Samples were also collected within the same Zeitgeber period to account for possible variations in relative

microbiota levels due to circadian rhythm/diurnal regulation. In fact, *L. reuteri* is one gut microbiome member demonstrating changes in relative abundance in human samples due to circadian/diurnal regulation [75]. TCDD disrupted diurnal regulation of hepatic gene expression, including bile acid biosynthesis genes, which may contribute to *L. reuteri* enrichment [76].

The same dose range (sesame oil vehicle and 0.01–30 µg/kg TCDD) and dosing regimen (every 4 days for 28 days) has been used in previous studies to examine TCDD-elicited effects in mice relevant to NAFLD development and progression [9,11–15,30,76–78]. This model recapitulates similar NAFLD progression and pathologies with hepatocyte vacuolization at doses as low as 0.3 µg/kg TCDD. In addition, immune cell infiltration (steatohepatitis) was observed at doses as low 3 µg/kg TCDD with collagen deposition (fibrosis) reported at 30 µg/kg TCDD [9]. Using this study design, TCDD also disrupted the bile acid metabolism and enterohepatic circulation with increased hepatic and serum total bile acids and the secondary bile acid DCA [9]. Likewise, increased serum bile acid levels, including DCA, have been reported in patients with steatohepatitis and fibrosis [79–82]. Furthermore, NAFLD patients with increased bile acid levels have increased levels of bacterial genes from the *bai* operon associated with 7α-dehydroxylation of bile acids leading to the production of DCA from cholic acid [83].

Although the consequences of TCDD-elicited immune system effects on the gut microbiome were not assessed in this study, it is most likely a factor impacting *L. reuteri* enrichment. TCDD causes macrophage and dendritic cell migration out of the *lamina propria* with increased accumulation in the liver, possibly exacerbating hepatic inflammation and affecting intestinal immune responses [14]. The ability of *L. reuteri* to produce AhR ligands, upregulate IL-22, and associate with the mucosa and Peyer's patches provides geographical proximity for immune/microbiome crosstalk mediated by the AhR [26,84,85]. In addition to immune cell regulation, TCDD treatment increases bone formation and decreases bone marrow adiposity [86]. Interestingly, *L. reuteri* supplementation also increases bone density, but only when mice were induced towards an inflammatory state [87]. Overall, the dose-dependent increase in *L. reuteri*

levels is consistent with increased bile acid levels, disruption of circadian/diurnal regulation and increased bone density [9,75,86,87].

In summary, Lactobacillus species were dose-dependently increased following AhR activation by TCDD concurrent with the increase in *bsh* genes and increased primary and secondary bile acids. Specifically, *L. reuteri*, a keystone gut microbiome species is involved in the microbial metabolism of bile acids and AhR ligands. The large and uniform enrichment of *L. reuteri* in this study also suggests environmental pressures, such as increased levels of bile acids and antimicrobial peptides elicited by AhR activation, may provide a complementary niche for *L. reuteri* that possess a gene repertoire not found in the closely related *L. murinus*. We also provide evidence regarding how *L. reuteri* metabolism could impact the AhR, FXR, and GPBAR1 signaling pathways, placing *L. reuteri* at the crossroads of bacterial/host interactions affecting glucose, bile acid, and immune regulation. Whether these microbial shifts in metabolism are adaptive and limit the intensity of adverse consequences or exacerbate steatosis to steatohepatitis with fibrosis progression warrants further investigation.

REFERENCES

REFERENCES

1. Younossi, Z.M.; Koenig, A.B.; Abdelatif, D.; Fazel, Y.; Henry, L.; Wymer, M. Global Epidemiology of Nonalcoholic Fatty Liver Disease-Meta-Analytic Assessment of Prevalence, Incidence, and Outcomes. Hepatology 2016, 64, 73–84, doi:10.1002/hep.28431.

2. Anstee, Q.M.; Targher, G.; Day, C.P. Progression of NAFLD to Diabetes Mellitus, Cardiovascular Disease or Cirrhosis. Nat. Rev. Gastroenterol. Hepatol. 2013, 10, 330–344, doi:10.1038/nrgastro.2013.41.

3. Tilg, H.; Moschen, A.R. Evolution of Inflammation in Nonalcoholic Fatty Liver Disease: The Multiple Parallel Hits Hypothesis. Hepatology 2010, 52, 1836–1846, doi:10.1002/hep.24001.

4. Cave, M.; Appana, S.; Patel, M.; Falkner, K.C.; McClain, C.J.; Brock, G. Polychlorinated Biphenyls, Lead, and Mercury Are Associated with Liver Disease in American Adults: NHANES 2003–2004. Environ. Health Perspect. 2010, 118, 1735–1742, doi:10.1289/ehp.1002720.

5. Zheng, S.; Yang, Y.; Wen, C.; Liu, W.; Cao, L.; Feng, X.; Chen, J.; Wang, H.; Tang, Y.; Tian, L.; et al. Effects of Environmental Contaminants in Water Resources on Nonalcoholic Fatty Liver Disease. Environ. Int. 2021, 154, 106555, doi:10.1016/j.envint.2021.106555.

6. Kumar, J.; Lind, L.; Salihovic, S.; van Bavel, B.; Ingelsson, E.; Lind, P.M. Persistent Organic Pollutants and Liver Dysfunction Biomarkers in a Population-Based Human Sample of Men and Women. Environ. Res. 2014, 134, 251–256, doi:10.1016/j.envres.2014.07.023.

7. Rantakokko, P.; Männistö, V.; Airaksinen, R.; Koponen, J.; Viluksela, M.; Kiviranta, H.; Pihlajamäki, J. Persistent Organic Pollutants and Non-Alcoholic Fatty Liver Disease in Morbidly Obese Patients: A Cohort Study. Environ. Health 2015, 14, 79, doi:10.1186/s12940-015-0066-z.

8. Zhang, L.; Nichols, R.G.; Correll, J.; Murray, I.A.; Tanaka, N.; Smith, P.B.; Hubbard, T.D.; Sebastian, A.; Albert, I.; Hatzakis, E.; et al. Persistent Organic Pollutants Modify Gut Microbiota–Host Metabolic Homeostasis in Mice through Aryl Hydrocarbon Receptor Activation. Environ. Health Perspect. 2015, 123, 679–688, doi:10.1289/ehp.1409055.

9. Fader, K.A.; Nault, R.; Zhang, C.; Kumagai, K.; Harkema, J.R.; Zacharewski, T.R. 2,3,7,8-Tetrachlorodibenzo-p-Dioxin (TCDD)-Elicited Effects on Bile Acid Homeostasis: Alterations in Biosynthesis, Enterohepatic Circulation, and Microbial Me-tabolism. Sci. Rep. 2017, 7, 5921, doi:10.1038/s41598-017-05656-8.

10. Petriello, M.C.; Hoffman, J.B.; Vsevolozhskaya, O.; Morris, A.J.; Hennig, B. Dioxin-like PCB 126 Increases Intestinal Inflam-mation and Disrupts Gut Microbiota and Metabolic Homeostasis. Environ. Pollut. 2018, 242, 1022–1032, doi:10.1016/j.envpol.2018.07.039.

11. Stedtfeld, R.D.; Chai, B.; Crawford, R.B.; Stedtfeld, T.M.; Williams, M.R.; Xiangwen, S.; Kuwahara, T.; Cole, J.R.; Kaminski, N.E.; Tiedje, J.M.; et al. Modulatory Influence of

Segmented Filamentous Bacteria on Transcriptomic Response of Gnotobiotic Mice Exposed to TCDD. Front. Microbiol. 2017, 8, 1708, doi:10.3389/fmicb.2017.01708.

12. Nault, R.; Fader, K.A.; Lydic, T.A.; Zacharewski, T.R. Lipidomic Evaluation of Aryl Hydrocarbon Receptor-Mediated Hepatic Steatosis in Male and Female Mice Elicited by 2,3,7,8-Tetrachlorodibenzo-p-dioxin. Chem. Res. Toxicol. 2017, 30, 1060–1075, doi:10.1021/acs.chemrestox.6b00430.

13. Nault, R.; Fader, K.A.; Ammendolia, D.A.; Dornbos, P.; Potter, D.; Sharratt, B.; Kumagai, K.; Harkema, J.R.; Lunt, S.Y.; Matthews, J.; et al. Dose-Dependent Metabolic Reprogramming and Differential Gene Expression in TCDD-Elicited Hepatic Fibrosis. Toxicol. Sci. 2016, 154, 253–266, doi:10.1093/toxsci/kfw163.

14. Fader, K.A.; Nault, R.; Ammendolia, D.A.; Harkema, J.R.; Williams, K.J.; Crawford, R.B.; Kaminski, N.E.; Potter, D.; Sharratt, B.; Zacharewski, T.R. 2,3,7,8-Tetrachlorodibenzo-p-Dioxin Alters Lipid Metabolism and Depletes Immune Cell Populations in the Jejunum of C57BL/6 Mice. Toxicol. Sci. 2015, 148, 567–580, doi:10.1093/toxsci/kfv206.

15. Angrish, M.M.; Dominici, C.Y.; Zacharewski, T.R. TCDD-Elicited Effects on Liver, Serum, and Adipose Lipid Composition in C57BL/6 Mice. Toxicol. Sci. 2013, 131, 108–115, doi:10.1093/toxsci/kfs277.

16. Katsiki, N.; Mikhailidis, D.P.; Mantzoros, C.S. Non-Alcoholic Fatty Liver Disease and Dyslipidemia: An Update. Metabolism 2016, 65, 1109–1123, doi:10.1016/j.metabol.2016.05.003.

17. Cholico, G.N.; Fling, R.R.; Zacharewski, N.A.; Fader, K.A.; Nault, R.; Zacharewski, T. Thioesterase Induction by 2,3,7,8-Tetrachlorodibenzo-p-Dioxin Results in a Futile Cycle That Inhibits Hepatic β-Oxidation. bioRxiv 2021, doi:10.1101/2021.01.21.427582.

18. Fernandez-Salguero, P.M.; Hllbert, D.M.; Rudikoff, S.; Ward, J.M.; Gonzalez, F.J. Aryl-Hydrocarbon Receptor-Deficient Mice Are Resistant to 2,3,7,8-Tetrachlorodibenzo-p-Dioxin-Induced Toxicity. Toxicol. Appl. Pharmacol. 1996, 140, 173–179, doi:10.1006/taap.1996.0210.

19. Bock, K.W. Aryl Hydrocarbon Receptor (AHR)-Mediated Inflammation and Resolution: Non-Genomic and Genomic Signaling. Biochem. Pharmacol. 2020, 182, 114220, doi:10.1016/j.bcp.2020.114220.

20. Schiering, C.; Wincent, E.; Metidji, A.; Iseppon, A.; Li, Y.; Potocnik, A.J.; Omenetti, S.; Henderson, C.J.; Wolf, C.R.; Nebert, D.W.; et al. Feedback Control of AHR Signalling Regulates Intestinal Immunity. Nature 2017, 542, 242–245, doi:10.1038/nature21080.

21. Grabherr, F.; Grander, C.; Effenberger, M.; Adolph, T.E.; Tilg, H. Gut Dysfunction and Non-Alcoholic Fatty Liver Disease. Front. Endocrinol. 2019, 10, 611, doi:10.3389/fendo.2019.00611.

22. Leung, C.; Rivera, L.; Furness, J.B.; Angus, P.W. The Role of the Gut Microbiota in NAFLD. Nat. Rev. Gastroenterol. Hepatol. 2016, 13, 412–425, doi:10.1038/nrgastro.2016.85.

23. Tian, J.; Feng, Y.; Fu, H.; Xie, H.Q.; Jiang, J.X.; Zhao, B. The Aryl Hydrocarbon Receptor: A Key Bridging Molecule of External and Internal Chemical Signals. Environ. Sci. Technol. 2015, 49, 9518–9531, doi:10.1021/acs.est.5b00385.

24. Rothhammer, V.; Quintana, F.J. The Aryl Hydrocarbon Receptor: An Environmental Sensor Integrating Immune Responses in Health and Disease. Nat. Rev. Immunol. 2019, 19, 184–197, doi:10.1038/s41577-019-0125-8.

25. Qiu, J.; Heller, J.J.; Guo, X.; Chen, Z.M.E.; Fish, K.; Fu, Y.X.; Zhou, L. The Aryl Hydrocarbon Receptor Regulates Gut Immunity through Modulation of Innate Lymphoid Cells. Immunity 2012, 36, 92–104, doi:10.1016/j.immuni.2011.11.011.

26. Zelante, T.; Iannitti, R.G.; Cunha, C.; DeLuca, A.; Giovannini, G.; Pieraccini, G.; Zecchi, R.; D'Angelo, C.; Massi-Benedetti, C.; Fallarino, F.; et al. Tryptophan Catabolites from Microbiota Engage Aryl Hydrocarbon Receptor and Balance Mucosal Reac-tivity via Interleukin-22. Immunity 2013, 39, 372–385, doi:10.1016/j.immuni.2013.08.003.

27. Murray, I.A.; Nichols, R.G.; Zhang, L.; Patterson, A.D.; Perdew, G.H. Expression of the Aryl Hydrocarbon Receptor Contrib-utes to the Establishment of Intestinal Microbial Community Structure in Mice. Sci. Rep. 2016, 6, 33969, doi:10.1038/srep33969.

28. Lefever, D.E.; Xu, J.; Chen, Y.; Huang, G.; Tamas, N.; Guo, T.L. TCDD Modulation of Gut Microbiome Correlated with Liver and Immune Toxicity in Streptozotocin (STZ)-Induced Hyperglycemic Mice. Toxicol. Appl. Pharmacol. 2016, 304, 48–58, doi:10.1016/j.taap.2016.05.016.

29. Neamah, W.H.; Busbee, P.B.; Alghetaa, H.; Abdulla, O.A.; Nagarkatti, M.; Nagarkatti, P. AhR Activation Leads to Alterations in the Gut Microbiome with Consequent Effect on Induction of Myeloid Derived Suppressor Cells in a CXCR2-Dependent Manner. Int. J. Mol. Sci. 2020, 18, 9613.

30. Stedtfeld, R.D.; Brett Sallach, J.; Crawford, R.B.; Stedtfeld, T.M.; Williams, M.R.; Waseem, H.; Johnston, C.T.; Li, H.; Teppen, B.J.; Kaminski, N.E.; et al. TCDD Administered on Activated Carbon Eliminates Bioavailability and Subsequent Shifts to a Key Murine Gut Commensal. Appl. Microbiol. Biotechnol. 2017, 101, 7409–7415, doi:10.1007/s00253-017-8460-9.

31. Shao, J.-W.; Ge, T.-T.; Chen, S.-Z.; Wang, G.; Yang, Q.; Huang, C.-H.; Xu, L.-C.; Chen, Z. Role of Bile Acids in Liver Diseases Mediated by the Gut Microbiome. World J. Gastroenterol. 2021, 27, 3010–3021, doi:10.3748/wjg.v27.i22.3010.

32. Marion, S.; Desharnais, L.; Studer, N.; Dong, Y.; Notter, M.D.; Poudel, S.; Menin, L.; Janowczyk, A.; Hettich, R.L.; Hapfelmeier, S.; et al. Biogeography of Microbial Bile Acid Transformations along the Murine Gut. J. Lipid Res. 2020, 61, 1450–1463, doi:10.1194/jlr.RA120001021.

33. Foley, M.H.; O'Flaherty, S.; Allen, G.; Rivera, A.J.; Stewart, A.K.; Barrangou, R.; Theriot, C.M. Lactobacillus Bile Salt Hydrolase Substrate Specificity Governs Bacterial Fitness and Host Colonization. Proc. Natl. Acad. Sci. USA 2021, 118, e2017709118, doi:10.1073/pnas.2017709118.

34. Matsubara, T.; Li, F.; Gonzalez, F.J. FXR Signaling in the Enterohepatic System. Mol. Cell. Endocrinol. 2013, 368, 17–29, doi:10.1016/j.mce.2012.05.004.

35. Shapiro, H.; Kolodziejczyk, A.A.; Halstuch, D.; Elinav, E. Bile Acids in Glucose Metabolism in Health and Disease. J. Exp. Med. 2018, 215, 383–396, doi:10.1084/jem.20171965.

36. Pols, T.W.H.; Noriega, L.G.; Nomura, M.; Auwerx, J.; Schoonjans, K. The Bile Acid Membrane Receptor TGR5: A Valuable Metabolic Target. Dig. Dis 2011, 29, 37–44, doi:10.1159/000324126.

37. Fiorucci, S.; Mencarelli, A.; Palladino, G.; Cipriani, S. Bile-Acid-Activated Receptors: Targeting TGR5 and Farnesoid-X-Receptor in Lipid and Glucose Disorders. Trends Pharmacol. Sci. 2009, 30, 570–580, doi:10.1016/j.tips.2009.08.001.

38. O'Flaherty, S.; Briner Crawley, A.; Theriot, C.M.; Barrangou, R. The Lactobacillus Bile Salt Hydrolase Repertoire Reveals Niche-Specific Adaptation. mSphere 2018, 3, e00140-18, doi:10.1128/mSphere.00140-18.

39. Shao, L.; Ling, Z.; Chen, D.; Liu, Y.; Yang, F.; Li, L. Disorganized Gut Microbiome Contributed to Liver Cirrhosis Progression: A Meta-Omics-Based Study. Front. Microbiol. 2018, 9, 3166, doi:10.3389/fmicb.2018.03166.

40. Fazili, T.; Riddell, S.; Kiska, D.; Endy, T.; Giurgea, L.; Sharngoe, C.; Javaid, W. Streptococcus Anginosus Group Bacterial In-fections. Am. J. Med. Sci. 2017, 354, 257–261, doi:10.1016/j.amjms.2017.05.011.

41. Workman, S.D.; Strynadka, N.C.J. A Slippery Scaffold: Synthesis and Recycling of the Bacterial Cell Wall Carrier Lipid. J. Mol. Biol. 2020, 432, 4964–4982, doi:10.1016/j.jmb.2020.03.025.

42. Johnston, J.M.; Bulloch, E.M. Advances in Menaquinone Biosynthesis: Sublocalisation and Allosteric Regulation. Curr. Opin. Struct. Biol. 2020, 65, 33–41, doi:10.1016/j.sbi.2020.05.005.

43. Hernández, S.B.; Cava, F.; Pucciarelli, M.G.; García-del Portillo, F.; de Pedro, M.A.; Casadesús, J. Bile-Induced Peptidoglycan Remodelling in S Almonella Enterica: Bile-Induced Peptidoglycan Remodelling. Environ. Microbiol. 2015, 17, 1081–1089, doi:10.1111/1462-2920.12491.

44. Ravcheev, D.A.; Thiele, I. Genomic Analysis of the Human Gut Microbiome Suggests Novel Enzymes Involved in Quinone Biosynthesis. Front. Microbiol. 2016, 7, 128, doi:10.3389/fmicb.2016.00128.

45. Aron-Wisnewsky, J.; Vigliotti, C.; Witjes, J.; Le, P.; Holleboom, A.G.; Verheij, J.; Nieuwdorp, M.; Clément, K. Gut Microbiota and Human NAFLD: Disentangling Microbial Signatures from Metabolic Disorders. Nat. Rev. Gastroenterol. Hepatol. 2020, 17, 279–297, doi:10.1038/s41575-020-0269-9.

46. Qiao, Y.; Sun, J.; Xia, S.; Li, L.; Li, Y.; Wang, P.; Shi, Y.; Le, G. Effects of Different Lactobacillus Reuteri on Inflammatory and Fat Storage in High-Fat Diet-Induced Obesity Mice Model. J. Funct. Foods 2015, 14, 424–434, doi:10.1016/j.jff.2015.02.013.

47. Ting, W.-J.; Kuo, W.-W.; Hsieh, D.; Yeh, Y.-L.; Day, C.-H.; Chen, Y.-H.; Chen, R.-J.; Padma, V.; Chen, Y.-H.; Huang, C.-Y. Heat Killed Lactobacillus Reuteri GMNL-263 Reduces Fibrosis Effects on the Liver and Heart in High Fat Diet-Hamsters via TGF-β Suppression. Int. J. Mol. Sci. 2015, 16, 25881–25896, doi:10.3390/ijms161025881.

48. Andreasen, A.S.; Larsen, N.; Pedersen-Skovsgaard, T.; Berg, R.M.G.; Møller, K.; Svendsen, K.D.; Jakobsen, M.; Pedersen, B.K. Effects of Lactobacillus Acidophilus NCFM on Insulin Sensitivity and the Systemic Inflammatory Response in Human Subjects. Br. J. Nutr. 2010, 104, 1831–1838, doi:10.1017/S0007114510002874.

49. Khare, A.; Gaur, S. Cholesterol-Lowering Effects of Lactobacillus Species. Curr. Microbiol. 2020, 77, 638–644, doi:10.1007/s00284-020-01903-w.

50. Roh, Y.S.; Cho, A.; Cha, Y.-S.; Oh, S.-H.; Lim, C.W.; Kim, B. Lactobacillus Aggravate Bile Duct Ligation-Induced Liver In-flammation and Fibrosis in Mice. Toxicol. Res. 2018, 34, 241–247, doi:10.5487/TR.2018.34.3.241.

51. Martoni, C.J.; Labbé, A.; Ganopolsky, J.G.; Prakash, S.; Jones, M.L. Changes in Bile Acids, FGF-19 and Sterol Absorption in Response to Bile Salt Hydrolase Active L. Reuteri NCIMB 30242. Gut Microbes 2015, 6, 57–65, doi:10.1080/19490976.2015.1005474.

52. Kumar, R.; Grover, S.; Batish, V.K. Hypocholesterolaemic Effect of Dietary Inclusion of Two Putative Probiotic Bile Salt Hy-drolase-Producing Lactobacillus Plantarum Strains in Sprague–Dawley Rats. Br. J. Nutr. 2011, 105, 561–573, doi:10.1017/S0007114510003740.

53. Lee, N.Y.; Shin, M.J.; Youn, G.S.; Yoon, S.J.; Choi, Y.R.; Kim, H.S.; Gupta, H.; Han, S.H.; Kim, B.K.; Lee, D.Y.; et al. Lactobacillus Attenuates Progression of Nonalcoholic Fatty Liver Disease by Lowering Cholesterol and Steatosis. Clin. Mol. Hepatol. 2021, 27, 110–124, doi:10.3350/cmh.2020.0125.

54. Kemis, J.H.; Linke, V.; Barrett, K.L.; Boehm, F.J.; Traeger, L.L.; Keller, M.P.; Rabaglia, M.E.; Schueler, K.L.; Stapleton, D.S.; Gatti, D.M.; et al. Genetic Determinants of Gut Microbiota Composition and Bile Acid Profiles in Mice. PLoS Genet. 2019, 15, e1008073, doi:10.1371/journal.pgen.1008073.

55. Fung, T.C.; Vuong, H.E.; Luna, C.D.G.; Pronovost, G.N.; Aleksandrova, A.A.; Riley, N.G.; Vavilina, A.; McGinn, J.; Rendon, T.; Forrest, L.R.; et al. Intestinal Serotonin and Fluoxetine Exposure Modulate Bacterial Colonization in the Gut. Nat. Microbiol. 2019, 4, 2064–2073, doi:10.1038/s41564-019-0540-4.

56. Tannock, G.W.; Dashkevicz, M.P.; Feighner, S.D. Lactobacilli and Bile Salt Hydrolase in the Murine Intestinal Tract. Appl. Environ. Microbiol. 1989, 55, 1848–1851, doi:10.1128/aem.55.7.1848-1851.1989.

57. Winston, J.A.; Rivera, A.; Cai, J.; Patterson, A.D.; Theriot, C.M. Secondary Bile Acid Ursodeoxycholic Acid Alters Weight, the Gut Microbiota, and the Bile Acid Pool in Conventional Mice. PLoS ONE 2021, 16, e0246161, doi:10.1371/journal.pone.0246161.

58. Chae, J.P.; Valeriano, V.D.; Kim, G.-B.; Kang, D.-K. Molecular Cloning, Characterization and Comparison of Bile Salt Hy-drolases from Lactobacillus Johnsonii PF01. J. Appl. Microbiol. 2013, 114, 121–133, doi:10.1111/jam.12027.

59. De Smet, I.; Van Hoorde, L.; Vande Woestyne, M.; Christiaens, H.; Verstraete, W. Significance of Bile Salt Hydrolytic Activities of Lactobacilli. J. Appl. Bacteriol. 1995, 79, 292–301, doi:10.1111/j.1365-2672.1995.tb03140.x.

60. Bustos, A.Y.; Saavedra, L.; de Valdez, G.F.; Raya, R.R.; Taranto, M.P. Relationship between Bile Salt Hydrolase Activity, Changes in the Internal PH and Tolerance to Bile Acids in Lactic Acid Bacteria. Biotechnol. Lett. 2012, 34, 1511–1518, doi:10.1007/s10529-012-0932-5.

61. Sato, H.; Macchiarulo, A.; Thomas, C.; Gioiello, A.; Une, M.; Hofmann, A.F.; Saladin, R.; Schoonjans, K.; Pellicciari, R.; Auwerx, J. Novel Potent and Selective Bile Acid Derivatives as TGR5 Agonists: Biological Screening, Structure−Activity Relationships, and Molecular Modeling Studies. J. Med. Chem. 2008, 51, 1831–1841, doi:10.1021/jm7015864.

62. Wahlström, A.; Sayin, S.I.; Marschall, H.-U.; Bäckhed, F. Intestinal Crosstalk between Bile Acids and Microbiota and Its Impact on Host Metabolism. Cell Metab. 2016, 24, 41–50, doi:10.1016/j.cmet.2016.05.005.

63. Vranová, E.; Coman, D.; Gruissem, W. Network Analysis of the MVA and MEP Pathways for Isoprenoid Synthesis. Annu. Rev. Plant Biol. 2013, 64, 665–700, doi:10.1146/annurev-arplant-050312-120116.

64. Stacchiotti, V.; Rezzi, S.; Eggersdorfer, M.; Galli, F. Metabolic and Functional Interplay between Gut Microbiota and Fat-Soluble Vitamins. Crit. Rev. Food Sci. Nutr. 2020, 61, 3211–3232, doi:10.1080/10408398.2020.1793728.

65. Brooijmans, R.; Smit, B.; Santos, F.; van Riel, J.; de Vos, W.M.; Hugenholtz, J. Heme and Menaquinone Induced Electron Transport in Lactic Acid Bacteria. Microb Cell Fact. 2009, 8, 28, doi:10.1186/1475-2859-8-28.

66. Ianniello, R.G.; Zheng, J.; Zotta, T.; Ricciardi, A.; Gänzle, M.G. Biochemical Analysis of Respiratory Metabolism in the Het-erofermentative Lactobacillus Spicheri and Lactobacillus Reuteri. J. Appl. Microbiol. 2015, 119, 763–775, doi:10.1111/jam.12853.

67. Plichta, D.R.; Somani, J.; Pichaud, M.; Wallace, Z.S.; Fernandes, A.D.; Perugino, C.A.; Lähdesmäki, H.; Stone, J.H.; Vlamakis, H.; Chung, D.C.; et al. Congruent Microbiome Signatures in Fibrosis-Prone Autoimmune Diseases: IgG4-Related Disease and Systemic Sclerosis. Genome Med. 2021, 13, 35, doi:10.1186/s13073-021-00853-7.

68. Quinn, R.A.; Whiteson, K.; Lim, Y.W.; Zhao, J.; Conrad, D.; LiPuma, J.J.; Rohwer, F.; Widder, S. Ecological Networking of Cystic Fibrosis Lung Infections. NPJ Biofilms Microbiomes 2016, 2, 4, doi:10.1038/s41522-016-0002-1.

69. Chu, N.-N.; Chen, W.-L.; Xu, H.-R.; Li, X.-N. Pharmacokinetics and Safety of Ezetimibe/Simvastatin Combination Tablet: An Open-Label, Single-Dose Study in Healthy Chinese Subjects. Clin. Drug Investig. 2012, 32, 791–798, doi:10.1007/s40261-012-0013-5.

70. Ashrafizadeh, M.; Ahmadi, Z. Effects of Statins on Gut Microbiota (Microbiome). Rev. Clin. Med. 2019, 6, 5.

71. Whitaker, E.; Alshammari, A. Bacteriostatic Effect of Simvastatin on Selected Oral Streptococci in Vitro. Contemp. Clin. Dent. 2017, 8, 59, doi:10.4103/ccd.ccd_848_16.

72. Wu, S.; Jiang, P.; Zhao, X.-M.; Chen, W.-H. Treatment Regimens May Compromise Gut-Microbiome-Derived Signatures for Liver Cirrhosis. Cell Metab. 2021, 33, 455–456, doi:10.1016/j.cmet.2021.02.012.

73. Loomba, R.; Seguritan, V.; Li, W.; Long, T.; Klitgord, N.; Bhatt, A.; Dulai, P.S.; Caussy, C.; Bettencourt, R.; Highlander, S.K.; et al. Gut Microbiome-Based Metagenomic Signature for Non-Invasive Detection of Advanced Fibrosis in Human Nonalcoholic Fatty Liver Disease. Cell Metab. 2017, 25, 1054–1062.e5, doi:10.1016/j.cmet.2017.04.001.

74. McCoy, K.D.; Ohland, C.L. Innate Responses to Gut Microbiota; Critical Assessment of the Necessary Experimental Controls. Curr. Opin. Microbiol. 2021, 59, 34–41, doi:10.1016/j.mib.2020.07.008.

75. Thaiss, C.A.; Zeevi, D.; Levy, M.; Zilberman-Schapira, G.; Suez, J.; Tengeler, A.C.; Abramson, L.; Katz, M.N.; Korem, T.; Zmora, N.; et al. Transkingdom Control of Microbiota Diurnal Oscillations Promotes Metabolic Homeostasis. Cell 2014, 159, 514–529, doi:10.1016/j.cell.2014.09.048.

76. Fader, K.A.; Nault, R.; Doskey, C.M.; Fling, R.R.; Zacharewski, T.R. 2,3,7,8-Tetrachlorodibenzo-p-Dioxin Abolishes Circadian Regulation of Hepatic Metabolic Activity in Mice. Sci. Rep. 2019, 9, 6514, doi:10.1038/s41598-019-42760-3.

77. Nault, R.; Fader, K.A.; Harkema, J.R.; Zacharewski, T. Loss of Liver-Specific and Sexually Dimorphic Gene Expression by Aryl Hydrocarbon Receptor Activation in C57BL/6 Mice. PLoS ONE 2017, 12, e0184842, doi:10.1371/journal.pone.0184842.

78. Fling, R.R.; Doskey, C.M.; Fader, K.A.; Nault, R.; Zacharewski, T.R. 2,3,7,8-Tetrachlorodibenzo-p-Dioxin (TCDD) Dysregulates Hepatic One Carbon Metabolism during the Progression of Steatosis to Steatohepatitis with Fibrosis in Mice. Sci. Rep. 2020, 10, 14831, doi:10.1038/s41598-020-71795-0.

79. Lee, G.; You, H.J.; Bajaj, J.S.; Joo, S.K.; Yu, J.; Park, S.; Kang, H.; Park, J.H.; Kim, J.H.; Lee, D.H.; et al. Distinct Signatures of Gut Microbiome and Metabolites Associated with Significant Fibrosis in Non-Obese NAFLD. Nat. Commun. 2020, 11, 4982, doi:10.1038/s41467-020-18754-5.

80. Jiao, N.; Baker, S.S.; Chapa-Rodriguez, A.; Liu, W.; Nugent, C.A.; Tsompana, M.; Mastrandrea, L.; Buck, M.J.; Baker, R.D.; Genco, R.J.; et al. Suppressed Hepatic Bile Acid Signalling despite Elevated Production of Primary and Secondary Bile Acids in NAFLD. Gut 2018, 67, 1881–1891, doi:10.1136/gutjnl-2017-314307.

81. Aranha, M.M.; Cortez-Pinto, H.; Costa, A.; da Silva, I.B.M.; Camilo, M.E.; de Moura, M.C.; Rodrigues, C.M.P. Bile Acid Levels Are Increased in the Liver of Patients with Steatohepatitis: Eur. J. Gastroenterol. Hepatol. 2008, 20, 519–525, doi:10.1097/MEG.0b013e3282f4710a.

82. Kakiyama, G.; Pandak, W.M.; Gillevet, P.M.; Hylemon, P.B.; Heuman, D.M.; Daita, K.; Takei, H.; Muto, A.; Nittono, H.; Ridlon, J.M.; et al. Modulation of the Fecal Bile Acid Profile

by Gut Microbiota in Cirrhosis. J. Hepatol. 2013, 58, 949–955, doi:10.1016/j.jhep.2013.01.003.

83. Jiao, N.; Loomba, R.; Yang, Z.-H.; Wu, D.; Fang, S.; Bettencourt, R.; Lan, P.; Zhu, R.; Zhu, L. Alterations in Bile Acid Metabo-lizing Gut Microbiota and Specific Bile Acid Genes as a Precision Medicine to Subclassify NAFLD. Physiol. Genom. 2020, 53, 336–348.

84. Plant, L.; Conway, P. Association of Lactobacillus Spp. with Peyer's Patches in Mice. Clin. Diagn Lab. Immunol. 2001, 8, 320–324, doi:10.1128/CDLI.8.2.320-324.2001.

85. Wang, P.; Li, Y.; Xiao, H.; Shi, Y.; Le, G.; Sun, J. Isolation of Lactobacillus Reuteri from Peyer's Patches and Their Effects on SIgA Production and Gut Microbiota Diversity. Mol. Nutr. Food Res. 2016, 60, 2020–2030, doi:10.1002/mnfr.201501065.

86. Fader, K.A.; Nault, R.; Raehtz, S.; McCabe, L.R.; Zacharewski, T.R. 2,3,7,8-Tetrachlorodibenzo-p-Dioxin Dose-Dependently Increases Bone Mass and Decreases Marrow Adiposity in Juvenile Mice. Toxicol. Appl. Pharmacol. 2018, 348, 85–98, doi:10.1016/j.taap.2018.04.013.

87. Collins, F.L.; Irwin, R.; Bierhalter, H.; Schepper, J.; Britton, R.A.; Parameswaran, N.; McCabe, L.R. Lactobacillus Reuteri 6475 Increases Bone Density in Intact Females Only under an Inflammatory Setting. PLoS ONE 2016, 11, 1–17, doi:10.1371/journal.pone.0153180.

88. Langmead, B.; Salzberg, S.L. Fast Gapped-Read Alignment with Bowtie 2. Nat. Methods 2012, 9, 357–359, doi:10.1038/nmeth.1923.

89. Danecek, P.; Bonfield, J.K.; Liddle, J.; Marshall, J.; Ohan, V.; Pollard, M.O.; Whitwham, A.; Keane, T.; McCarthy, S.A.; Davies, R.M.; et al. Twelve Years of SAMtools and BCFtools. GigaScience 2021, 10, giab008, doi:10.1093/gigascience/giab008.

90. Quinlan, A.R.; Hall, I.M. BEDTools: A Flexible Suite of Utilities for Comparing Genomic Features. Bioinformatics 2010, 26, 841–842, doi:10.1093/bioinformatics/btq033.

91. Mallick, H.; Rahnavard, A.; McIver, L.J.; Ma, S.; Zhang, Y.; Nguyen, L.H.; Tickle, T.L.; Weingart, G.; Ren, B.; Schwager, E.H.; et al. Multivariable Association Discovery in Population-Scale Meta-Omics Studies. Biorxiv 2021, doi:10.1101/2021.01.20.427420.

92. Love, M.I.; Huber, W.; Anders, S. Moderated Estimation of Fold Change and Dispersion for RNA-Seq Data with DESeq2. Genome Biol. 2014, 15, 550, doi:10.1186/s13059-014-0550-8.

93. Franzosa, E.A.; Morgan, X.C.; Segata, N.; Waldron, L.; Reyes, J.; Earl, A.M.; Giannoukos, G.; Boylan, M.R.; Ciulla, D.; Gevers, D.; et al. Relating the Metatranscriptome and Metagenome of the Human Gut. Proc. Natl. Acad. Sci. USA 2014, 111, E2329–E2338, doi:10.1073/pnas.1319284111.

94. Wang, Q.; Fish, J.A.; Gilman, M.; Sun, Y.; Brown, C.T.; Tiedje, J.M.; Cole, J.R. Xander : Employing a Novel Method for Efficient Gene-Targeted Metagenomic Assembly. Microbiome 2015, 3, 32, doi:10.1186/s40168-015-0093-6.

95. Fish, J.A.; Chai, B.; Wang, Q.; Sun, Y.; Brown, C.T.; Tiedje, J.M.; Cole, J.R. FunGene: The Functional Gene Pipeline and Re-pository. Front. Microbiol. 2013, 4, 291, doi:10.3389/fmicb.2013.00291.

CHAPTER 4: CONCLUSIONS AND FUTURE RESEARCH

CONCLUSIONS

TCDD-elicited effects on one carbon metabolism in the context of NAFLD

Disruptions in OCM are associated with NAFLD [1–3]. In the liver, regulatory mechanisms i.e., gene expression, allosteric regulation, and MAT isoforms, dictate the biosynthesis and supply of hepatic SAM needed for epigenic and high flux anabolic reactions including the biosynthesis of phospholipids, creatine, and polyamines [4]. Hepatic OCM was evaluated in the context of TCDD elicited NAFLD-like phenotypes at early (8 days) and late(28 days) time points (Chapter 3). The early time point showed dose-dependent decreases in the hepatic SAM/SAH ratio, cystathionine and dimethylglycine with minimal changes in OCM gene expression (Chapter 3, Figures 8 & 9). Conversely, OCM gene expression was highly repressed at 28 days despite little evidence for direct AhR regulation (Chapter 3, Figure 8). There was also OCM gene repression at 30 µg/kg TCDD after 28 days of treatment with evidence of hepatic fibrosis [5]. These results suggest secondary AhR-mediated mechanisms of toxicity i.e., induction of CYP1A1 with increased oxidative stress, contribute to repression of OCM rather than direct AhR regulation.

Despite reduced *Mat1a* expression and protein levels at the late time point, SAM levels were relatively unchanged compared to control mice. Reductions in GNMT and MAT1A levels may account for the recovery of the SAM/SAH ratio (Chapter 3, Figure 8). Reduced GNMT/MAT1A levels concurrent with normalized SAM/SAH ratio also suggested reduced OCM flux. It is not apparent what AhR-mediated effects contributed most towards OCM dysregulation. For example, several factors may also impact the metabolic state and OCM flux including allosteric and transcriptional regulation discussed in this manuscript as well as posttranslational modifications that were not investigated. Reduced serum methionine clearance is observed in patients with liver damage [6]. This report suggested reduced methionine clearance may be occurring in TCDD-treated mice following the repression of *Mat1a* and elevated hepatic methionine levels (Chapter 3).

Reduced OCM flux and repressed *Pemt* expression may also decrease PC biosynthesis capacity required for VLDL assembly. This is consistent with reports of increased hepatic lipid accumulation and reduced VLDL secretion in TCDD-treated mice [7–9]. Disruption of other VLDL metabolic processes may also be occurring due to oxidative stress. For example, excess polyunsaturated fatty acids increase reactive oxygen species that result in apoB aggregates and degradation of apoB through a posttranslational proteolytic process in hepatocytes [10]. Lastly, the gene expression patterns of major OCM i.e., *Mat1a*/*Mat2a* switch, *Gnmt*/*Bhmt* repression, and Odc induction, closely resembles OCM in late stages of NALFD progression [1,4,11,12]. Collectively, results presented in this manuscript demonstrate that the dose dependent activation of AhR repressed OCM only after repeated treatments similar to the OCM dysregulation reported in NAFLD and HCC.

TCDD-elicited shifts the gut microbiome consistent with NAFLD progression

Secondary BAs participate in regulation of BA and glucose metabolism through receptors in the intestine and liver [13]. TCDD disrupts bile acid metabolism and enterohepatic circulation in mice resulting in elevated serum and hepatic primary and secondary bile acids [5]. Our studies evaluated TCDD-elicited shifts in the gut microbiome at taxonomic and functional levels using shotgun metagenomics. Metagenomic analyses identified alterations in microbial species populations and disrupted metabolic pathways following TCDD treatment associated with bile acid metabolism consistent with NAFLD. TCDD enriched for deconjugating bile acid species i.e., *Lactobacillus reuteri* and *Turicibacter sanguinis,* concomitant with increased abundance in bile salt hydrolase genes found within enriched species. Genes involved in mevalonate dependent isoprenoid biosynthesis pathway were enriched in *L. reuteri* and *L. johnsonii* (Chapter 2). This pathway as well as menaquinone biosynthesis were also elevated in cirrhosis patients. Furthermore, the amino acid aminotransferase gene (UniRef90_A0A2S1ENB9) was annotated to

L. reuteri and enriched by TCDD, a gene that is required for indole-3-aldehyde production in *L. reuteri* [23].

Turcibacter sanguinis was also one of the top species enriched by TCDD treatment and may warrant further investigations due to previous reports on its relevant microbial/host signaling. For example, Turicibacter has also been shown to be an abundant species found in the interior of Peyer's patches [14]. Further, mice mononcolonized with *T. sanguinis* exhibit altered host lipid metabolism [15]. *T. sangunis* is reported to have BSH deconjugation activity that is consistent with metagenomic *bsh* analysis presented in this report (Chapter 4, Figure 14) as well as bile acid epimerization of DCA to isoDCA, a secondary bile acid reported to be elevated in NAFLD [16].

One of the more unexpected findings in this report was the increased abundance of genes associated with the mevalonate dependent isoprenoid pathway in fecal samples from cirrhosis patients. This pathway is found predominantly in Streptococcus and Lactobacillus species which is reflected in the mouse and human results presented in this thesis (Chapter 4). Statins are often prescribed to NAFLD patients to ameliorate high cholesterol levels associated with Metabolic Syndrome to reduce risk of more complex metabolic diseases [17]. Most statins including simvastatin are inhibitors of 3-hydroxy-3-methylglutaryl-CoA reductase (HMGCR) and are mainly eliminated through biliary secretion and excretion in the feces [18]. Several studies have demonstrated antimicrobial effects of statins targeting species that possess the mevalonate isoprenoid pathway including *Staphylococcus aureus* and *Streptococcus anginsosus* [19,20]. However, the mechanisms of inhibition and species-specific effects are not fully elucidated [20]. In *S. aureus*, simvastatin may directly inhibit mevalonate IPP biosynthesis whereas the simvastatin inhibitory effects can be rescued with supplementation of mevalonate[21]. It is tempting to speculate that statins may inhibit the growth of *L. reuteri* and other species with HMG-CoA reductases and mevalonate dependent isoprenoid biosynthesis, however, no studies investigating the direct antimicrobial effects of statins on *L. reuteri* have been conducted. It is most

likely that the combined inhibition of cholesterol biosynthesis and the lipid lowering abilities of statins that contributes to pleiotropic effects on the gut microbiome.

Tryptophan metabolizing bacteria including *L. reuteri* can produce endogenous AhR ligands that upregulate the expression of *Il22* in group 3 innate lymphoid cells (ILC3s), the primary producers of IL-22 in the small intestine. ILC3s are also necessary for the development of Peyer's patches and intestinal immune system development [22]. The IL-22/microbial axis mediated by AhR signaling is critical to the intestinal barrier that includes the production of antimicrobial peptides and regulation of intestinal mucous production [23,24]. Interestingly, select strains of *L. reuteri* colonize Peyer's patches in mice [25,26]. Results in this thesis, support TCDD-elicited activation of the AhR enriches for bacteria with bile salt hydrolase activity. Moreover, *L. reuteri* was the most enriched species by TCDD with gene annotation associated with endogenous AhR ligand production and the relatively rare bacterial mevalonate dependent isoprenoid biosynthesis pathway. Whether statins are negatively or positively affecting symbiotic members of the gut microbial community in NAFLD progression remains unresolved. It is also not clear whether these TCDD-elicited shifts in the gut microbiome are antagonistic or agonistic towards the development and progression of the NAFLD-like phenotypes reported.

FUTURE RESEARCH

This report investigated disruptions in hepatic OCM and gut microbiome metabolic pathways associated with TCDD treatment in mice. Repeated oral gavage with TCDD every 4 days for 28 days recapitulates NAFLD-like phenotypes in mice with dose-dependent development of steatosis and progression to steatohepatitis with fibrosis in mice. In this dissertation, comparisons were made between AhR-mediated NAFLD-phenotype in mice to human NAFLD, cirrhosis, and HCC published datasets in relation to OCM and shifts in the gut microbiomes relevant to disease progression.

Considerations for future research regarding OCM

The metabolomic analysis in this report offers a snapshot into metabolite levels and gene expression associated with hepatic OCM. Conclusions towards metabolic fluxes through OCM can only be inferred from these results. Further, distinctions between early and late time points in this report suggest the involvement of several mechanisms including oxidative stress that could impact the regulation of homocysteine metabolism. Tracer studies using labeled intermediates such as methionine would offer more comprehensive insight into the metabolic fates of homocysteine and shifts in OCM fluxes towards the biosynthesis of glutathione, methionine, and SAM.

Another limitation of these OCM metabolic analyses in this report is the lack of subcellular analyses needed to characterize shifts in phospholipid composition that affects VLDL metabolism. Specifically, lower PC levels reduces the PC/PE ratio and negatively correlates with ER membrane integrity in PEMT-/- mice[27]. Whether *Pemt* inhibition by TCDD contributes to reduced PC incorporation into VLDL particle during assembly or induces ER membrane stress is not clear. Hepatic lipid analyses of ER membranes and VLDL particles in TCDD-treated animals could better evaluate the impact of OCM dysregulation and *Pemt* repression on PC levels with relevance to VLDL assembly and secretion.

Considerations for research regarding TCDD and HCC

Several observations in this report mirror the expression and metabolic changes in OCM associated with human cirrhosis and HCC including the repression of OCM gene expression and elevated polyamines. Hepatic expression of *Mat1a* is a marker of differentiated adult hepatocytes and often repressed in HCC. The *Mat1a*/M*at2a* switch and reduced *Bhmt*/*Gnmt* expression profiler reported in this manuscript is also associated with a poorer HCC prognosis [11,12]. Using hepatic single cell RNA sequencing (scRNA-seq) datasets from studies using the same TCDD treatment regimen, cells were identified having similar HCC-like repression profiles [28]. These

HCC-like cells exhibiting OCM dysregulation could also be evaluated for shifts in gene expression profiles in other metabolic pathways relevant to HCC development and metastasis. For example, single cell technologies highlight the intra-tumor heterogeneity of HCC tumors with small subsets of cells demonstrating distinct expression profiles associating with more aggressive cell phenotypes [29]. Further, scRNA-seq captures expression profiles of less abundant cell types including immune cells that impact the tumor microenvironment and HCC progression which may be indistinguishable in bulk RNA-seq datasets. Analysis of HCC tumors using scRNA-seq identified dysregulation of the methionine salvage pathway and polyamine biosynthesis in T-Cells associated with T-cell exhaustion and worse prognosis [30].

Considerations for TCDD and the gut microbiome

Short term TCDD treatment in mice causes reductions in hepatic primary and secondary bile acid levels and reductions in hepatic biliary secretion of BAs [31]. Conversely, longer treatment regimens like the studies presented in this report demonstrate elevated primary and secondary BAs [5]. Results presented in this thesis studied both earlier and late time points in the liver. Investigations into temporal shifts in the gut microbiome at early time points of the study may identify early metabolic and taxonomic shifts in the gut microbiome and may capture temporal shifts in the gut microbiome through the duration of the study.

Due to the high enrichment *L. reuteri* and *L. reuteri*'s close association with AhR signaling in intestinal barrier homeostasis and BA metabolism, functional metabolic pathway analyses in this report focused on identifying *L. reuteri* genes enriched by TCDD treatment. The metagenomic studies in this report were also conducted in three independent cohorts to ensure reproducibility and account for coprophagia. This study design resulted in enrichment of *L. reuteri* suggesting TCDD-elicited AhR activation highly selects for *L. reuteri.* The AhR also directly promotes IL-22 production in ILC3s with subsequent antimicrobial peptide production and promotion of goblet cell hyperplasia [22]. It has also been shown that only some *L. reuteri* strains colonize Peyer's patches

[26]. These results present in this report support an enrichment of select *L. reuteri* strains. For example, only 2 out of the 4 unique *bsh* sequences annotated to *L. reuteri* were enriched by TCDD (Chapter 4, Figure 14). *L. reuteri* strains in the gut lumen and Peyer's patches could be isolated and their genomes sequenced for comparative analysis in the identification of genes and metabolic pathways found only in the strains associated with Peyer's patches. Further, metagenomic analysis of mucus isolated from Peyer's patches could provide taxonomic and functional shifts in bacterial community members in the context of TCDD treatment. From the same samples, scRNA-seq analysis could assess TCDD-elicited host responses in the diverse set of epithelium and immune and cells found in Peyer's patches.

REFERENCES

REFERENCES

1. Bae, D.H.; Lane, D.J.R.; Jansson, P.J.; Richardson, D.R. The Old and New Biochemistry of Polyamines. *Biochimica et Biophysica Acta - General Subjects* **2018**, *1862*, 2053–2068, doi:10.1016/j.bbagen.2018.06.004.

2. Pascale, R.M.; Feo, C.F.; Calvisi, D.F.; Feo, F. Deregulation of Methionine Metabolism as Determinant of Progression and Prognosis of Hepatocellular Carcinoma. *Translational gastroenterology and hepatology* **2018**, *3*, 36, doi:10.21037/tgh.2018.06.04.

3. Song, J.; Da Costa, K.A.; Fischer, L.M.; Kohlmeier, M.; Kwock, L.; Wang, S.; Zeisel, S.H. Polymorphism of the PEMT Gene and Susceptibility to Nonalcoholic Fatty Liver Disease (NAFLD). *The FASEB Journal* **2005**, *19*, 1266–1271, doi:10.1096/fj.04-3580com.

4. Mato, J.M.; Martinez-Chantar, M.L.; Lu, S.C. *S*-Adenosylmethionine Metabolism and Liver Disease. *Annals of hepatology* **2013**, *12*, 183–189, doi:1032614 [pii].

5. Fader, K.A.; Nault, R.; Zhang, C.; Kumagai, K.; Harkema, J.R.; Zacharewski, T.R. 2,3,7,8-Tetrachlorodibenzo-p-Dioxin (TCDD)-Elicited Effects on Bile Acid Homeostasis: Alterations in Biosynthesis, Enterohepatic Circulation, and Microbial Metabolism. *Sci Rep* **2017**, *7*, 5921, doi:10.1038/s41598-017-05656-8.

6. Kinsell, L.W.; Harper, H.A.; Barton, H.C.; Michaels, G.D.; Weiss, H.A. Rate of Disappearance From Plasma of Intravenously Administered Methionine in Patients With Liver Damage. *Science* **1947**, *106*, 589–590, doi:10.1126/science.106.2763.589.

7. Nault, R.; Fader, K.A.; Lydic, T.A.; Zacharewski, T.R. Lipidomic Evaluation of Aryl Hydrocarbon Receptor-Mediated Hepatic Steatosis in Male and Female Mice Elicited by 2,3,7,8- Tetrachlorodibenzo-p-dioxin., doi:10.1021/acs.chemrestox.6b00430.

8. Angrish, M.M.; Dominici, C.Y.; Zacharewski, T.R. TCDD-Elicited Effects on Liver, Serum, and Adipose Lipid Composition in C57BL/6 Mice. *Toxicological Sciences* **2013**, *131*, 108–115, doi:10.1093/toxsci/kfs277.

9. Lee, J.H.; Wada, T.; Febbraio, M.; He, J.; Matsubara, T.; Lee, M.J.; Gonzalez, F.J.; Xie, W. A Novel Role for the Dioxin Receptor in Fatty Acid Metabolism and Hepatic Steatosis. *Gastroenterology* **2010**, *139*, 653–663, doi:10.1053/J.GASTRO.2010.03.033.

10. Pan, M.; Maitin, V.; Parathath, S.; Andreo, U.; Lin, S.X.; Germain, C.St.; Yao, Z.; Maxfield, F.R.; Williams, K.J.; Fisher, E.A. Presecretory Oxidation, Aggregation, and Autophagic Destruction of Apoprotein-B: A Pathway for Late-Stage Quality Control. *Proc. Natl. Acad. Sci. U.S.A.* **2008**, *105*, 5862–5867, doi:10.1073/pnas.0707460104.

11. Chen, P.-M.; Tsai, C.-H.; Huang, C.-C.; Hwang, H.-H.; Li, J.-R.; Liu, C.-C.; Ko, H.-A.; Chiang, E.-P.I. Downregulation of Methionine Cycle Genes MAT1A and GNMT Enriches Protein-Associated Translation Process and Worsens Hepatocellular Carcinoma Prognosis. *IJMS* **2022**, *23*, 481, doi:10.3390/ijms23010481.

12. Jin, B.; Gong, Z.; Yang, N.; Huang, Z.; Zeng, S.; Chen, H.; Hu, S.; Pan, G. Downregulation of Betaine Homocysteine Methyltransferase (BHMT) in Hepatocellular Carcinoma Associates with Poor Prognosis. *Tumor Biol.* **2016**, *37*, 5911–5917, doi:10.1007/s13277-015-4443-6.

13. Chow, M.D.; Lee, Y.H.; Guo, G.L. The Role of Bile Acids in Nonalcoholic Fatty Liver Disease and Nonalcoholic Steatohepatitis. *Molecular Aspects of Medicine* **2017**, *56*, 34–44, doi:10.1016/j.mam.2017.04.004.

14. Qiao, Y.; Sun, J.; Xie, Z.; Shi, Y.; Le, G. Propensity to High-Fat Diet-Induced Obesity in Mice Is Associated with the Indigenous Opportunistic Bacteria on the Interior of Peyer's Patches. *J. Clin. Biochem. Nutr.* **2014**, *55*, 120–128, doi:10.3164/jcbn.14-38.

15. Fung, T.C.; Vuong, H.E.; Luna, C.D.G.; Pronovost, G.N.; Aleksandrova, A.A.; Riley, N.G.; Vavilina, A.; McGinn, J.; Rendon, T.; Forrest, L.R.; et al. Intestinal Serotonin and Fluoxetine Exposure Modulate Bacterial Colonization in the Gut. *Nat Microbiol* **2019**, *4*, 2064–2073, doi:10.1038/s41564-019-0540-4.

16. Kemis, J.H.; Linke, V.; Barrett, K.L.; Boehm, F.J.; Traeger, L.L.; Keller, M.P.; Rabaglia, M.E.; Schueler, K.L.; Stapleton, D.S.; Gatti, D.M.; et al. Genetic Determinants of Gut Microbiota Composition and Bile Acid Profiles in Mice. *PLoS Genet* **2019**, *15*, e1008073, doi:10.1371/journal.pgen.1008073.

17. Pastori, D.; Pani, A.; Di Rocco, A.; Menichelli, D.; Gazzaniga, G.; Farcomeni, A.; D'Erasmo, L.; Angelico, F.; Del Ben, M.; Baratta, F. Statin Liver Safety in Non-alcoholic Fatty Liver Disease: A Systematic Review and Metanalysis. *Brit J Clinical Pharma* **2022**, *88*, 441–451, doi:10.1111/bcp.14943.

18. Elsby, R.; Hilgendorf, C.; Fenner, K. Understanding the Critical Disposition Pathways of Statins to Assess Drug–Drug Interaction Risk During Drug Development: It's Not Just About OATP1B1. *Clin Pharmacol Ther* **2012**, *92*, 584–598, doi:10.1038/clpt.2012.163.

19. Whitaker, E.; Alshammari, A. Bacteriostatic Effect of Simvastatin on Selected Oral Streptococci in Vitro. *Contemp Clin Dent* **2017**, *8*, 59, doi:10.4103/ccd.ccd_848_16.

20. Hennessy, E.; Adams, C.; Reen, F.J.; O'Gara, F. Is There Potential for Repurposing Statins as Novel Antimicrobials? *Antimicrob Agents Chemother* **2016**, *60*, 5111–5121, doi:10.1128/AAC.00192-16.

21. Horn, M.P.; Knecht, S.M.; Rushing, F.L.; Birdsong, J.; Siddall, C.P.; Johnson, C.M.; Abraham, T.N.; Brown, A.; Volk, C.B.; Gammon, K.; et al. Simvastatin Inhibits *Staphylococcus Aureus* Host Cell Invasion through Modulation of Isoprenoid Intermediates. *J Pharmacol Exp Ther* **2008**, *326*, 135–143, doi:10.1124/jpet.108.137927.

22. Melo-Gonzalez, F.; Hepworth, M.R. Functional and Phenotypic Heterogeneity of Group 3 Innate Lymphoid Cells. *Immunology* **2017**, *150*, 265–275, doi:10.1111/imm.12697.

23. Zelante, T.; Iannitti, R.G.; Cunha, C.; DeLuca, A.; Giovannini, G.; Pieraccini, G.; Zecchi, R.; D'Angelo, C.; Massi-Benedetti, C.; Fallarino, F.; et al. Tryptophan Catabolites from Microbiota Engage Aryl Hydrocarbon Receptor and Balance Mucosal Reactivity via Interleukin-22. *Immunity* **2013**, *39*, 372–385, doi:10.1016/j.immuni.2013.08.003.

24. Kou, Z.; Dai, W. Aryl Hydrocarbon Receptor: Its Roles in Physiology. *Biochemical Pharmacology* **2021**, *185*, 114428, doi:10.1016/j.bcp.2021.114428.

25. Wang, P.; Li, Y.; Xiao, H.; Shi, Y.; Le, G.; Sun, J. Isolation of *Lactobacillus Reuteri* from Peyer's Patches and Their Effects on SIgA Production and Gut Microbiota Diversity. *Mol. Nutr. Food Res.* **2016**, *60*, 2020–2030, doi:10.1002/mnfr.201501065.

26. Qi, C.; Sun, J.; Li, Y.; Gu, M.; Goulette, T.; You, X.; Sela, D.A.; Wang, X.; Xiao, H. Peyer's Patch-Specific *Lactobacillus Reuteri* Strains Increase Extracellular Microbial DNA and Antimicrobial Peptide Expression in the Mouse Small Intestine. *Food Funct.* **2018**, *9*, 2989–2997, doi:10.1039/C8FO00109J.

27. Li, Z.; Agellon, L.B.; Allen, T.M.; Umeda, M.; Jewell, L.; Mason, A.; Vance, D.E. The Ratio of Phosphatidylcholine to Phosphatidylethanolamine Influences Membrane Integrity and Steatohepatitis. *Cell Metabolism* **2006**, *3*, 321–331, doi:10.1016/j.cmet.2006.03.007.

28. Nault, R.; Fader, K.A.; Bhattacharya, S.; Zacharewski, T.R. Single-Nuclei RNA Sequencing Assessment of the Hepatic Effects of 2,3,7,8-Tetrachlorodibenzo-p-Dioxin. *Cellular and Molecular Gastroenterology and Hepatology* **2020**, 1–13, doi:10.1016/j.jcmgh.2020.07.012.

29. Li, X.-Y.; Shen, Y.; Zhang, L.; Guo, X.; Wu, J. Understanding Initiation and Progression of Hepatocellular Carcinoma through Single Cell Sequencing. *Biochimica et Biophysica Acta (BBA) - Reviews on Cancer* **2022**, *1877*, 188720, doi:10.1016/j.bbcan.2022.188720.

30. Hung, M.H.; Lee, J.S.; Ma, C.; Diggs, L.P.; Heinrich, S.; Chang, C.W.; Ma, L.; Forgues, M.; Budhu, A.; Chaisaingmongkol, J.; et al. Tumor Methionine Metabolism Drives T-Cell Exhaustion in Hepatocellular Carcinoma. *Nat Commun* **2021**, *12*, 1455, doi:10.1038/s41467-021-21804-1.

31. Csanaky, I.L.; Lickteig, A.J.; Klaassen, C.D. Aryl Hydrocarbon Receptor (AhR) Mediated Short-Term Effects of 2,3,7,8-Tetrachlorodibenzo- p -Dioxin (TCDD) on Bile Acid Homeostasis in Mice. *Toxicology and Applied Pharmacology* **2018**, *343*, 48–61, doi:10.1016/j.taap.2018.02.005.